

Nuclear forces from chiral effective field theory — a primer —

Evgeny Epelbaum

*Forschungszentrum Jülich, Institut für Kernphysik (Theorie) and Jülich Center for Hadron
Physics, D-52425 Jülich, Germany;
Helmholtz-Institut für Strahlen- und Kernphysik (Theorie) and Bethe Center for Theoretical
Physics, Universität Bonn, D-53115 Bonn, Germany*

ABSTRACT

This paper is a write-up of introductory lectures on the modern approach to the nuclear force problem based on chiral effective field theory given at the 2009 Joliot-Curie School, Lacanau, France, 27 September - 3 October 2009.

Contents

1	Introduction	2
2	Nuclear potentials and nucleon-nucleon scattering	3
3	Chiral perturbation theory: An elementary introduction	8
3.1	Chiral symmetry of QCD	9
3.2	Effective Lagrangian for Goldstone bosons	11
3.3	Power counting	15
3.4	Inclusion of nucleons	19
4	EFT for two nucleons	23
4.1	ChPT and nucleon-nucleon scattering	23
4.2	Analytic properties of the non-relativistic scattering amplitude	25

4.3	EFT for two nucleons at very low energy	28
4.4	Chiral EFT for two nucleons with perturbative pions	32
4.5	Towards including pions nonperturbatively: playing with toy models	34
4.5.1	The model	34
4.5.2	KSW-like approach	36
4.5.3	Weinberg-like approach with a finite cutoff	39
4.5.4	Toy model with local interactions: a numerical example	42
5	Nuclear forces from chiral EFT	45
5.1	Derivation of nuclear potentials from field theory	45
5.2	Method of unitary transformation	48
5.3	The 1π - and the leading 2π -exchange potentials	51
6	Summary	57

1 Introduction

One of the oldest but still actual problems in nuclear physics is related to the determination of the interaction between the nucleons. A quantitative understanding of the nuclear force is crucial in order to describe the properties of nuclei and nuclear matter in terms of hadronic degrees of freedom. The conventional way to parametrize the nuclear force utilizes the meson-exchange picture, which goes back to the seminal work by Yukawa [1]. His idea, followed by the experimental discovery of π - and heavier mesons (ρ , ω , \dots), stimulated the development of boson-exchange models which still provide a basis for many modern, highly sophisticated phenomenological nucleon-nucleon (NN) potentials.

According to our present understanding, the nuclear force is due to residual strong interactions between the color-charge neutral hadrons. A direct derivation of the nuclear force from QCD, the underlying theory of strong interactions, is not yet possible, see however Ref. [2] for a recent attempt using lattice QCD. In order to provide reliable input for few- and many-body calculations, a (semi-)phenomenological approach has been followed over the past few decades aiming to achieve the best possible description of the available low-energy NN data. As will be discussed in section 2, the two-nucleon potential can be decomposed in only few different spin-space structures, so that the corresponding radial functions can be parameterized using an extensive set of data. Although the resulting models provide an excellent description of experimental data in many cases, there are certain major conceptual deficiencies that cannot be overcome. In particular, one important concern is related to the problem of the construction of *consistent* many-body forces. These can only be meaningfully defined in a consistent scheme with a given two-nucleon interaction [3]. Notice that because of the large variety of different possible structures in the three-nucleon force, following the same phenomenological path as in the NN system

and parametrizing its most general structure seems not to be feasible without additional theoretical guidance. Clearly, the same problem of consistency arises in the context of reactions with electroweak probes, whose description requires the knowledge of the corresponding consistent nuclear current operator. Further, one lacks within phenomenological treatments a method of systematically improving the theory of the nuclear force in terms of the dominant dynamical contributions. Finally, and most important, the phenomenological scheme provides only a loose connection to QCD.

Chiral perturbation theory (ChPT) is an effective field theory (EFT) of QCD which exploits its symmetries and symmetry-breaking pattern and allows to analyze the properties of hadronic systems at low energies in a systematic and model independent way. We will see in section 3 that QCD with two flavors of the u - and d -quarks and, to a less extent, with three flavors of the u -, d - and s -quarks, exhibits an approximate chiral symmetry which is explicitly broken due to non-vanishing (but small) quark masses. In addition, the chiral symmetry is also spontaneously broken down to its vector subgroup. These symmetry/symmetry-breaking pattern manifest themselves in the hadron spectrum leading, in particular, to a natural explanation of the very small masses (compared to other hadrons) of pions which play the role of the corresponding Goldstone bosons. Most important, the Goldstone boson nature of the pions implies that they interact weakly at low energy and allows to calculate low-energy observables in the pion and single-nucleon sector in perturbation theory. The situation in the few-nucleon sector is conceptually much more complicated due to the strong nature of the nuclear force which manifests itself in the appearance of self-bound atomic nuclei and invalidates a naive application of perturbation theory. As pointed out by Weinberg, the breakdown of perturbation theory in the few-nucleon sector can be traced back to the infrared enhancement of reducible time-ordered diagrams which involve purely nucleonic intermediate states and can be resummed by iterating the corresponding dynamical equation [4, 5]. These important observation made in Weinberg's seminal papers opened a new era in nuclear physics and has triggered an intense research activity along these lines. In these lectures I will outline the basic concepts of chiral effective field theory and its application to nucleon-nucleon scattering and the derivation of the nuclear force.

The manuscript is organized as follows. In section 2 I discuss the general structure of the nuclear force and outline the main ingredients of the conventional NN potentials. Section 3 provides an elementary introduction to chiral perturbation theory. Generalization of EFT to strongly interacting nuclear systems is discussed in section 4. Derivation of the nuclear forces in chiral EFT is outlined in section 5. A brief summary is given in section 6.

2 Nuclear potentials and nucleon-nucleon scattering

The most general structure of a non-relativistic two-nucleon potential is expressible in terms of just a few operators. The potential can be viewed as an operator acting in the position, spin and isospin spaces of the nucleons. It is instructive to discuss its isospin structure separately from the operators acting in the position-spin space.

The isospin structure of the two-nucleon force falls into the four different classes according to the

classification of Ref. [6]:

$$\begin{aligned}
\text{Class I:} & \quad V_I = \alpha_I + \beta_I \boldsymbol{\tau}_1 \cdot \boldsymbol{\tau}_2, \\
\text{Class II:} & \quad V_{II} = \alpha_{II} \tau_1^3 \tau_2^3, \\
\text{Class III:} & \quad V_{III} = \alpha_{III} (\tau_1^3 + \tau_2^3), \\
\text{Class IV:} & \quad V_{IV} = \alpha_{IV} (\tau_1^3 - \tau_2^3) + \beta_{IV} [\boldsymbol{\tau}_1 \times \boldsymbol{\tau}_2]^3.
\end{aligned} \tag{2.1}$$

Here, α_i, β_i are position-spin operators and $\boldsymbol{\tau}_i$ are Pauli isospin matrices of a nucleon i . The operator β_{IV} has to be odd under a time reversal transformation. While class (I) forces are isospin-invariant, all other classes (II), (III) and (IV) are isospin-breaking. Class (II) forces, V_{II} , maintain charge symmetry but break charge independence. They are usually referred to as charge independence breaking (CIB) forces. Charge symmetry represents invariance under reflection about the 1-2 plane in charge space. The charge symmetry operator P_{cs} transforms proton and neutron states into each other and is given by $P_{cs} = e^{i\pi T_2}$ with $\mathbf{T} \equiv \sum_i \boldsymbol{\tau}_i/2$ being the total isospin operator. Class (III) forces break charge symmetry but do not lead to isospin mixing in the NN system, i.e. they do not give rise to transitions between isospin-singlet and isospin-triplet two-nucleon states. Finally, class (IV) forces break charge symmetry and cause isospin mixing in the NN system.

Exercise: show that class-III two-nucleon forces do not lead to isospin mixing in the two-nucleon system, i.e. they commute with the operator T^2 . Does this still hold true for systems with three and more nucleons?

Let us now discuss the position-spin structure of the potential. For the sake of simplicity, I restrict myself to the isospin-invariant case. The available vectors are given by the position, momentum and spin operators for individual nucleons: $\vec{r}_1, \vec{r}_2, \vec{p}_1, \vec{p}_2, \vec{\sigma}_1, \vec{\sigma}_2$. The translational and Galilean invariance of the potential implies that it may only depend on the relative distance between the nucleons, $\vec{r} \equiv \vec{r}_1 - \vec{r}_2$, and the relative momentum, $\vec{p} \equiv (\vec{p}_1 - \vec{p}_2)/2$. Further constraints due to (i) rotational invariance, (ii) invariance under a parity operation, (iii) time reversal invariance, (iv) hermiticity as well as (v) invariance with respect to interchanging the nucleon labels, $1 \leftrightarrow 2$, lead to the following operator form of the potential [7]:

$$\left\{ \mathbf{1}_{\text{spin}}, \vec{\sigma}_1 \cdot \vec{\sigma}_2, S_{12}(\vec{r}), S_{12}(\vec{p}), \vec{L} \cdot \vec{S}, (\vec{L} \cdot \vec{S})^2 \right\} \times \{ \mathbf{1}_{\text{isospin}}, \boldsymbol{\tau}_1 \cdot \boldsymbol{\tau}_2 \}, \tag{2.2}$$

where $\vec{L} \equiv \vec{r} \times \vec{p}$, $\vec{S} \equiv (\vec{\sigma}_1 + \vec{\sigma}_2)/2$ and $S_{12}(\vec{x}) \equiv 3\vec{\sigma}_1 \cdot \hat{x} \vec{\sigma}_2 \cdot \hat{x} - \vec{\sigma}_1 \cdot \vec{\sigma}_2$ with $\hat{x} \equiv \vec{x}/|\vec{x}|$. The operators entering the above equation are multiplied by scalar operator-like functions that depend on r^2, p^2 and L^2 .

Throughout this work, two-nucleon observables will be computed by solving the Lippmann-Schwinger equation in momentum space. It is, therefore, instructive to look at the momentum-space representation of the potential, $V(\vec{p}', \vec{p}) \equiv \langle \vec{p}' | V | \vec{p} \rangle$, with \vec{p} and \vec{p}' denoting the two-nucleon center of mass momenta before and after the interaction takes place. Following the same logic as above, the most general form of the potential potential in momentum space can be shown to be:

$$\left\{ \mathbf{1}_{\text{spin}}, \vec{\sigma}_1 \cdot \vec{\sigma}_2, S_{12}(\vec{q}), S_{12}(\vec{k}), i\vec{S} \cdot \vec{q} \times \vec{k}, \vec{\sigma}_1 \cdot \vec{q} \times \vec{k} \vec{\sigma}_2 \cdot \vec{q} \times \vec{k} \right\} \times \{ \mathbf{1}_{\text{isospin}}, \boldsymbol{\tau}_1 \cdot \boldsymbol{\tau}_2 \}, \tag{2.3}$$

where $\vec{q} \equiv \vec{p}' - \vec{p}$ and $\vec{k} \equiv (\vec{p}' + \vec{p})/2$. The operators are multiplied with the scalar functions that depend on p^2 , p'^2 and $\vec{p} \cdot \vec{p}'$. Notice that contrary to Eq. (2.2) which involves the *operator* \vec{p} , \vec{p} and \vec{p}' that enter Eq. (2.3) denote the corresponding eigenvalues. It should also be emphasized that further spin-momentum operators contribute in the case of class-IV isospin-breaking interactions.

For low-energy processes I will be focused in here, it is convenient to switch to the partial wave basis $|\vec{p}\rangle \rightarrow |plm_l\rangle$. A two-nucleon state $|p(ls)jm_j\rangle$ in the partial-wave basis depends on the orbital angular momentum l , spin s , the total angular momentum j and the corresponding magnetic quantum number m_j . The partial wave decomposition of the potential in Eq. (2.3) is given by:

$$\langle p'(l's')j'm'_j | V | p(ls)jm_j \rangle \equiv \delta_{j'j} \delta_{m'_j m_j} \delta_{s's} V_{l'l}^{sj}(p', p), \quad (2.4)$$

with

$$\begin{aligned} V_{l'l}^{sj}(p', p) &= \sum_{m'_l, m_l} \int d\hat{p}' d\hat{p} c(l', s, j; m'_l, m_j - m'_l, m_j) c(l, s, j; m_l, m_j - m_l, m_j) \\ &\times Y_{l'm'_l}^*(\hat{p}') Y_{lm_l}(\hat{p}) \langle s m_j - m'_l | V(\vec{p}', \vec{p}) | s m_j - m_l \rangle, \end{aligned} \quad (2.5)$$

where $c(l, s, j; m_l, m_j - m_l, m_j)$ are Clebsch-Gordan coefficients and $Y_{lm_l}(\hat{p})$ denote the spherical harmonics. The first two Kronecker δ 's on the right-hand side of the first line in Eq. (2.4) reflect the conservation of the total angular momentum. Rotational invariance of the potential prevents the dependence of the matrix elements on the magnetic quantum number m_j . The conservation of the total spin of the nucleons can be easily verified explicitly for all operators entering Eq. (2.3). I stress, however, that transitions between the spin-singlet and spin-triplet channels are possible in a more general case of the broken isospin symmetry. For each individual operator entering Eq. (2.3), the expression (2.5) can be simplified and finally expressed as an integral over $\hat{p} \cdot \hat{p}'$ with the integrand being written in terms of the corresponding scalar function and Legendre polynomials. Explicit formulae can be found e.g. in [8], see also Ref. [9] for a recent work on this topic.

The Lippmann-Schwinger (LS) equation for the half-shell T -matrix in the partial wave basis has the form

$$T_{l'l}^{sj}(p', p) = V_{l'l}^{sj}(p', p) + \sum_{l''} \int_0^\infty \frac{dp'' p''^2}{(2\pi)^3} V_{l'l''}^{sj}(p', p'') \frac{m}{p^2 - p''^2 + i\eta} T_{l''l}^{sj}(p'', p), \quad (2.6)$$

with m denoting the nucleon mass and $\eta \rightarrow 0^+$. In the uncoupled case, l is conserved. The relation between the on-shell S - and T -matrices is given by

$$S_{l'l}^{sj}(p) = \delta_{l'l} - \frac{i}{8\pi^2} p m T_{l'l}^{sj}(p). \quad (2.7)$$

The phase shifts in the uncoupled cases can be obtained from the S -matrix via

$$S_{jj}^{0j} = \exp\left(2i\delta_j^{0j}\right), \quad S_{jj}^{1j} = \exp\left(2i\delta_j^{1j}\right), \quad (2.8)$$

where I use the notation δ_l^{sj} . The so-called Stapp parametrization of the S -matrix in the coupled channels ($j > 0$) is defined as:

$$S = \begin{pmatrix} S_{j-1j-1}^{1j} & S_{j-1j+1}^{1j} \\ S_{j+1j-1}^{1j} & S_{j+1j+1}^{1j} \end{pmatrix} = \begin{pmatrix} \cos(2\epsilon) \exp(2i\delta_{j-1}^{1j}) & i \sin(2\epsilon) \exp(i\delta_{j-1}^{1j} + i\delta_{j+1}^{1j}) \\ i \sin(2\epsilon) \exp(i\delta_{j-1}^{1j} + i\delta_{j+1}^{1j}) & \cos(2\epsilon) \exp(2i\delta_{j+1}^{1j}) \end{pmatrix},$$

and is related to another frequently used parametrization due to Blatt and Biedenharn in terms of $\tilde{\delta}$ and $\tilde{\epsilon}$ via the following equations:

$$\delta_{j-1} + \delta_{j+1} = \tilde{\delta}_{j-1} + \tilde{\delta}_{j+1}, \quad \sin(\delta_{j-1} - \delta_{j+1}) = \frac{\tan(2\epsilon)}{\tan(2\tilde{\epsilon})}, \quad \sin(\tilde{\delta}_{j-1} - \tilde{\delta}_{j+1}) = \frac{\sin(2\epsilon)}{\sin(2\tilde{\epsilon})}. \quad (2.9)$$

The appearance of the electromagnetic interaction requires special care when calculating scattering observables due to its long-range nature. In particular, the S -matrix has to be formulated in terms of asymptotic Coulomb states. The electromagnetic interaction between the nucleons is driven by the Coulomb force and, to a lesser extent, magnetic moment interactions and vacuum polarization. It should also be emphasized that the expansion of the scattering amplitude in partial waves converges very slowly in the presence of the magnetic moment interactions. For explicit expressions and a detailed discussion on their implementation when calculating nucleon-nucleon observables the reader is referred to [10].

The deuteron wave function and binding energy E_d are obtained from the homogeneous part of Eq. (2.6):

$$\phi_l(p) = \frac{1}{E_d - p^2/m} \sum_{l'} \int_0^\infty \frac{dp' p'^2}{(2\pi)^3} V_{ll'}^{sj}(p, p') \phi_{l'}(p'), \quad (2.10)$$

where $s = j = 1$, $l = l' = 0, 2$. Once phase shifts are calculated, nucleon-nucleon scattering observables can be computed in a standard way, see [11, 12].

The appearance of only a few structures in the most general expression for the two-nucleon force, see Eq. (2.3), and the large amount of available low-energy nucleon-nucleon scattering data motivated and enabled the development of modern high-precision phenomenological potential models such as e.g. the CD-Bonn 2000 [13], Argonne V_{18} (AV18) [14] and Nijmegen I, II potentials [15]. The general strategy involves incorporating the proper long-range behavior due to the electromagnetic interaction and the one-pion exchange potential which is important to correctly describe the low-energy behavior of the amplitude, cf. section 4.2, and parametrizing the medium- and short-range contributions in a general way. AV18, a local r -space potential, can be viewed as a representative example. It includes (i) electromagnetic interactions multiplied by short-range functions to account for the finite size of the nucleon, (ii) regularized one-pion exchange potential including isospin-breaking corrections due to different masses of the charged and neutral pions, (iii) some additional phenomenological isospin-breaking terms of a shorter range, (iv) medium-range (short-range) contributions of Yukawa-type (Woods-Saxon type) multiplying the operators in Eq. (2.2). With about 40 adjustable parameters, it describes the proton-proton and neutron-proton scattering data with $\chi_{\text{datum}}^2 = 1.09$. Other high-precision potentials are constructed in a similar way and allow to reproduce the data or phase shifts from e.g. the Nijmegen

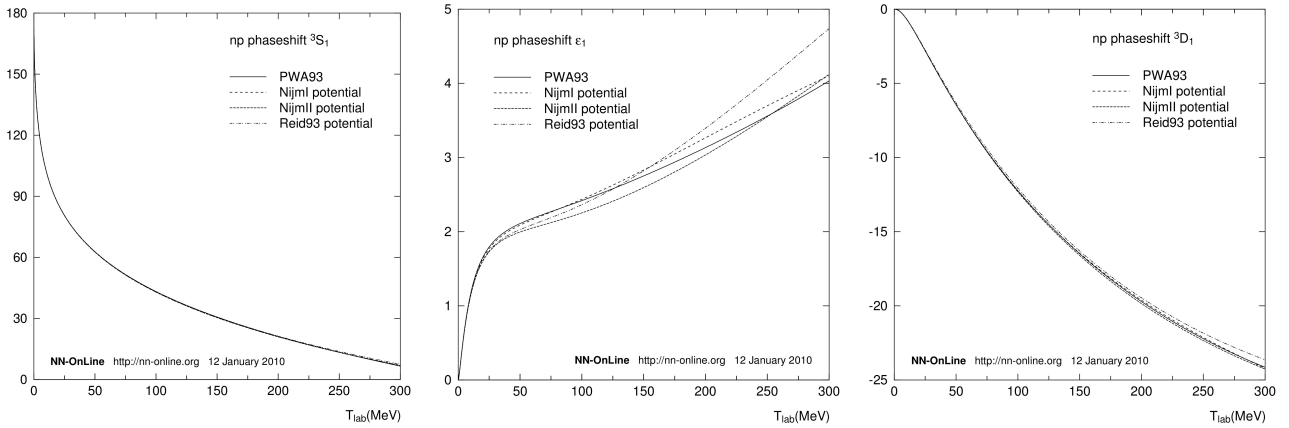


Figure 1: 3S_1 (left panel) and 3D_1 (right panel) phase shifts and the mixing angle ϵ_1 (middle panel) calculated from several modern high-precision potentials in comparison with the results of the Nijmegen PWA. The phase shifts and the mixing angle are shown in degrees. Plots are generated through the NN-Online web site <http://nn-online.org>.

partial wave analysis (PWA) with a comparable accuracy. This is visualized in Fig.1. I refer the reader to Ref. [16] for a recent review article on the modern high-precision potentials.

While various phenomenological potentials provide an accurate representation of the nucleon-nucleon phase shifts and most of the deuteron properties, the situation is much less satisfactory when it comes to the much weaker but necessary three-nucleon forces. Such three-body forces are needed to describe the nuclear binding energies and levels, as most systematically shown by the Urbana-Argonne group [17]. Systematic studies of the dynamics and reactions of systems with three or four-nucleons further sharpen the case for the necessity of including three-nucleon forces, see e.g. [18]. A phenomenological path to modeling the three-nucleon force following the same strategy as in the two-nucleon case seems to be not feasible (at least, at present). Indeed, in the case of two nucleons, the potential can be decomposed in only a few different spin-space structures, and the corresponding radial functions can be adjusted to the extensive set of data. Such an approach would, however, fail for the three-nucleon force due to the large variety of different possible structures, a scarcer data base and considerably more time consuming calculations required.

While the conventional approach based on the high-precision two-nucleon potentials accompanied with the existing three-nucleon force models enjoyed many successes and is frequently used in e.g. nuclear structure and reaction calculations, it remains incomplete as there are certain deficiencies that can only be overcome based on EFT approaches. These are: (i) it is very difficult - if not impossible - to assign a trustworthy theoretical error, (ii) gauge and chiral symmetries are difficult to implement, (iii) none of the three-nucleon forces is consistent with the underlying nucleon-nucleon interaction models/approaches and (iv) the connection to QCD is not at all obvious.

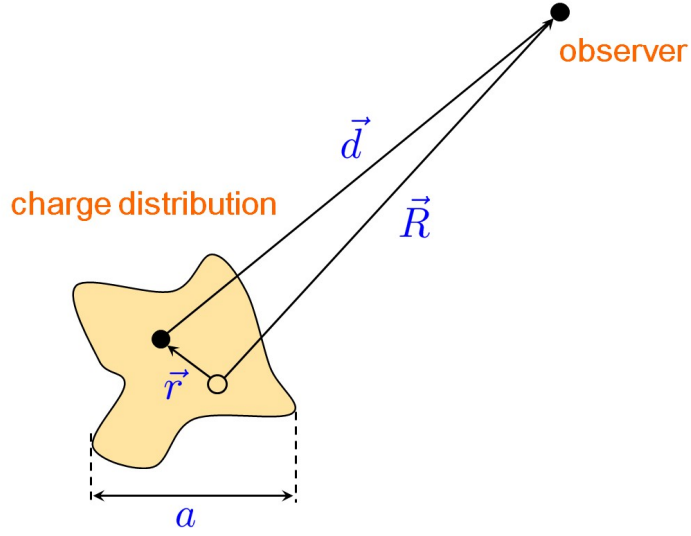


Figure 2: A localized charge distribution generates an electrostatic potential which can be described in terms of the multipole expansion.

3 Chiral perturbation theory: An elementary introduction

Effective field theories have proved to be an important and very useful tool in nuclear and particle physics. One understands under an effective (field) theory an approximate theory whose scope is to describe phenomena which occur at a chosen length (or energy) range. The main idea of this method can be illustrated with the following example from classical electrodynamics. Consider a localized charge distribution in space of a size a . The resulting electrostatic potential at any given position \vec{R} can be calculated by integrating over the elementary charges and using the familiar expression for the Coulomb potential generated by a point charge:

$$V(\vec{R}) \propto \int d^3r \frac{\rho(\vec{r})}{|\vec{R} - \vec{r}|} \quad (3.11)$$

Expanding $1/|\vec{R} - \vec{r}|$ for $r \ll R$,

$$\frac{1}{|\vec{R} - \vec{r}|} = \frac{1}{R} + \sum_i r_i \frac{R_i}{R^3} + \frac{1}{2} \sum_{ij} r_i r_j \frac{3R_i R_j - \delta_{ij} R^2}{R^5} + \dots, \quad (3.12)$$

with i, j denoting the Cartesian components allows to rewrite the integral as

$$\int d^3r \frac{\rho(\vec{r})}{|\vec{R} - \vec{r}|} = \frac{q}{R} + \frac{1}{R^3} \sum_i R_i P_i + \frac{1}{6R^5} \sum_{ij} (3R_i R_j - \delta_{ij} R^2) Q_{ij} + \dots \quad (3.13)$$

where the total charge q , dipole moment P_i and quadrupole moment Q_{ij} are defined via

$$q = \int d^3r \rho(\vec{r}), \quad P_i = \int d^3r \rho(\vec{r}) r_i, \quad Q_{ij} = \int d^3r \rho(\vec{r}) (3r_i r_j - \delta_{ij} r^2). \quad (3.14)$$

The expression in Eq. (3.13) represents the well-known multipole expansion for the electrostatic potential. When truncated, it provides an approximation to the “underlying theory” given by the exact expression (3.11). The multipoles entering every term in this expansion contain certain amount of information about the charge distribution and can, of course, be calculated provided $\rho(\vec{r})$ is known. The multipole expansion is, however, particularly useful if $\rho(\vec{r})$ is unknown (except for the fact that it is localized). It then allows to describe the electrostatic potential at every point in space far from the charge distribution with, in principle, an arbitrarily high accuracy provided one has enough data (e.g. experimentally measured values of the electrostatic potential at some points) to determine the desired number of the multipoles.

Chiral Perturbation Theory (CHPT) is the effective theory of QCD (more generally, of the Standard Model) which was formulated by Weinberg [19] and developed in to a systematic tool for analyzing low-energy hadronic observables by Gasser and Leutwyler [20, 21]. In this section, I give a brief overview of the foundations of this approach. My main purpose here is to outline the logical steps which are needed in order to set up this theoretical framework. I will also give references to the existing extensive literature on this subject which is suitable for further reading.

3.1 Chiral symmetry of QCD

Symmetries provide powerful constraints on effective interactions and thus play the crucial role for effective field theories. In the following, I will discuss the symmetries of QCD which are relevant in the context of ChPT. Consider the QCD Lagrangian in the two-flavor case of the light up and down quarks

$$\mathcal{L}_{\text{QCD}} = \bar{q} (i\gamma_\mu D^\mu - \mathcal{M}) q - \frac{1}{4} G_{\mu\nu}^a G^{a\mu\nu}, \quad (3.15)$$

where $D_\mu = \partial_\mu - ig_s G_\mu^a T^a$ with T^a , (with $a = 1 \dots 8$) are the $\text{SU}(3)_{\text{color}}$ Gell-Mann matrices and q the quark fields. Further, $G_{\mu\nu}^a$ are the gluon field strength tensors, and the quark mass matrix is given by $\mathcal{M} = \text{diag}(m_u, m_d)$. I do not show in Eq. (3.15) the θ - and gauge fixing terms which are not relevant for our consideration. It is instructive to write the QCD Lagrangian in terms of the left- and right-handed quark field components defined by $q_R = (1/2)(1 + \gamma_5)q$, $q_L = (1/2)(1 - \gamma_5)q$:

$$\mathcal{L}_{\text{QCD}} = \bar{q}_L i \not{D} q_L + \bar{q}_R i \not{D} q_R - \bar{q}_L \mathcal{M} q_R - \bar{q}_R \mathcal{M} q_L - \frac{1}{4} G_{\mu\nu}^a G^{a\mu\nu}. \quad (3.16)$$

We see that the left- and right-handed quark fields are only connected through the mass term. Given the smallness of the light quark masses [22]¹,

$$m_u \simeq 1.5 \dots 3.3 \text{ MeV}, \quad m_d \simeq 3.5 \dots 6.0 \text{ MeV}, \quad (3.17)$$

¹The following values correspond to the $\overline{\text{MS}}$ scheme at scale $\mu = 2 \text{ GeV}$.

as compared to the typical hadron masses of the order of 1 GeV, the quark mass term can, to a good approximation, be neglected. The Lagrangian in Eq. (3.16) is, therefore, approximately invariant under independent global flavor rotations of the left- and right-handed quark fields:

$$q_L \longrightarrow q'_L = L q_L = \exp(-i\boldsymbol{\theta}_L \cdot \boldsymbol{\tau}/2) q_L, \quad q_R \longrightarrow q'_R = R q_R = \exp(-i\boldsymbol{\theta}_R \cdot \boldsymbol{\tau}/2) q_R, \quad (3.18)$$

where $\boldsymbol{\tau}$ denote the Pauli matrices in the flavor space and $\boldsymbol{\theta}_{L,R}$ are the corresponding rotation angles. The corresponding symmetry group $SU(2)_L \times SU(2)_R$ is referred to as the $SU(2)$ chiral group. According to Noether's theorem, there are six conserved currents

$$L_\mu^i = \bar{q}_L \gamma_\mu \frac{\tau^i}{2} q_L, \quad R_\mu^i = \bar{q}_R \gamma_\mu \frac{\tau^i}{2} q_R, \quad (3.19)$$

which can equally well be expressed in terms of the vector and axial-vector currents $V_\mu^i = L_\mu^i + R_\mu^i$ and $A_\mu^i = R_\mu^i - L_\mu^i$. The corresponding conserved charges generate the algebra of the chiral group

$$[Q_I^i, Q_I^j] = i\epsilon^{ijk} Q_I^k \quad \text{with } I = L, R, \quad [Q_L^i, Q_R^j] = 0, \quad (3.20)$$

or, equivalently,

$$[Q_V^i, Q_V^j] = i\epsilon^{ijk} Q_V^k, \quad [Q_A^i, Q_A^j] = i\epsilon^{ijk} Q_A^k, \quad [Q_V^i, Q_A^j] = i\epsilon^{ijk} Q_A^k. \quad (3.21)$$

Application of the above commutation relations to hadronic reactions was at the heart of the current algebra calculations in the early seventies of the last century.

The Lagrangian for massless u- and d-quarks is, in fact, invariant under even a larger group of transformations in the flavor space, namely $SU(2)_L \times SU(2)_R \times U(1)_V \times U(1)_A$. While the vector $U(1)$ corresponds to quark number conservation, the axial $U(1)_A$ current is known to be broken by quantum effects (the so-called $U(1)_A$ anomaly) and thus does not represent a symmetry of the quantum theory.

In spite of the fact that QCD for two light flavors is approximately chiral invariant, its ground state is not symmetric with respect to $SU(2)_L \times SU(2)_R$ but only with respect to its vector subgroup $SU(2)_V \subset SU(2)_L \times SU(2)_R$ generated by the charges $\{Q_V^i\}$. This means that the axial charges do not annihilate the vacuum, that is $Q_V^i|0\rangle = 0$ while $Q_A^i|0\rangle \neq 0$. Evidence of the spontaneous breakdown of the chiral symmetry comes from various sources. For example, hadrons occur in nearly degenerate isospin multiplets corresponding to $SU(2)_V$ which implies that this group is realized in the usual Wigner-Weyl mode. If this were the case for the chiral group, one would observe larger chiral multiplets containing particles of opposite parity since the charges Q_V^i and Q_A^i have opposite parity. Generally, no such parity doubling is observed in the hadron spectrum. Another strong argument in favor of the spontaneous breakdown of the chiral symmetry comes from the existence of unnaturally light (in comparison with other hadrons) pseudoscalar mesons (pions) being natural candidates for the corresponding Nambu-Goldstone bosons. Pions are not exactly massless but acquire a small mass due to the explicit chiral symmetry breaking by the nonvanishing quark masses. These and further arguments coming from both the theory and experiment indicate undoubtedly that the chiral $SU(2)_L \times SU(2)_R$ group is spontaneously broken down to $SU(2)_V$.

I now pause to summarize the content of this section. QCD Lagrangian in the two-flavor case of the up- and down-quarks is approximately invariant under global chiral $SU(2)_L \times SU(2)_R$ transformations. The chiral symmetry is broken explicitly due to the nonvanishing quark masses, $m_u \neq 0$, $m_d \neq 0$. In addition to this explicit symmetry breaking, $SU(2)_L \times SU(2)_R$ is also broken spontaneously down to the isospin group $SU(2)_V$. The three corresponding pseudoscalar Goldstone bosons are identified with pions whose small masses emerge due to nonvanishing quark masses. There exist a large mass gap in the hadron spectrum: $M_\rho \simeq 770 \text{ MeV} \gg M_\pi \simeq 140 \text{ MeV}$.

3.2 Effective Lagrangian for Goldstone bosons

We now turn to the *effective* description of low-energy QCD dynamics. The simplest possible case emerges when the energy is chosen so small that only pions need to be treated as explicit degrees of freedom. All other hadrons are much heavier and can be integrated out from the theory. The main ingredient of any effective field theory is the most general effective Lagrangian that involves *all* possible terms which are consistent with the symmetries of the underlying theory. Let us, for the time being, consider the so-called chiral limit of QCD, i.e. the idealized world in which quarks are massless and the chiral symmetry of \mathcal{L}_{QCD} is exact. The task is then to construct the most general chiral invariant Lagrangian for pion fields. In order to do that we first need to figure out how pions transform with respect to chiral rotations. Our knowledge of the pion transformation properties with respect to $SU(2)_L \times SU(2)_R$ can be summarized by the following two observations:

- Pions build an isospin triplet and thus transform linearly under $SU(2)_V \subset SU(2)_L \times SU(2)_R$ according to the corresponding irreducible representation;
- The chiral group must be realized *nonlinearly*. This follows immediately from the geometrical argument based on the fact that the Lie algebra of $SU(2)_L \times SU(2)_R$ in Eq. (3.20) is isomorphic to that of $SO(4)$. We know that one needs three coordinates in order to construct the smallest nontrivial representation, the so-called fundamental representation, of the three-dimensional rotation group. Similarly, the smallest nontrivial representation of the four-dimensional rotation group $SO(4)$ is four-dimensional. We have, however, only three “coordinates” at our disposal (the triplet of the pion fields)!

To construct a non-linear realization of $SO(4)$ we begin with the usual representation describing four-dimensional rotations of a vector $(\boldsymbol{\pi}, \sigma) \equiv (\pi_1, \pi_2, \pi_3, \sigma)$. For an infinitesimal rotation parametrized by six angles $\{\theta_i^{V,A}\}$, with $i = 1, 2, 3$, we have:

$$\begin{pmatrix} \boldsymbol{\pi} \\ \sigma \end{pmatrix} \xrightarrow{SO(4)} \begin{pmatrix} \boldsymbol{\pi}' \\ \sigma' \end{pmatrix} = \left[\mathbf{1}_{4 \times 4} + \sum_{i=1}^3 \theta_i^V V_i + \sum_{i=1}^3 \theta_i^A A_i \right] \begin{pmatrix} \boldsymbol{\pi} \\ \sigma \end{pmatrix}, \quad (3.22)$$

where

$$\sum_{i=1}^3 \theta_i^V V_i = \begin{pmatrix} 0 & -\theta_3^V & \theta_2^V & 0 \\ \theta_3^V & 0 & -\theta_1^V & 0 \\ -\theta_2^V & \theta_1^V & 0 & 0 \\ 0 & 0 & 0 & 0 \end{pmatrix}, \quad \sum_{i=1}^3 \theta_i^A A_i = \begin{pmatrix} 0 & 0 & 0 & \theta_1^A \\ 0 & 0 & 0 & \theta_2^A \\ 0 & 0 & 0 & \theta_3^A \\ -\theta_1^A & -\theta_2^A & -\theta_3^A & 0 \end{pmatrix}. \quad (3.23)$$

Notice that the set of rotations generated by V_i builds a subgroup of $SO(4)$, namely the group of three-dimensional rotations $SO(3) \subset SO(4)$ which is locally isomorphic to $SU(2)$. The four real quantities $(\boldsymbol{\pi}, \sigma)$ define the smallest nontrivial chiral multiplet and represent the field content of the well-known linear sigma model. To switch from the above linear realization (i.e. representation) of $SO(4)$ to the nonlinear one, we observe that, in fact, only three of the four components of $(\boldsymbol{\pi}, \sigma)$ are independent with respect to four-dimensional rotations. These three independent components correspond to coordinates on a four-dimensional sphere since $\boldsymbol{\pi}$ and σ are subject to the constraint

$$\boldsymbol{\pi}^2 + \sigma^2 = F^2, \quad (3.24)$$

where F is a constant of dimension mass. Making use of this equation to eliminate σ in Eq. (3.22) we end up with the following transformation properties of $\boldsymbol{\pi}$ under $SO(4)$:

$$\begin{aligned} \boldsymbol{\pi} &\xrightarrow{\theta^V} \boldsymbol{\pi}' = \boldsymbol{\pi} + \boldsymbol{\theta}^V \times \boldsymbol{\pi}, \\ \boldsymbol{\pi} &\xrightarrow{\theta^A} \boldsymbol{\pi}' = \boldsymbol{\pi} + \boldsymbol{\theta}^A \sqrt{F^2 - \boldsymbol{\pi}^2}, \end{aligned} \quad (3.25)$$

where $\boldsymbol{\theta}^{V,A} \equiv \{\theta_i^{V,A}\}$ with $i = 1, 2, 3$. The nonlinear terms (in $\boldsymbol{\pi}$) on the right-hand side of the second equation give rise to the nonlinear realization of $SO(4)$. This is exactly what we wanted to achieve: the chiral group $SU(2)_L \times SU(2)_R \simeq SO(4)$ is realized nonlinearly on the triplet of pions which, however, transform linearly under isospin $SU(2)_V \simeq SO(3)$ rotations parametrized through the angles $\{\boldsymbol{\theta}_V\}$.

As a last remark note that the four-dimensional rotations of $(\boldsymbol{\pi}, \sigma)$ can be conveniently written using the 2×2 matrix notation by introducing the unitary matrix²

$$U = \frac{1}{F} (\sigma \mathbf{1}_{2 \times 2} + i \boldsymbol{\pi} \cdot \boldsymbol{\tau}), \quad (3.26)$$

and demanding the transformation properties of U under chiral rotations to be:

$$U \longrightarrow U' = LUR^\dagger. \quad (3.27)$$

Here, L and R are $SU(2)_L \times SU(2)_R$ matrices defined in Eq. (3.18).

Exercise: verify that infinitesimal transformations of $(\boldsymbol{\pi}, \sigma)$ induced by Eq. (3.27) with $\boldsymbol{\theta}^V = (\boldsymbol{\theta}_R + \boldsymbol{\theta}_L)/2$ and $\boldsymbol{\theta}^A = (\boldsymbol{\theta}_R - \boldsymbol{\theta}_L)/2$ have indeed the same form as the ones given in Eq. (3.22).

²For U to be unitary, σ and $\boldsymbol{\pi}$ have to fulfill Eq. (3.24).

Clearly, the transition to the nonlinear realization is achieved by

$$U = \frac{1}{F} (\sigma \mathbf{1}_{2 \times 2} + i \boldsymbol{\pi} \cdot \boldsymbol{\tau}) \longrightarrow U = \frac{1}{F} \left(\sqrt{F^2 - \boldsymbol{\pi}^2} \mathbf{1}_{2 \times 2} + i \boldsymbol{\pi} \cdot \boldsymbol{\tau} \right), \quad (3.28)$$

leaving pions as the only remaining degrees of freedom. Notice that the ground state of the theory is characterized by a vanishing vacuum expectation values of $\boldsymbol{\pi}$ and corresponds to a particular point on the considered four-dimensional sphere (one of two crossing points between the sphere and the σ -axis). In accordance with the spontaneous breaking of chiral symmetry, it is not $SO(4)$ - but only $SO(3) \simeq SU(2)_V$ -invariant.

It is now a simple exercise to construct the most general chiral-invariant Lagrangian for pions in terms of the matrix U . The building blocks are given by U , U^\dagger and derivatives of these quantities. Notice that since I consider here only global chiral rotations, i.e. L and R do not depend on space-time, the quantities like e.g. $\partial_\mu \partial_\nu U$ transform in the same way as U itself, i.e. according to Eq. (3.27). Chiral invariant terms in the effective Lagrangian can be constructed by taking a trace over products of U , U^\dagger and their derivatives. Lorentz invariance implies that the number of derivatives must be even, so that the effective Lagrangian can be written as

$$\mathcal{L}_\pi = \mathcal{L}_\pi^{(2)} + \mathcal{L}_\pi^{(4)} + \dots \quad (3.29)$$

Notice that $\mathcal{L}_\pi^{(0)}$ is simply a constant since $UU^\dagger = \mathbf{1}_{2 \times 2}$. The lowest-order Lagrangian involves just a single term

$$\mathcal{L}_\pi^{(2)} = \frac{F^2}{4} \langle \partial_\mu U \partial^\mu U^\dagger \rangle, \quad (3.30)$$

where $\langle \dots \rangle$ denotes the trace in the flavor space. Terms involving $\partial_\mu \partial^\mu U$ or $\partial_\mu \partial^\mu U^\dagger$ are not independent and can be brought to the form of Eq. (3.30) by using partial integration. The constant $F^2/4$ ensures that the Lagrangian has a proper dimension (both F and π have a dimension of mass) and is chosen in such a way that Eq. (3.30) matches the usual free Lagrangian for massless scalar field when written in terms of pions:

$$\mathcal{L}_\pi^{(2)} = \frac{1}{2} \partial_\mu \boldsymbol{\pi} \cdot \partial^\mu \boldsymbol{\pi} + \frac{1}{2F^2} (\partial_\mu \boldsymbol{\pi} \cdot \boldsymbol{\pi})^2 + \mathcal{O}(\pi^6). \quad (3.31)$$

The a-priori unknown constants that accompany the terms in the effective Lagrangian are commonly called the low-energy constants (LECs), cf. the multipoles in Eq. (3.13). The LEC F can be identified with the pion decay constant in our idealized world (with quark masses being set to zero) [20]. In the real world, it is measured to be $F_\pi = 92.4$ MeV. Notice further that the pions are massless in the idealized world. Higher-order Lagrangians $\mathcal{L}_\pi^{(4)}$, $\mathcal{L}_\pi^{(6)}$, \dots , can be constructed along the same lines by using partial integration and equations of motion to eliminate the redundant terms.

Let us now pause to summarize what has been achieved so far. We have explicitly constructed a particular nonlinear realization of $SU(2)_L \times SU(2)_R$ in terms of pion fields which, as desired, build a representation of $SU(2)_V \subset SU(2)_L \times SU(2)_R$ and learned how to write down the most general possible effective Lagrangian. The constructed nonlinear realization of the chiral group is, however, not unique. Different realizations emerge by choosing different parametrizations of the matrix U in Eq. (3.27) in

terms of pion fields such as, for example, the exponential parametrization $U = \exp(i\boldsymbol{\pi} \cdot \boldsymbol{\tau}/F)$. Generally, only the first three terms in the expansion of U in powers of the pion field are fixed by unitarity,

$$U(\boldsymbol{\pi}) = \mathbf{1}_{2 \times 2} + i \frac{\boldsymbol{\tau} \cdot \boldsymbol{\pi}}{F} - \frac{\boldsymbol{\pi}^2}{2F^2} - i\alpha \frac{\boldsymbol{\pi}^2 \boldsymbol{\tau} \cdot \boldsymbol{\pi}}{F^3} + (8\alpha - 1) \frac{\boldsymbol{\pi}^4}{8F^4} + \mathcal{O}(\boldsymbol{\pi}^5). \quad (3.32)$$

Here, α is an arbitrary constant which reflects the freedom in parametrizing the matrix U . This raises the concern that observables that one intends to compute in the EFT are possibly affected by this non-uniqueness which would be a disaster. Fortunately, this is not the case. As shown by Coleman, Callan, Wess and Zumino [23, 24], all realizations of the chiral group are equivalent to each other modulo nonlinear field redefinitions

$$\pi_i \rightarrow \pi'_i = \pi_i F[\boldsymbol{\pi}] \quad \text{with} \quad F[\mathbf{0}] = 1. \quad (3.33)$$

According to Haag's theorem [25], such nonlinear field redefinitions do not affect S-matrix elements.

So far, I considered the chiral limit corresponding to the idealized world with the masses of the up- and down-quarks being set to zero. This is fine as a first approximation but, of course, one would like to systematically improve on it by taking into account corrections due to nonvanishing quark masses. For that, we have to include in the effective Lagrangian all possible terms which break chiral symmetry in exactly the same way as does the quark mass term in \mathcal{L}_{QCD} . Consider, for example, the quark mass term with $m_u = m_d = m_q \neq 0$ which breaks chiral but preserves isospin symmetry. Recalling the geometrical interpretation with the four-dimensional rotation group and coordinates $(\boldsymbol{\pi}, \sigma)$, the quark mass term can be viewed as a vector that points along the $(\mathbf{0}, \sigma)$ -direction. Its effects can be systematically taken into account by including in the effective Lagrangian not only $SO(4)$ -scalars but also the corresponding components of all possible $SO(4)$ -tensors and multiplying the resulting terms by the appropriate powers of m_q , see [26] for more details and the explicit construction along these lines. A simpler (but equivalent) method makes use of the following trick. Consider the massless QCD Lagrangian in the presence of an external hermitian scalar field s interacting with the quarks via the term $-\bar{q}s q$. The resulting Lagrangian is chiral invariant provided the scalar source s transforms under chiral rotations according to:

$$s \rightarrow s' = LsR^\dagger = RsL^\dagger, \quad (3.34)$$

where the second equality follows from the hermiticity of s . To recover QCD from the new theory, the external field needs to be set to the value $s = \mathcal{M}$. To account for the explicit chiral symmetry breaking, we first write down the effective Lagrangian for the new theory by listing all possible chiral invariant terms constructed from s and (derivatives of) U and U^\dagger and then set $s = \mathcal{M}$. Since the quark masses are treated as a small perturbation, the leading symmetry-breaking terms should contain a minimal possible number of derivatives and just one insertion of s . Given that $U \rightarrow U^\dagger$ under parity transformation, there exist only one symmetry-breaking term without derivatives:

$$\mathcal{L}_{SB} = \frac{F^2 B}{2} \langle sU + sU^\dagger \rangle \Big|_{s=\mathcal{M}} = F^2 B(m_u + m_d) - \frac{B}{2}(m_u + m_d)\boldsymbol{\pi}^2 + \mathcal{O}(\boldsymbol{\pi}^4), \quad (3.35)$$

where B is a LEC. The first term is a constant and does not contribute to the S -matrix. The second one gives rise to the pion mass $-(1/2)M^2\boldsymbol{\pi}^2$ with $M^2 = (m_u + m_d)B$. Note that to leading order

in $m_{u,d}$, one has equal masses for all pions π^+ , π^- and π^0 . Further, the LEC B can be shown to be related to the quark condensate according to $\langle 0|\bar{u}u|0\rangle = \langle 0|\bar{d}d|0\rangle = -F_\pi^2 B(1 + \mathcal{O}(\mathcal{M}))$ [20]. Modulo corrections of higher order in the quark masses, the experimentally measured pion mass M_π coincides with M : $M_\pi^2 = M^2 + \mathcal{O}(m_q^2)$.

How important are chiral-symmetry breaking terms as compared to chiral-invariant ones? When constructing the most general chiral-invariant effective Lagrangian, various terms were classified according to the number of derivatives. When calculating observables, the derivatives acting on pion fields generate powers of external momenta which are assumed to be low. The EFT considered so far is typically applied to processes characterized by pion momenta of the order of the pion mass.³ It is, therefore, natural to count the pion mass in the effective Lagrangian on the same footing as a derivative. We thus end up with the following lowest-order Lagrangian:

$$\mathcal{L}_\pi^{(2)} = \frac{F^2}{4} \langle \partial_\mu U \partial^\mu U^\dagger + 2B(\mathcal{M}U + \mathcal{M}U^\dagger) \rangle. \quad (3.36)$$

For the sake of completeness, the next-higher order Lagrangian reads [20]:

$$\begin{aligned} \mathcal{L}_\pi^{(4)} &= \frac{l_1}{4} \langle \partial_\mu U \partial^\mu U^\dagger \rangle^2 + \frac{l_2}{4} \langle \partial_\mu U \partial_\nu U^\dagger \rangle \langle \partial^\mu U \partial^\nu U^\dagger \rangle + \frac{l_3}{16} \langle 2B\mathcal{M}(U + U^\dagger) \rangle^2 + \dots \\ &- \frac{l_7}{16} \langle 2B\mathcal{M}(U - U^\dagger) \rangle^2, \end{aligned} \quad (3.37)$$

where the ellipses refer to terms that involve external sources and the l_i are the corresponding LECs.

3.3 Power counting

Having constructed the most general effective Lagrangian for pions in harmony with the chiral symmetry of QCD, we now need to figure out how to compute observables. At first sight, the effective Lagrangian seems to be of less practical value due to an infinite number of the unknown LECs. Even worse, all interaction terms entering \mathcal{L}_π are non-renormalizable in the usual sense⁴ contrary to field theories such as e.g. QED and QCD. What at first sight appears to cause a problem, namely non-renormalizability of the theory, in fact, turns out to be a crucial feature for the whole approach to be useful. As demonstrated in the seminal paper by Weinberg [19], the effective Lagrangian \mathcal{L}_π can be used to compute low-energy observables (such as e.g. scattering amplitudes) in a systematically improvable way via an expansion in powers of Q/Λ_χ , where Q represents the soft scale associated with external momenta or the pion mass M_π while Λ_χ , the so-called chiral-symmetry-breaking scale, is the hard scale that drives the LECs in \mathcal{L}_π . This expansion is referred to as the chiral expansion, and the whole approach carries the name of chiral perturbation theory. Consider an arbitrary multi-pion scattering process with all initial and final pion momenta of the order of M_π . In order to decide on the importance of a particular Feynman diagram, we have to determine the power of the soft scale associated with it. For that we

³For an example of EFT in a different kinematical regime with nonrelativistic mesons see [27].

⁴This implies that the structure of local ultraviolet divergences generated by loop diagrams with vertices from $\mathcal{L}_\pi^{(2)}$ is different from $\mathcal{L}_\pi^{(2)}$.



Figure 3: Tadpole contribution from $\mathcal{L}_\pi^{(2)}$ (left) and tree contribution from $\mathcal{L}_\pi^{(4)}$ (right) to the pion self energy.

first need to clarify an important issue related to the counting of virtual momenta which are being integrated over in the loop integrals. What scale do we associate with such virtual momenta? When calculating Feynman diagrams in ChPT, one generally encounters two kinds of loop integrals. First, there are cases in which the integrand dies out fast enough when the loop momenta go to infinity so that the corresponding integrals are well-defined. Since the hard scale only enters the LECs and thus factorizes out, the integrands involve only soft scales (external momenta and the pion mass) and the loop momenta. Given that the integration is carried over the whole range of momenta, the resulting mass dimension of the integral is obviously driven by the soft scales. Thus, in this case we can safely count all virtual momenta as the soft scale. The second kind of integrals involves ultraviolet divergences and requires regularization and renormalization. Choosing renormalization conditions in a suitable way, one can ensure that virtual momenta are (effectively) of the order of the soft scale. This is achieved automatically if one uses a mass-independent regularization such as e.g. dimensional regularization (DR). Consider, for example, the integral

$$I = \int \frac{d^4 l}{(2\pi)^4} \frac{i}{l^2 - M^2 + i\epsilon}, \quad (3.38)$$

that enters the pion self energy due to the tadpole diagram shown in Fig. 3. Evaluating this quadratically divergent integral in dimensional regularization one obtains

$$I \rightarrow I^{\text{reg}} = \mu^{4-d} \int \frac{d^d l}{(2\pi)^d} \frac{i}{l^2 - M^2} = \frac{M^2}{16\pi^2} \ln \left(\frac{M^2}{\mu^2} \right) + 2M^2 L(\mu) + \mathcal{O}(d-4), \quad (3.39)$$

where γ_E is the Euler constant and μ is the scale introduced by dimensional regularization and the quantity $L(\mu)$ is given by

$$L(\mu) = \frac{\mu^{d-4}}{16\pi^2} \left\{ \frac{1}{d-4} - \frac{1}{2}(\ln(4\pi) + \Gamma'(1) + 1) \right\}, \quad \Gamma'(1) = -0.577215\dots \quad (3.40)$$

The second term on the right-hand side of the above expression diverges in the limit $d \rightarrow 4$ but can be absorbed into an appropriate redefinition of the LECs in $\mathcal{L}_\pi^{(4)}$ (renormalization). Notice that, as desired, the mass dimension of the finite term is driven by the soft scale M . I further emphasize that the scale μ introduced by dimensional regularization has to be chosen of the order $\mu \sim M_\pi$ in order to prevent the appearance of large logarithms in DR expressions. Last but not least, note that one can, in principle, use different regularization methods such as e.g. cutoff regularization provided

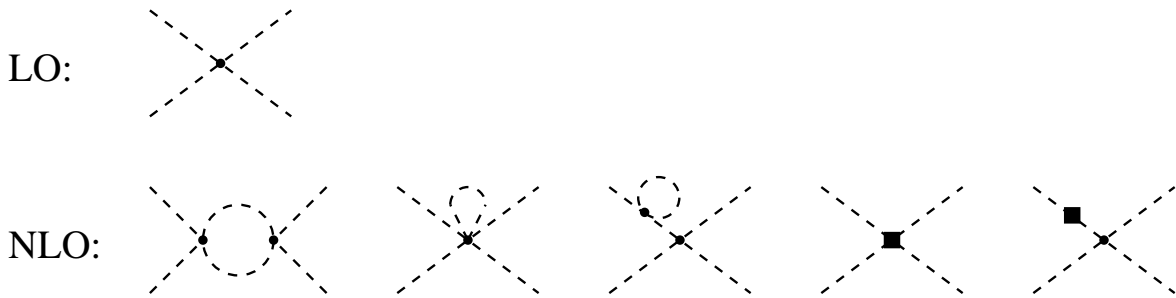


Figure 4: Diagrams contributing to pion-pion scattering in at leading- and next-to-leading order in ChPT. Solid dots and filled rectangles represent vertices from $\mathcal{L}_\pi^{(2)}$ and $\mathcal{L}_\pi^{(4)}$, respectively.

they respect chiral symmetry.⁵ Contrary to dimensionally-regularized expressions, cutoff-regularized integrals do not scale properly i.e. their mass dimension is not generated exclusively by the soft scales. The renormalized expressions emerging after absorbing the positive powers and logarithms of the cutoff into an appropriate redefinition of the LECs do, however, feature the expected scaling behavior.

I am now in the position to discuss the chiral power counting, i.e. the expression that determines the power ν of the expansion parameter Q/Λ_χ for a given Feynman diagram. This can be achieved by carefully counting the powers of small momenta associated with derivatives entering the vertices in \mathcal{L}_π , pion propagators, integrations over the loop momenta and the δ -functions. Using certain topological identities, one obtains the following expression for the chiral dimension of a connected Feynman diagram:

$$\nu = 2 + 2L + \sum_i V_i \Delta_i, \quad \Delta_i = d_i - 2, \quad (3.41)$$

where L refers to the number of loops. This result has been first obtained by Weinberg in [19]. Notice that in order for perturbation theory to work, \mathcal{L}_π must contain no interactions with $\Delta_i \leq 0$ since, otherwise, adding new vertices would not increase or even lower the chiral dimension ν . This feature is guaranteed by the spontaneously broken chiral symmetry of QCD which ensures that only non-renormalizable interactions with at least two derivatives or powers of the pion mass appear in \mathcal{L}_π . In particular, chiral symmetry forbids the renormalizable derivative-less interaction of the type π^4 .

Consider now pion-pion scattering as an illustrative example. Eq. (3.41) tells us that the leading contribution to the scattering amplitude is generated by tree diagrams ($L = 0$) constructed from the lowest-order vertices with $\Delta_i = 0$ i.e. the ones from $\mathcal{L}_\pi^{(2)}$, see Fig. 4. The amplitude scales as Q^2 . The corrections result from one-loop graphs involving all vertices from $\mathcal{L}_\pi^{(2)}$ as well as tree graphs with a single insertion from $\mathcal{L}_\pi^{(4)}$, see Fig. 4. They appear at order Q^4 and are suppressed by two powers of momenta or one power of the quark masses compared to the leading-order contribution. It is easy to verify that all diagrams in the bottom line of this figure scale, indeed, as Q^4 . For example, for the first

⁵When cutoff regularization is used, a special care is required regarding the treatment of non-covariant pieces in the pion propagator, see. [28].

diagram, four powers of momenta arise from the vertices and another four powers of momenta emerge from the loop integration. One should further take into account four powers of momenta generated in the denominator by the pion propagators. Thus, the total power of the soft scale is indeed four. All ultraviolet divergences entering the loop integrals are local and absorbable into redefinition of the LECs in $\mathcal{L}_\pi^{(4)}$ (when using dimensional regularization), as it represents the most general, approximately chiral invariant, local interaction of Goldstone bosons at order Q^4 . The divergent parts of the LECs l_i have been worked out in [20] using the heat-kernel method. The finite parts of the l_i 's are not fixed by chiral symmetry and have to be determined from the data or lattice QCD calculations. In the Goldstone boson sector, even a number of two-loop calculations (i.e. at order Q^6) have already been performed, see Ref. [29] for a review article. In particular, an impressive theoretical prediction has been made for the isoscalar S-wave $\pi\pi$ scattering length a_0^0 by Colangelo et al. [30] who combined the two-loop calculation [31] with dispersion relations to predict $a_0^0 = 0.220 \pm 0.005$. To compare, the leading-order calculation by Weinberg yielded $a_0^0 = 0.16$ [32] while the next-to-leading value obtained by Gasser and Leutwyler is $a_0^0 = 0.20$ [20]. The results of the recent E865 experiment at Brookhaven [33] and the NA48/2 experiment at CERN [34] combined with the older measurement by the Geneva-Saclay collaboration beautifully confirmed the prediction of the two-loop analysis of Ref. [30] yielding the value $a_0^0 = 0.217 \pm 0.008$ (exp) ± 0.006 (th) [35]. This combined result accounts for isospin breaking corrections, see Ref. [35] for more details.

The procedure outlined above can, in principle, be extended to arbitrarily high orders in the low-energy expansion. Clearly, the accuracy of the calculations depends crucially on the value of the hard scale Λ_χ which sets the (maximal) radius of convergence of the chiral expansion. The ρ -meson is the first meson of the non-Goldstone type and shows up as a resonance in p-wave $\pi\pi$ scattering. Such resonances represent truly non-perturbative phenomena that cannot be described in standard ChPT⁶. Consequently, their appearance signals the breakdown of the chiral expansion. This leads to the estimation $\Lambda_\chi \sim M_\rho \simeq 770$ MeV. A related observation that matches naturally the above estimation was made by Manohar and Georgi who pointed out that Λ_χ cannot be larger than $4\pi F_\pi \simeq 1200$ MeV since this number sets the scale that controls the running of the renormalized LECs when shifting the renormalization point.

Last but not least, I would like to summarize and underline the special role and importance of the chiral symmetry for the whole approach. First of all, it implies severe constraints on the interactions in the effective Lagrangian and relates the strengths of various multi-pion vertices. For example, the leading-order Lagrangian $\mathcal{L}_\pi^{(2)}$ in Eq. (3.36) gives rise to infinitely many vertices, when expanded in powers of pion fields, whose strengths are determined by just two (!) LECs F and B . $\mathcal{L}_\pi^{(2)}$ allows to compute the leading contribution to scattering amplitudes for multi-pion processes and to relate the strengths of the corresponding matrix elements, thus featuring a remarkable predictive power. Moreover, as we saw through the explicit construction, the spontaneously broken chiral symmetry of QCD prevents the appearance of derivative-less interactions between pions in the effective Lagrangian. The only derivative-less interactions in \mathcal{L}_π are due to explicit chiral symmetry breaking in \mathcal{L}_{QCD} and are suppressed by powers of the light quark masses. When calculating S-matrix elements, the derivatives entering the vertices generate powers of external momenta. Consequently, the interaction

⁶For an extension of ChPT to the resonance region, the so-called unitarized ChPT, see [36] and references therein.

between pions becomes weak at vanishingly low energies and would even completely disappear if chiral symmetry were exact. This turns out to be a general feature of Goldstone bosons and is not restricted to the $SU(2)_L \times SU(2)_R$ group. This allows to compute low-energy hadronic observables in a systematic way via the chiral expansion, i.e. the dual expansion in powers of momenta and quark masses about the kinematical point corresponding to the free theory (assuming that the actual quark masses in the real world are low enough for such an expansion to converge).

3.4 Inclusion of nucleons

So far we only discussed interactions between Goldstone bosons. We now extend these considerations to include nucleons. More precisely, we are interested in describing reactions involving pions with external momenta of the order of M_π and (essentially) non-relativistic nucleons whose three-momenta are of the order of M_π . Similarly to the triplet of pion fields, the isospin doublet of the nucleon fields should transform nonlinearly under the chiral $SU(2)_L \times SU(2)_R$ but linearly under the vector subgroup $SU(2)_V$. The unitary matrix U introduced in Eq. (3.26) is less useful when constructing the Lagrangian involving the nucleons. It is more convenient to introduce its square root u , $U = u^2$. The transformation properties of u under chiral rotations can be read off from Eq. (3.27):

$$u \rightarrow u' = \sqrt{LuR^\dagger} \equiv Luh^{-1} = huR^\dagger, \quad (3.42)$$

where I have introduced the unitary matrix $h = h(L, R, U)$ given by $h = \sqrt{LU R^\dagger}^{-1} L \sqrt{U}$ which is sometimes referred to as a compensator field. The last equality in Eq. (3.42) follows from $U' = u' u' = Luh^{-1} u' = L u u R^\dagger$. Notice that since pions transform linearly under isospin rotations corresponding to $L = R = V$ with $U \rightarrow U' = V U V^\dagger$ and, accordingly, $u \rightarrow u' = V u V^\dagger$, the compensator field in this particular case becomes U -independent and coincides with V .

Exercise: calculate the explicit form of the compensator field $h(L, R, \pi)$ for infinitesimal chiral transformations using Eq. (3.32) and keeping only terms that are at most linear in the pion fields. Verify that h indeed reduces to the isospin transformation for $L = R = V$.

It can be shown that $\{U, N\}$ define a nonlinear realization of the chiral group if one demands that

$$N \rightarrow N' = h N. \quad (3.43)$$

I do not give here the proof of this statement and refer the interesting reader to Ref. [23, 24]. Moreover, this nonlinear realization obviously fulfills the desired feature that pions and nucleons transform linearly under isospin rotations. Similarly to the purely Goldstone boson case, one can show that all other possibilities to introduce the nucleon fields are identical with the above realization modulo nonlinear field redefinitions. The most general chiral invariant Lagrangian for pions and nucleons can be constructed from *covariantly* transforming building blocks, i.e. $O_i \rightarrow O'_i = h O_i h^{-1}$, by writing down all possible terms of the form $\bar{N} O_1 \dots O_n N$. The covariant (first) derivative of the pion field is given by

$$u_\mu \equiv iu^\dagger (\partial_\mu U) u^\dagger = -\frac{\tau \cdot \partial_\mu \pi}{F} + \mathcal{O}(\pi^3) \rightarrow u'_\mu = h u_\mu h^{-1}, \quad (3.44)$$



Figure 5: Leading pion loop contribution to the nucleon self energy. Solid line represents the nucleon.

and is sometimes referred to as chiral vielbein. The derivative of the nucleon field, $\partial_\mu N$, does not transform covariantly, i.e. $\partial_\mu N \rightarrow (\partial_\mu N)' \neq h \partial_\mu N$ since the compensator field h does, in general, depend on space-time (through its dependence on U). The covariant derivative of the nucleon field $D_\mu N$, $D_\mu N \rightarrow (D_\mu N)' = h D_\mu N$, is given by

$$D_\mu N \equiv (\partial_\mu + \Gamma_\mu)N, \quad \text{with} \quad \Gamma_\mu \equiv \frac{1}{2} \left(u^\dagger \partial_\mu u + u \partial_\mu u^\dagger \right) = \frac{i}{4F^2} \boldsymbol{\tau} \cdot \boldsymbol{\pi} \times \partial_\mu \boldsymbol{\pi} + \mathcal{O}(\pi^4). \quad (3.45)$$

The so-called connection Γ_μ can be used to construct higher covariant derivatives of the pion field, for example:

$$u_{\mu\nu} \equiv \partial_\mu u_\nu - [\Gamma_\mu, u_\nu]. \quad (3.46)$$

To first order in the derivatives, the most general pion-nucleon Lagrangian takes the form [37]

$$\mathcal{L}_{\pi N}^{(1)} = \bar{N} \left(i\gamma^\mu D_\mu - m + \frac{g_A}{2} \gamma^\mu \gamma_5 u_\mu \right) N, \quad (3.47)$$

where m and g_A are the bare nucleon mass and the axial-vector coupling constant and the superscript of $\mathcal{L}_{\pi N}$ denotes the power of the soft scale Q . Contrary to the pion mass, the nucleon mass does not vanish in the chiral limit and introduces an additional hard scale in the problem. Consequently, terms proportional to D_0 and m in Eq. (3.47) are individually large. It can, however, be shown that $(i\gamma^\mu D_\mu - m)N \sim \mathcal{O}(Q)$ [38]. The appearance of the additional hard scale associated with the nucleon mass invalidates the power counting for dimensionally regularized expressions since the contributions from loop integrals involving nucleon propagators are not automatically suppressed. To see this consider the correction to the nucleon mass m_N due to the pion loop shown in Fig. 5. Assuming that the nucleon and pion propagators scale as $1/Q$ and $1/Q^2$, respectively, and taking into account Q^4 from the loop integration and Q^2 from the derivatives entering the g_A -vertices, the pion loop contribution to the nucleon self energy $\Sigma(p)$ is expected to be of the order $\sim Q^3$. Consequently, the corresponding nucleon mass shift $\delta m_N = \Sigma(m_N)$ is expected to be $\propto M_\pi^3$ (since no other soft scale is left). Explicit calculation, however, shows that the resulting nucleon mass shift does not vanish in the chiral limit [37]:

$$\delta m_N|_{\text{loop, rel}} \stackrel{\mathcal{M} \rightarrow 0}{=} -\frac{3g_A^2 m^3}{F^2} \left(L(\mu) + \frac{1}{32\pi^2} \ln \frac{m^2}{\mu^2} \right) + \mathcal{O}(d-4), \quad (3.48)$$

where the quantity $L(\mu)$ is defined in Eq. (3.40). The result in Eq. (3.48) implies that the nucleon mass receives a contribution which is formally of the order $\sim m(m/4\pi F)^2$ and is not suppressed compared to m . The bare nucleon mass m that enters the lowest-order Lagrangian $\mathcal{L}_{\pi N}^{(1)}$ gets renormalized. This is in contrast to the purely mesonic sector where loop contributions are always suppressed by powers of

the soft scale and the parameters F and B in the lowest-order Lagrangian $L_\pi^{(2)}$ remain unchanged by higher-order corrections (if mass-independent regularization is used). I emphasize, however, that even though DR expressions do not automatically obey the dimensional power counting with nucleons being treated relativistically, the proper scaling in agreement with naive dimensional analysis can be restored via appropriately chosen renormalization conditions [39]. Stated differently, one can (and should in order for the EFT to be useful) choose renormalization conditions in such a way, that all momenta flowing through diagrams are effectively of the order of Q . Another, simpler way to ensure the proper power counting exploits the so-called heavy-baryon formalism [40, 41] which is closely related to the nonrelativistic expansion due to Foldy and Wouthuysen [42] and is also widely used in heavy-quark effective field theories. The idea is to decompose the nucleon four-momentum p^μ according to

$$p_\mu = mv_\mu + k_\mu, \quad (3.49)$$

with v_μ the four-velocity of the nucleon satisfying $v^2 = 1$ and k_μ its small residual momentum, $v \cdot k \ll m$. One can thus decompose the nucleon field N in to the velocity eigenstates

$$N_v = e^{imv \cdot x} P_v^+ N, \quad h_v = e^{imv \cdot x} P_v^- N, \quad (3.50)$$

where $P_v^\pm = (1 \pm \gamma_\mu v^\mu)/2$ denote the corresponding projection operators. In the nucleon rest-frame with $v_\mu = (1, 0, 0, 0)$, the quantities N_v and h_v coincide with the familiar large and small components of the free positive-energy Dirac field (modulo the modified time dependence). One, therefore, usually refers to N_v and h_v as to the large and small components of N . The relativistic Lagrangian $\mathcal{L}_{\pi N}^{(1)}$ in Eq. (3.47) can be expressed in terms of N_v and h_v as:

$$\mathcal{L}_{\pi N}^{(1)} = \bar{N}_v \mathcal{A} N_v + \bar{h}_v \mathcal{B} N_v + \bar{N}_v \gamma_0 \mathcal{B}^\dagger \gamma_0 h_v - \bar{h}_v \mathcal{C} h_v, \quad (3.51)$$

where

$$\mathcal{A} = i(v \cdot D) + g_A(S \cdot u), \quad \mathcal{B} = -\gamma_5 \left[2i(S \cdot D) + \frac{g_A}{2}(v \cdot u) \right], \quad \mathcal{C} = 2m + i(v \cdot D) + g_A(S \cdot u), \quad (3.52)$$

and $S_\mu = i\gamma_5 \sigma_{\mu\nu} v^\nu$ is the nucleon spin operator. One can now use the equations of motion for the large and small component fields to completely eliminate h_v from the Lagrangian. Utilizing the more elegant path integral formulation [43], the heavy degrees of freedom can be integrated out performing the Gaussian integration over the (appropriately shifted) variables h_v, \bar{h}_v . This leads to the effective Lagrangian of the form [41]

$$\mathcal{L}_{\pi N} = \bar{N}_v \left[\mathcal{A} + (\gamma_0 \mathcal{B}^\dagger \gamma_0) \mathcal{C}^{-1} \mathcal{B} \right] N_v = \bar{N}_v [i(v \cdot D) + g_A(S \cdot u)] N_v + \mathcal{O}\left(\frac{1}{m}\right). \quad (3.53)$$

Notice that the (large) nucleon mass term has disappeared from the Lagrangian, and the dependence on m in $\mathcal{L}_{\pi N}^{\text{eff}}$ resides entirely in new vertices suppressed by powers of $1/m$. The heavy-baryon propagator of the nucleon is simply $1/(v \cdot k + i\epsilon)$ and can be obtained from the $1/m$ expansion of the Dirac propagator using Eq. (3.49) and assuming $v \cdot k \ll m$:

$$\frac{\not{p} + m}{p^2 - m^2 + i\epsilon} = \frac{\Lambda_+}{v \cdot k + i\epsilon} + \mathcal{O}(m^{-1}), \quad (3.54)$$

where $\Lambda_+ = (\not{p} + m)/(2m)$ is a projection operator on the states of positive energy. The advantage of the heavy-baryon formulation (HBChPT) compared to the relativistic one can be illustrated using the previous example of the leading one-loop correction to the nucleon mass

$$\delta m_N|_{\text{loop, HB}} = -\frac{3g_A^2 M_\pi^3}{32\pi F^2}. \quad (3.55)$$

Contrary to the relativistic CHPT result in Eq. (3.48), the loop correction in HBChPT is finite (in DR) and vanishes in the chiral limit. The parameters in the lowest-order Lagrangian do not get renormalized due to higher-order corrections which are suppressed by powers of Q/Λ_χ . Notice further that Eq. (3.55) represents the leading contribution to the nucleon mass which is nonanalytic in quark masses. It agrees with the result obtained by Gasser et al. based on the relativistic Lagrangian in Eq. (3.47) [37]. In general, the power ν of a soft scale Q for connected contributions to the scattering amplitude can be read off from the extension of Eq. (3.41) to the single-nucleon sector which has the form:

$$\nu = 1 + 2L + \sum_i V_i \Delta_i, \quad \text{with} \quad \Delta_i = -2 + \frac{1}{2}n_i + d_i, \quad (3.56)$$

with n_i being the number of nucleon field operators at a vertex i with the chiral dimension Δ_i . Notice that no closed fermion loops appear in the heavy-baryon approach, so that exactly one nucleon line connecting the initial and final states runs through all diagrams in the single-baryon sector.

The heavy-baryon formulation outlined above can be straightforwardly extended to higher orders in the chiral expansion. At lowest orders in the derivative expansion, the effective Lagrangian \mathcal{L}^{Δ_i} for pions and nucleons takes the form [44]:

$$\begin{aligned} \mathcal{L}_{\pi N}^{(0)} &= \bar{N} [i v \cdot D + g_A u \cdot S] N, \\ \mathcal{L}_{\pi N}^{(1)} &= \bar{N} [c_1 \langle \chi_+ \rangle + c_2 (v \cdot u)^2 + c_3 u \cdot u + c_4 [S^\mu, S^\nu] u_\mu u_\nu + c_5 \langle \hat{\chi}_+ \rangle] N, \\ \mathcal{L}_{\pi N}^{(2)} &= \bar{N} \left[\frac{1}{2m} (v \cdot D)^2 - \frac{1}{2m} D \cdot D + d_{16} S \cdot u \langle \chi_+ \rangle + i d_{18} S^\mu [D_\mu, \chi_-] + \dots \right] N, \\ \mathcal{L}_{\pi NN}^{(0)} &= -\frac{1}{2} C_S (\bar{N} N) (\bar{N} N) + 2 C_T (\bar{N} S N) \cdot (\bar{N} S N), \\ \mathcal{L}_{\pi NN}^{(1)} &= \frac{D}{2} (\bar{N} N) (\bar{N} S \cdot u N), \\ \mathcal{L}_{\pi NN}^{(2)} &= -\tilde{C}_1 [(\bar{N} D N) \cdot (\bar{N} D N) + ((D \bar{N}) N) \cdot ((D \bar{N}) N)] \\ &\quad - 2(\tilde{C}_1 + \tilde{C}_2) (\bar{N} D N) \cdot ((D \bar{N}) N) - \tilde{C}_2 (\bar{N} N) \cdot [(D^2 \bar{N}) N + \bar{N} D^2 N] + \dots, \\ \mathcal{L}_{\pi NNN}^{(1)} &= -\frac{E}{2} (\bar{N} N) (\bar{N} \boldsymbol{\tau} N) \cdot (\bar{N} \boldsymbol{\tau} N). \end{aligned} \quad (3.57)$$

Here, the ellipses refer to terms which do not contribute to the nuclear forces up to next-to-next-to-leading order (N²LO) except for $\mathcal{L}_{\pi NN}^{(2)}$ where I have shown only a few terms in order to keep the presentation compact. Further, here and in what follows I omit the subscript v of the nucleon field operators. The quantity $\chi_+ = u^\dagger \chi u^\dagger + u \chi^\dagger u$ with $\chi = 2B\mathcal{M}$ involves the explicit chiral symmetry

breaking due to the finite light quark masses and $\tilde{O} \equiv O - \langle O \rangle/2$. Finally, c_i , d_i , C_i , \tilde{C}_i , D and E denote the corresponding LECs.

The presented elementary introduction into ChPT aims at providing the main conceptual ideas of this framework and is neither complete nor comprehensive. Excellent lecture notes on the discussed and related subjects [45–50] are highly recommended for further reading. A very comprehensive, textbook-like lecture notes can be found in Ref. [51]. Current frontiers and challenges in these fields are addressed in recent review articles [52, 53], see also Ref. [54].

4 EFT for two nucleons

4.1 ChPT and nucleon-nucleon scattering

As outlined in the previous section, ChPT can be straightforwardly extended to the single-nucleon sector (apart from the complication related to the treatment of the nucleon mass). A generalization to processes involving two and more nucleons is much more difficult. Contrary to the interaction between Goldstone bosons, nucleons do interact with each other in the limit of vanishingly small momenta and quark masses. Chiral symmetry does not constrain few-nucleon operators in the effective Lagrangian which contains derivative-less terms, see Eq. (3.57). In fact, the interaction between the nucleons at low energy is even strong enough to bind them together. Shallow bound states such as the deuteron, triton etc. represent non-perturbative phenomena that cannot be described in perturbation theory.

On the other hand, just following the naive dimensional analyses as we did in the previous section, the power counting can be straightforwardly generalized to connected Feynman diagrams involving N nucleons leading to

$$\nu = 2 - N + 2L + \sum_i V_i \Delta_i. \quad (4.58)$$

This implies the usual suppression for loop diagrams and thus suggests that the interaction is weak. This conclusion is certainly not correct. So, what goes wrong? The reason why the naive dimensional analysis yields a wrong result is due to the appearance of infrared divergences (in the HBChPT) in diagrams which contain purely nucleonic intermediate states [4, 5]. Consider the two-pion- (2π -) exchange box Feynman diagram shown in Fig. 6 (the diagram on the left-hand side). In the nucleon rest frame with $v_\mu = (1, 0, 0, 0)$, the four-momenta of the incoming nucleons are $(\vec{k}^2/(2m) + \mathcal{O}(m^{-3}), \vec{k})$ and $(\vec{k}^2/(2m) + \mathcal{O}(m^{-3}), -\vec{k})$. In the infrared regime with $\vec{k} = 0$, the contribution of the box diagram takes the form

$$\int \frac{d^4l}{(2\pi)^4} \frac{P(l)}{(l^0 + i\epsilon)(-l^0 + i\epsilon)(l^2 - M_\pi^2 + i\epsilon)^2}, \quad (4.59)$$

where l is the loop momentum and $P(l)$ is a polynomial whose explicit form is determined by the pion-nucleon vertex. The integral over l^0 possesses the so-called pinch singularity due to the poles at $l^0 = \pm i\epsilon$. Notice that such pinch singularities only show up in the case of at least two nucleons since for a single nucleon the contour of integration can be distorted to avoid the singularity. The singularities

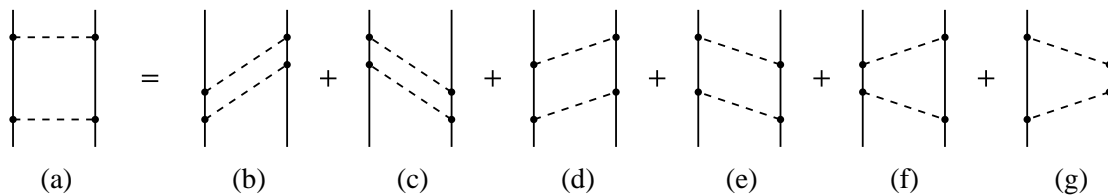


Figure 6: Two-pion exchange: Feynman diagram (a) and the corresponding time-ordered graphs (b-g). Solid (dashed) lines correspond to nucleons (pions).

that appear in the box diagram are not “real” but an artefact of the heavy-baryon approximation for the nucleon propagators (static nucleons) that is not valid for such diagrams.

Exercise: verify this statement by using the standard Dirac propagators for the nucleon field, see Eq. (3.54), and making the nonrelativistic expansion after carrying out the integration over l^0 .

An alternative and, perhaps, more instructive way to explore the origin of the infrared enhancement is by using the so-called “old-fashioned” time-ordered perturbation theory instead of the covariant one. In time-ordered perturbation theory, the T -matrix is given by

$$T_{\alpha\beta} = (H_I)_{\alpha\beta} + \sum_a \frac{(H_I)_{\alpha a} (H_I)_{a\beta}}{E_\beta - E_a + i\epsilon} + \sum_{ab} \frac{(H_I)_{\alpha a} (H_I)_{ab} (H_I)_{b\beta}}{(E_\beta - E_a + i\epsilon)(E_\beta - E_b + i\epsilon)} + \dots, \quad (4.60)$$

where H_I is the interaction Hamiltonian corresponding to the effective Lagrangian for pions and nucleons. This expression should be familiar from Quantum Mechanics. Its derivation and application to quantum field theory can be found e.g. in [55]. Here, I use Latin letters for intermediate states, which, in general, may contain any number of pions, in order to distinguish them from purely nucleonic states denoted by Greek letters. I remind the reader that no nucleon-antinucleon pairs can be created or destroyed if nucleons are treated nonrelativistically. Consequently, all states contain the same number of nucleons. It is useful to represent various contributions to the scattering amplitude in terms of time-ordered diagrams. For example, the Feynman box diagram for NN scattering via 2π -exchange can be expressed as a sum of six time-ordered graphs, see Fig. 6, which correspond to the following term in Eq. (4.60):

$$\sum_{abc} \frac{(H_{\pi NN})_{\alpha a} (H_{\pi NN})_{ab} (H_{\pi NN})_{bc} (H_{\pi NN})_{c\beta}}{(E_\beta - E_a + i\epsilon)(E_\beta - E_b + i\epsilon)(E_\beta - E_c + i\epsilon)}, \quad (4.61)$$

where $H_{\pi NN}$ denotes the πNN vertex. Actually, this expression can be obtained from carrying out the l^0 -integration in the corresponding Feynman diagram (using Dirac propagators for the nucleons). It is easy to see that the contributions of diagrams (d-g) are *enhanced* due to the presence of the small (of the order Q^2/m) energy denominator associated with the purely nucleonic intermediate state $|b\rangle$ which in the center-of-mass system (CMS) takes the form:

$$\frac{1}{E_\beta - E_b + i\epsilon} = \frac{1}{\vec{p}_\beta^2/m - \vec{p}_b^2/m + i\epsilon}. \quad (4.62)$$

Notice that the energy denominators corresponding to the πNN states $|a\rangle$ and $|c\rangle$ contain the pion energy $\omega_k \equiv \sqrt{\vec{k}^2 + M_\pi^2}$ and are of the order $M_\pi \sim Q$ in agreement with the dimensional analysis. According to Weinberg, the failure of perturbation theory in the few-nucleon sector is caused by the enhanced contributions of reducible diagrams, i.e. those ones which contain purely nucleonic intermediate states. It should, however, be emphasized that the infrared enhancement is not sufficient to justify the need of non-perturbative resummation of the amplitude if one counts $m = \mathcal{O}(\Lambda_\chi)$. According to Eq. (4.58) and taking into account the infrared enhancement $\sim m/Q$ due to the purely nucleonic intermediate states, loop contributions are still suppressed by $\sim Qm/\Lambda_\chi^2 \sim Q/\Lambda$ for $m \sim \Lambda_\chi$. To overcome this conceptual difficulty, Weinberg proposed to treat the nucleon mass as a separate hard scale according to the rule [4, 5]:

$$m \sim \frac{\Lambda_\chi^2}{Q} \gg \Lambda_\chi. \quad (4.63)$$

The resulting power counting is referred to as the Weinberg power counting. I will also discuss some alternative scenarios.

The infrared enhancement of the few-nucleon diagrams can be naturally taken into account by rearranging the expansion in Eq. (4.60) and casting it into the form of the Lippmann-Schwinger (LS) equation

$$T_{\alpha\beta} = (V_{\text{eff}})_{\alpha\beta} + \sum_{\gamma} \frac{(V_{\text{eff}})_{\alpha\gamma} T_{\gamma\beta}}{E_\beta - E_\gamma + i\epsilon}, \quad (4.64)$$

with the effective potential $(V_{\text{eff}})_{\alpha\beta}$ defined as a sum of all possible irreducible diagrams (i.e. the ones which do not contain purely nucleonic intermediate states):

$$(V_{\text{eff}})_{\alpha\beta} = (H_I)_{\alpha\beta} + \sum_a \frac{(H_I)_{\alpha a} (H_I)_{a\beta}}{E_\beta - E_a + i\epsilon} + \sum_{ab} \frac{(H_I)_{\alpha a} (H_I)_{ab} (H_I)_{b\beta}}{(E_\beta - E_a + i\epsilon)(E_\beta - E_b + i\epsilon)} + \dots \quad (4.65)$$

Here, the states $|a\rangle$, $|b\rangle$ contain at least one pion. The effective potential in Eq. (4.65) does not contain small energy denominators and can be worked out within the low-momentum expansion following the usual procedure of ChPT. After the potential is obtained at a given order in the chiral expansion, few-nucleon observables can be computed by solving the LS equation (4.64), which leads to a nonperturbative resummation of the contributions resulting from reducible diagrams. The resulting two-step approach will be referred to as ChEFT in order to distinguish it from ChPT in the Goldstone boson and single-nucleon sectors.

4.2 Analytic properties of the non-relativistic scattering amplitude

Before discussing various scenarios of organizing EFT for two nucleons, it is useful to recall general constraints imposed on the partial wave scattering amplitude by analyticity. Consider two non-relativistic nucleons interacting via a potential V . The corresponding S -matrix for an uncoupled channel with the orbital angular momentum l is parametrized in terms of a single phase shift δ_l and can be written in

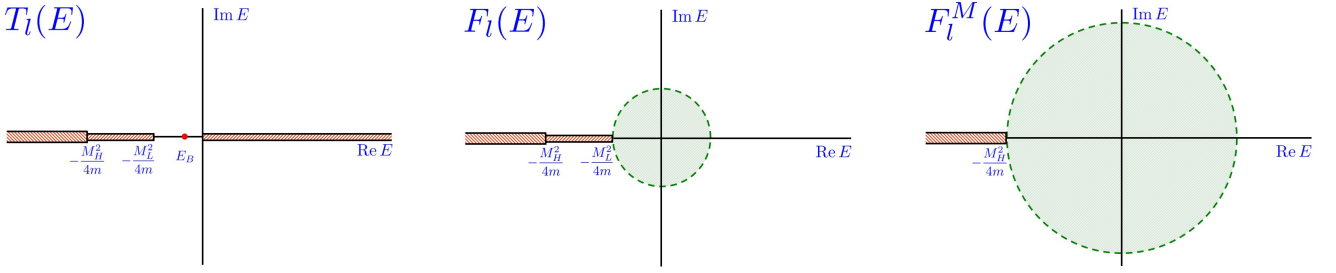


Figure 7: Some singularities of the partial wave T -matrix (left panel), effective range function $F_l(E)$ (middle panel) and the modified effective range function $F_l^M(E)$ (right panel). The shaded areas show the (maximal) range of applicability of the ERE and MERE.

terms of T -matrix as

$$S_l = e^{2i\delta_l(k)} = 1 - i \left(\frac{km}{8\pi^2} \right) T_l(k), \quad (4.66)$$

with k denoting the CMS scattering momentum. The T -matrix can then be expressed in terms of the so-called effective range function $F_l(k) \equiv k^{2l+1} \cot \delta_l(k)$ via

$$T_l(k) = -\frac{16\pi^2}{m} \frac{k^{2l}}{F_l(k) - ik^{2l+1}}. \quad (4.67)$$

In the complex energy plane, the scattering amplitude and thus also the T -matrix possess a so-called unitarity cut, a kinematic singularity due to two-body unitarity. The unitarity cut starts from the branch point at the threshold ($E = 0$) and goes to positive infinity. The dynamic singularities are associated with the interaction mechanism and are located at the negative real axis. For example, in the case of Yukawa potential $\sim \exp(-Mr)/r$ corresponding to an exchange of a meson of mass M , the amplitude has a left-hand cut starting at $k^2 = -M^2/4$. Bound and virtual states reside as poles at the negative real axis ($k = i|k|$ and $k = -i|k|$ for bound- and virtual-state poles, respectively) while resonances show up as poles at complex energies.

Exercise: verify the appearance of the left-hand cut in the scattering amplitude for the one-pion exchange potential

$$V(\vec{p}', \vec{p}) \propto \frac{\vec{\sigma}_1 \cdot \vec{q} \vec{\sigma}_2 \cdot \vec{q}}{\vec{q}^2 + M_\pi^2}, \quad \text{with} \quad \vec{q} \equiv \vec{p}' - \vec{p},$$

using the first Born approximation.

Contrary to the scattering amplitude, the effective range function does not possess the kinematic unitarity cut and can be shown to be a real meromorphic function of k^2 near the origin for non-singular potentials of a finite range [56, 57]. It can, therefore, be Taylor-expanded about the origin leading to the well-known effective range expansion (ERE)

$$F_l(k^2) = -\frac{1}{a} + \frac{1}{2}rk^2 + v_2k^4 + v_3k^6 + \dots, \quad (4.68)$$

with a , r and v_i being the scattering length, effective range and the so-called shape parameters. Generally, the maximal radius of convergence of the ERE is limited by the lowest-lying left-hand dynamic singularity associated with the potential. For Yukawa-type potentials with the range $r \sim M^{-1}$, the (maximal) radius of convergence of the ERE is given by $k^2 < M^2/4$. For (strong) nucleon-nucleon interaction with the one-pion- (1π -) exchange potential constituting the longest-range contribution, the ERE is expected to converge for energies up to $E_{\text{lab}} \sim M_\pi^2/(2m_N) = 10.5$ MeV. Notice that apart from the singularities associated with the structure of the potential, $F_l(k^2)$ may also contain discrete poles whose positions are determined by the strength of the interaction. The appearance of such poles near the origin would spoil the convergence of the ERE.

The framework of ERE can be generalized to the case in which the potential is given by a sum of a long-range ($r_l \sim m_l^{-1}$) and short-range ($r_s \sim m_s^{-1} \ll m_l^{-1}$) potentials V_L and V_S , respectively. Following van Haeringen and Kok [58], one can define the *modified* effective range function F_l^M via

$$F_l^M(k^2) \equiv M_l^L(k) + \frac{k^{2l+1}}{|f_l^L(k)|} \cot[\delta_l(k) - \delta_l^L(k)], \quad (4.69)$$

The Jost function $f_l^L(k)$ is defined according to $f_l^L(k) \equiv f_l^L(k, r)|_{r=0}$ with $f_l^L(k, r)$ being the Jost solution of the Schrödinger equation corresponding to the potential V_L , i.e. the particular solution that fulfills

$$\lim_{r \rightarrow \infty} e^{-ikr} f_l(k, r) = 1. \quad (4.70)$$

Further, $\delta_l^L(k)$ denotes to the phase shift associated with the potential V_L and the quantity $M_l^L(k)$ can be computed from $f_l^L(k, r)$ as follows:

$$M_l^L(k) = \left(-\frac{ik}{2}\right)^l \frac{1}{l!} \lim_{r \rightarrow 0} \left[\frac{d^{2l+1}}{dr^{2l+1}} r^l \frac{f_l(k, r)}{f_l(k)} \right]. \quad (4.71)$$

I denote here with the superscript “L” all quantities that can be computed solely from the long-range part of the potential. The modified effective range function $F_l^M(k^2)$ defined in this way does not contain the left-hand singularity associated with the long-range potential and reduces, per construction, to the ordinary effective range function $F_l(k^2)$ for $V_L = 0$. It is a real meromorphic function in a much larger region given by r_s^{-1} as compared to $F_l(k^2)$.⁷ If the long-range interaction is due to a Coulomb potential, $V_L(r) = \alpha/r$, the Jost solution and, consequently, the function $M_l^L(k)$ can be calculated analytically. For example, for $l = 0$ and the repulsive Coulomb potential, the MERE takes the following well-known form:

$$F_C(k^2) = C_0^2(\eta) k \cot[\delta(k) - \delta^C(k)] + 2k\eta h(\eta), \quad (4.72)$$

where the Coulomb phase shift is $\delta^C \equiv \arg \Gamma(1 + i\eta)$ and the quantity η is given by

$$\eta = \frac{m}{2k} \alpha. \quad (4.73)$$

⁷Note that the existence of $M_l^L(k)$ implies certain constraints on the small- r behavior of $V_L(r)$.

Further, the functions $C_0^2(\eta)$ (the Sommerfeld factor) and $h(\eta)$ read

$$C_0^2(\eta) = \frac{2\pi\eta}{e^{2\pi\eta} - 1}, \quad \text{and} \quad h(\eta) = \text{Re}[\Psi(i\eta)] - \ln(\eta). \quad (4.74)$$

Here, $\Psi(z) \equiv \Gamma'(z)/\Gamma(z)$ denotes the digamma function. For more details on the analytic properties of the scattering amplitude and related topics I refer the reader to the review article [59].

After these preparations, we are now in the position to discuss the implications of the long-range interaction on the energy dependence of the phase shift. It is natural to assume that the coefficients in the ERE and MERE (except for the scattering length) are driven by the scales m_l and m_s associated with the lowest left-hand singularities, see [60] for a related discussion. The knowledge of the long-range interaction V_L allows to compute the quantities $f_l^L(k)$, $M_l^L(k)$ and $\delta_l^L(k)$ entering the right-hand side of Eq. (4.69) and thus to express $\delta_l(k)$ and the ordinary effective range function $F_l(k^2)$ in terms of the modified one, $F_l^M(k^2)$. The MERE for $F_l^M(k^2)$ then yields an expansion of the subthreshold parameters entering Eq. (4.68) in powers of m_l/m_s . In particular, using the first few terms in the MERE as input allows to make predictions for *all* coefficients in the ERE. The appearance of the correlations between the subthreshold parameters in the above-mentioned sense which I will refer to as low-energy theorems (LETs) is the only signature of the long-range interaction at low energy (in the two-nucleon system). The LETs allow to test whether the long-range interactions are incorporated properly in nuclear chiral EFT and thus provide an important consistency check.

4.3 EFT for two nucleons at very low energy

Before discussing chiral EFT for two nucleons, let us consider, as a warm-up exercise, a simpler EFT for very low energies with $Q \ll M_\pi$. Then, no pions need to be taken into account explicitly, and the only relevant degrees of freedom are the nucleons themselves. The corresponding EFT with the hard scale $\Lambda \sim M_\pi$ is usually referred to as pionless EFT. The most general effective Lagrangian consistent with Galilean invariance, baryon number conservation and the isospin symmetry takes in the absence of external sources the following form:

$$\mathcal{L} = N^\dagger \left(i\partial_0 + \frac{\vec{\nabla}^2}{2m} \right) N - \frac{1}{2}C_S (N^\dagger N)(N^\dagger N) - \frac{1}{2}C_T (N^\dagger \vec{\sigma} N) \cdot (N^\dagger \vec{\sigma} N) + \dots, \quad (4.75)$$

where $C_{S,T}$ are LECs and the ellipses denote operators with derivatives. Isospin-breaking and relativistic corrections to Eq. (4.75) can be included perturbatively.

What can be expected from the pionless EFT as compared to the ERE? In the absence of external sources and restricting ourselves to the two-nucleon system, both approaches provide an expansion of NN low-energy observables in powers of k/M_π , have the same validity range and incorporate the same physical principles. Pionless EFT can, therefore, not be expected to do any better than ERE. Our goal will be thus to design the EFT in such a way that it matches the ERE for the scattering amplitude

$$T = -\frac{16\pi^2}{m} \frac{1}{\left(-\frac{1}{a} + \frac{1}{2}r_0k^2 + v_2k^4 + v_3k^6 + \dots\right) - ik}. \quad (4.76)$$

Here, I restrict myself to S-waves only. While the coefficients in the effective range expansion are, in general, driven by the range of the potential and thus expected to scale with the appropriate powers of M_π , the scattering length can, in principle, take any value. In particular, it diverges in the presence of a bound or virtual state at threshold. It is, therefore, useful to distinguish between a natural case with $|a| \sim M_\pi^{-1}$ and an unnatural case with $|a| \gg M_\pi^{-1}$. In the natural case, the T -matrix in Eq. (4.76) can be expanded in powers of k as:

$$T = T^{(0)} + T^{(1)} + T^{(2)} + \dots = \frac{16\pi^2 a}{m} \left[1 - iak + \left(\frac{ar_0}{2} - a^2 \right) k^2 + \dots \right], \quad (4.77)$$

where the superscripts of T denote the power of the soft scale Q . A natural value of the scattering length implies the absence of bound and virtual states close to threshold. The T -matrix can then be evaluated perturbatively in the EFT provided one uses an appropriate renormalization scheme (i.e. the one that does not introduce an additional large scale). When solving the LS equation with point-like contact interactions, one encounters divergent loop integrals of the kind

$$I_n = -\frac{m}{(2\pi)^3} \int d^3l l^{n-3}, \quad \text{with } n = 1, 3, 5, \dots, \quad I(k) = \frac{m}{(2\pi)^3} \int d^3l \frac{1}{k^2 - l^2 + i\eta}. \quad (4.78)$$

The integrals can be evaluated using a cutoff regularization:

$$\begin{aligned} I_n &\rightarrow I_n^\Lambda = -\frac{m}{(2\pi)^3} \int d^3l l^{n-3} \theta(\Lambda - l) = -\frac{m \Lambda^n}{2n\pi^2}, \\ I(k) &\rightarrow I^\Lambda(k) = \frac{m}{(2\pi)^3} \int \frac{d^3l \theta(\Lambda - l)}{k^2 - l^2 + i\eta} = I_1^\Lambda - \frac{i m k}{4\pi} - \frac{m k}{4\pi^2} \ln \frac{\Lambda - k}{\Lambda + k}, \end{aligned} \quad (4.79)$$

where the last equation is valid for $k < \Lambda$. To renormalize the scattering amplitude, I divide loop integrals into the divergent and finite parts and take the limit $\Lambda \rightarrow \infty$ ⁸:

$$\begin{aligned} I_n &\equiv \lim_{\Lambda \rightarrow \infty} I_n^\Lambda = \lim_{\Lambda \rightarrow \infty} \left(I_n^\Lambda + \frac{m \mu_n^n}{2n\pi^2} \right) - \frac{m \mu_n^n}{2n\pi^2} \equiv \Delta_n(\mu_n) + I_n^R(\mu_n), \\ I(k) &\equiv \lim_{\Lambda \rightarrow \infty} I^\Lambda(k) = \lim_{\Lambda \rightarrow \infty} \left(I_1^\Lambda + \frac{m \mu}{2\pi^2} \right) + \left[-\frac{m \mu}{2\pi^2} - \frac{i m k}{4\pi} \right] \equiv \Delta(\mu) + I^R(\mu, k). \end{aligned} \quad (4.80)$$

Here, $\Delta_n(\mu_n)$ and $\Delta(\mu)$ denote the divergent parts of the loop integrals while $I_n^R(\mu_n)$ and $I^R(\mu, k)$ are finite. The procedure is analogous to the standard treatment of divergences arising from pion loops in ChPT, see section 3. The splitting of loop integrals in Eq. (4.80) is not unique. The freedom in the choice of renormalization conditions is parameterized by μ and μ_n . The divergent parts $\Delta_n(\mu_n)$ and $\Delta(\mu)$ are to be canceled by contributions of counterterms. The renormalized expression for the amplitude, therefore, emerge from dropping the divergent parts in Eq. (4.80) and replacing the bare LECs by the renormalized ones $C_i \rightarrow C_i^r(\{\mu, \mu_n\})$. The proper choice of renormalization conditions

⁸While extremely convenient in the case under consideration, taking the limit $\Lambda \rightarrow \infty$ is, strictly speaking, not necessary in an EFT. It is sufficient to ensure that the error from keeping the cutoff finite is within the accuracy of the EFT expansion. In the considered case, taking $\Lambda \sim M_\pi$ would do equally good job in describing the scattering amplitude.

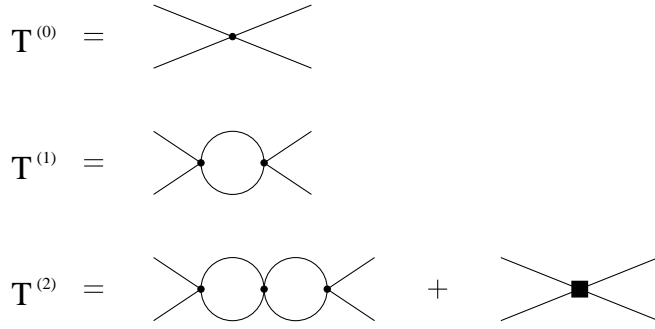


Figure 8: Leading, subleading and sub-subleading contributions to the S-wave T -matrix in the case of a natural scattering length. Solid dots (filled rectangles) refer to contact vertices without (with two) derivatives. Lines represent the nucleon propagators.

requires choosing $\mu, \mu_n \sim Q \ll M_\pi$. Dimensional regularization with the minimal subtraction can be viewed as a special case corresponding to $\mu = \mu_n = 0$. Another special case is given by DR with the power divergence subtraction (PDS) [61, 62]. In this scheme, the power law divergences, which are normally discarded in DR, are explicitly accounted for by subtracting from dimensionally regulated loop integrals not only $1/(d-4)$ -poles but also the $1/(d-3)$ -poles. Its formulation used in Refs. [61, 62] corresponds to the choice $\mu_n = 0$ and $\mu \rightarrow \mu\pi/2$ in Eq. (4.80).

The dimensional analysis for the renormalized scattering amplitude implies that the leading and sub-leading terms $T^{(0)}$ and $T^{(1)}$ are given by the tree- and one-loop graphs constructed with the lowest-order vertices from Eq. (4.75), see Fig. 8. $T^{(2)}$ receives a contribution from the two-loop graph with the lowest-order vertices and the tree graph with a subleading vertex [61, 62]. Higher-order corrections can be evaluated straightforwardly. Matching the resulting T -matrix to the ERE in Eq. (4.77) order by order in the low-momentum expansion allows to fix the LECs C_i^r . At next-to-next-to-leading order (N²LO), for example, one finds:

$$C_0^r = \frac{4\pi a}{m} \left[1 + \mathcal{O}(a\mu) \right], \quad C_2^r = \frac{2\pi a^2}{m} r_0, \quad (4.81)$$

where the LECs C_0 and C_2 are defined via the tree-level T -matrix: $T_{\text{tree}} = 4\pi(C_0 + C_2 k^2 + \dots)$. The LEC C_0 is related to $C_{S,T}$ in Eq. (4.75) as $C_0 = C_S - 3C_T$. Here and in the remaining part of this section, the expressions are given in DR with PDS.

For the physically interesting case of neutron-proton scattering, the two S-wave scattering lengths appear to be large:

$$a_{1S_0} = -23.714 \text{ fm} \sim -16.6 M_\pi^{-1}, \quad a_{3S_1} = 5.42 \text{ fm} \sim 3.8 M_\pi^{-1}. \quad (4.82)$$

Instead of using the low-momentum representation in Eq. (4.77) which is valid only for $k < 1/a$, it is

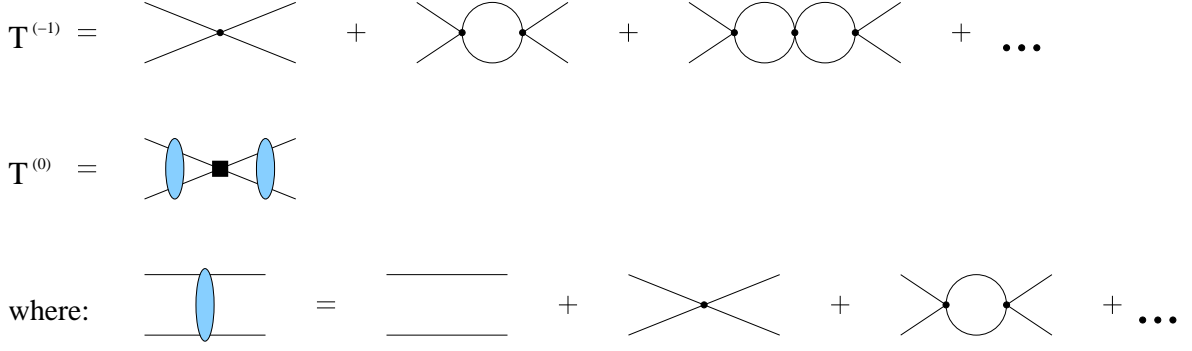


Figure 9: Leading and subleading contributions to the S-wave T -matrix in the case of an unnaturally large scattering length. For notation, see Fig. 8.

advantageous to expand the T -matrix in powers of k keeping $ak \sim 1$ [61, 62]:

$$\begin{aligned}
 T &= T^{(-1)} + T^{(0)} + T^{(1)} + \dots \\
 &= \frac{16\pi^2}{m} \frac{1}{(a^{-1} + ik)} \left[1 + \frac{r_0}{2(a^{-1} + ik)} k^2 + \left(\frac{r_0^2}{4(a^{-1} + ik)^2} + \frac{v_2}{(a^{-1} + ik)} \right) k^4 + \dots \right].
 \end{aligned} \tag{4.83}$$

The EFT expansion can be cast into the form of Eq. (4.83) if one assumes that the LECs C_i^r scale according to $C_{2n}^r \sim 1/Q^{n+1}$. The leading contribution $T^{(-1)}$ then results from summing up an infinite chain of bubble diagrams with the lowest-order vertices, see Fig. 9. All diagrams constructed only from C_0^r scale as $1/Q$. For example, for the one-loop graph one has Q^3 from the integration, $1/Q^2$ from the nucleon propagator and another $1/Q^2$ from the LECs C_0^r . The corrections are given by perturbative insertions of higher-order interactions dressed to all orders by the leading vertices. Matching the resulting T -matrix with the one in Eq. (4.83) one finds at NLO:

$$C_0^r = \frac{4\pi}{m} \frac{1}{a^{-1} - \mu}, \quad C_2^r = \frac{4\pi}{m} \frac{1}{(a^{-1} - \mu)^2} \frac{r_0}{2}. \tag{4.84}$$

Exercise: calculate the S-wave scattering amplitude up to NLO for the case of unnaturally large scattering length and verify the expressions for the LECs given in Eq. (4.84).

The real power of pionless EFT comes into play when one goes beyond the two-nucleon system by considering e.g. low-energy reactions involving external electroweak sources and/or three- and more nucleon systems. A discussion of these topics goes beyond the scope of these lectures. I refer an interested reader to the recent review articles [63–66].

4.4 Chiral EFT for two nucleons with perturbative pions

We have seen in the previous section how the EFT without explicit pions can be organized to describe strongly interacting nucleons at low energy. The limitation in energy of this approach, cf. the discussion in section 4.2, appears to be too strong for most nuclear physics applications. To go to higher energies it is necessary to include pions as explicit degrees of freedom. I have already outlined in section 4.1 one possible way to extend ChPT to the few-nucleon sector following Weinberg’s original proposal [4, 5]. In this approach, the nonperturbative dynamics is generated by iterating the lowest-order two-nucleon potential $V_{2N}^{(0)}$ which subsumes irreducible (i.e. non-iterative) contributions from tree diagrams with the leading vertices (i.e. $\Delta_i = 0$), see Eq. (4.58). The only possible contributions are due to derivative-less contact interaction and the static 1π -exchange, so that the resulting potential reads:

$$V_{2N}^{(0)} = -\frac{g_A^2}{4F_\pi^2} \frac{\vec{\sigma}_1 \cdot \vec{q} \vec{\sigma}_2 \cdot \vec{q}}{\vec{q}^2 + M_\pi^2} \vec{\tau}_1 \cdot \vec{\tau}_2 + C_S + C_T \vec{\sigma}_1 \cdot \vec{\sigma}_2. \quad (4.85)$$

Here, $\vec{\sigma}_i$ ($\vec{\tau}_i$) are the Pauli spin (isospin) matrices of the nucleon i , $\vec{q} = \vec{p}' - \vec{p}$ is the nucleon momentum transfer and \vec{p} (\vec{p}') refers to initial (final) nucleon momenta in the CMS. As pointed out in section 4.1, the justification for resumming $V_{2N}^{(0)}$ to all orders in the LS equation is achieved in the Weinberg approach via a fine tuning of the nucleon mass, see Eq. (4.63). With this counting rule, it follows immediately that every iteration of $V_{2N}^{(0)}$ in Eq. (4.64) generates a contribution of the order Q^0/Λ_χ . On the other hand, in the pionless EFT with unnaturally large scattering length outlined in section 4.3, the non-perturbative resummation of the amplitude was enforced by fine-tuning the LECs accompanying the contact interactions while treating the nucleon mass on the same footing as all other hard scales. While these two scenarios are essentially equivalent in the pionless case, they lead to an important difference in organizing EFT with explicit pions. The approach due to Kaplan, Savage and Wise (KSW) [61, 62] represents a straightforward generalization of the pionless EFT to *perturbatively* include diagrams with exchange of one or more pions. The scaling of the contact interactions is assumed to be the same as in pionless EFT (provided one uses DR with PDS or an equivalent scheme to regularize divergent loop integrals). Notice that in contrast to pionless EFT, the pion mass is treated as a soft scale with $Q \sim M_\pi \sim a^{-1}$. The only new ingredients in the calculation of the amplitude up to next-to-leading order in the KSW expansion are given by the dressed 1π -exchange potential and derivative-less interaction $\propto M_\pi^2$, see Fig. 10. 2π -exchange is suppressed and starts to contribute at N²LO. At each order in the perturbative expansion, the amplitude is made independent on the renormalization scale by an appropriate running of the LECs.⁹ Compact analytic expressions for the scattering amplitude represent another nice feature of the KSW approach.

As explained in section 4.2, the appearance of a long-range interaction implies strong constraints on the energy dependence of the amplitude and imposes certain correlations between the coefficients in the ERE (LETs). EFT with explicit pions aims at a correct description of non-analyticities in the scattering amplitude associated with exchange of pions which in this framework represent truly long-range phenomena. Thus, the correct treatment of the long-range interaction by including pions perturbatively

⁹Strictly speaking, an exact scale independence of the NLO amplitude in the KSW approach with explicit pions is achieved at the cost of resumming a certain class of higher-order terms, see the discussion in Ref. [67].

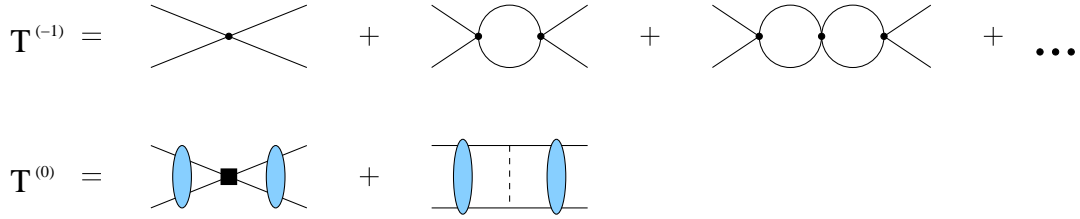


Figure 10: Leading and subleading contributions to the S-wave T -matrix in the case of unnaturally large scattering length in the KSW approach with explicit pions. Filled rectangle denotes contact interactions with two derivatives or a single insertion of M_π^2 . For remaining notation, see Fig. 8.

can be ultimately judged by testing the corresponding low-energy theorems. This idea was picked up by Cohen and Hansen [68, 69]. Fixing the LECs accompanying the contact interactions from the scattering length and effective range, they obtained the following predictions for the first three S-wave shape parameters at NLO in the KSW scheme [68, 69]:

$$\begin{aligned}
v_2 &= \frac{g_A^2 m}{16\pi F_\pi^2} \left(-\frac{16}{3a^2 M_\pi^4} + \frac{32}{5a M_\pi^3} - \frac{2}{M_\pi^2} \right), \\
v_3 &= \frac{g_A^2 m}{16\pi F_\pi^2} \left(\frac{16}{a^2 M_\pi^6} - \frac{128}{7a M_\pi^5} + \frac{16}{3M_\pi^4} \right), \\
v_4 &= \frac{g_A^2 m}{16\pi F_\pi^2} \left(-\frac{256}{5a^2 M_\pi^8} + \frac{512}{9a M_\pi^7} - \frac{16}{M_\pi^6} \right).
\end{aligned} \tag{4.86}$$

Plugging in the numbers for the nucleon and pion masses, $g_A \simeq 1.27$, $F_\pi = 92.4$ MeV and the corresponding scattering lengths, see Eq. (4.82), Cohen and Hansen obtained the results quoted in Table 1.¹⁰ A clear failure for the LETs in both channels serves as an indication that the long-range physics is not properly taken into account if pions are treated perturbatively. The convergence of the KSW expansion was further tested in Ref. [71] where the amplitude is calculated up to N²LO. While the results for the 1S_0 and some other partial waves including spin-singlet channels were found to be in a reasonable agreement with the Nijmegen PWA, large corrections show up in spin-triplet channels already at momenta of the order of ~ 100 MeV and lead to strong disagreements with the data. The perturbative inclusion of the pion-exchange contributions does not allow to increase the region of validity of the EFT compared to the pionless theory, see however, Ref. [72] for a new formulation which is claimed to yield a convergent expansion. The failure of the KSW approach in the spin-triplet channels was attributed in [71] to the iteration of the tensor part of the 1π -exchange potential. This appears to be in line with phenomenological successes of Weinberg's approach which treats pion exchange contributions nonperturbatively. The most advanced analyses of the NN system at next-to-next-to-next-to-leading order (N³LO) in Weinberg's power counting scheme demonstrate the ability to accurately describe NN scattering data up to center-of-mass momenta at least of the order $\sim 2M_\pi$ [8, 73].

¹⁰A slightly different values compared to the ones quoted in this table are extracted from the Nijmegen PWA in Ref. [70].

	1S_0 partial wave			3S_1 partial wave		
	v_2 [fm ³]	v_3 [fm ⁵]	v_4 [fm ⁷]	v_2 [fm ³]	v_3 [fm ⁵]	v_4 [fm ⁷]
LETs	−3.3	17.8	−108	−0.95	4.6	−25
Nijmegen PWA	−0.48	3.8	−17	0.4	0.67	−4

Table 1: A comparison of the predicted S-wave shape parameters from Ref. [68] with coefficients extracted from the Nijmegen PWA.

4.5 Towards including pions nonperturbatively: playing with toy models

While the power counting approach due to Weinberg allows for a nonperturbative resummation of the 1π -exchange potential, there is a price to pay. Contrary to the KSW approach, the leading NN potential is non-renormalizable in the traditional sense, i.e. iterations of the LS equation generate divergent terms with structures that are not included in the original potential. Moreover, resummation of the 1π -exchange potential in the LS equation can only be carried out numerically. This prevents the use of regularization prescriptions such as e.g. DR which avoid the appearance of a hard scale and maintain the manifest power counting for regularized loop contributions making renormalization considerably more subtle. Most of the available calculations employ various forms of cutoff regularization with the cutoff being kept finite. The purpose of this section is to provide an in-depth discussion on regularization and renormalization in this context by considering a simple and exactly solvable quantum mechanical model for two nucleons interacting via the long- and short-range forces. This may be regarded as a toy model for chiral EFT in the two-nucleon sector. In this model, resummation of the long-range interaction can be carried out analytically. This allows to employ and compare the subtractive renormalization that maintains the manifest power counting and the cutoff formulation of the effective theory. I also explore the consequences of taking very large values of the cutoff in this model. The presentation follows closely the one of Ref. [67].

4.5.1 The model

Consider two spin-less nucleons interacting via the two-range separable potential

$$V(p', p) = v_l F_l(p') F_l(p) + v_s F_s(p') F_s(p), \quad F_l(p) \equiv \frac{\sqrt{p^2 + m_s^2}}{p^2 + m_l^2}, \quad F_s(p) \equiv \frac{1}{\sqrt{p^2 + m_s^2}}, \quad (4.87)$$

where the masses m_l and m_s fulfill the condition $m_l \ll m_s$. Further, the dimensionless quantities v_l and v_s denote the strengths of the long- and short-range interactions, respectively. The choice of the explicit form of $F_{l,s}(p)$ is motivated by the simplicity of calculations.

The potential in Eq. (4.87) does not depend on the angle between \vec{p} and \vec{p}' and, therefore, only gives rise to S-wave scattering. The projection onto the S-wave in this case is trivial and simply yields the

factor of 4π from the integration over the angles. For an interaction of a separable type, the off-shell T-matrix and, consequently, also the coefficients in the ERE, see Eqs. (4.67) and (4.68), can be calculated analytically by solving the corresponding LS equation

$$T(p', p; k) = V(p', p) + 4\pi \int \frac{l^2 dl}{(2\pi)^3} V(p', l) \frac{m}{k^2 - l^2 + i\epsilon} T(l, p; k), \quad (4.88)$$

where m is the nucleon mass and k corresponds to the on-shell momentum which is related to the two-nucleon center-of-mass energy via $E_{\text{CMS}} = k^2/m$. Note that we have absorbed the factor 4π into the normalization of the T-matrix which is, therefore, different from the one in Eq. (2.6). In particular, the relation between the S- and T-matrices is given by $S(p) = 1 - ipmT(p, p; p)/(2\pi)$.

As explained in section 4.2, the coefficients in the ERE generally scale with the mass corresponding to the long-range interaction that gives rise to the first left-hand singularities in the T-matrix. Thus, in the considered two-range model, the coefficients in the ERE can be expanded in powers of m_l/m_s leading to the “chiral” expansion:

$$\begin{aligned} a &= \frac{1}{m_l} \left(\alpha_a^{(0)} + \alpha_a^{(1)} \frac{m_l}{m_s} + \alpha_a^{(2)} \frac{m_l^2}{m_s^2} + \dots \right), \\ r &= \frac{1}{m_l} \left(\alpha_r^{(0)} + \alpha_r^{(1)} \frac{m_l}{m_s} + \alpha_r^{(2)} \frac{m_l^2}{m_s^2} + \dots \right), \\ v_i &= \frac{1}{m_l^{2i-1}} \left(\alpha_{v_i}^{(0)} + \alpha_{v_i}^{(1)} \frac{m_l}{m_s} + \alpha_{v_i}^{(2)} \frac{m_l^2}{m_s^2} + \dots \right), \end{aligned} \quad (4.89)$$

where $\alpha_a^{(m)}$, $\alpha_r^{(m)}$ and $\alpha_{v_i}^{(m)}$ are dimensionless constants whose values are determined by the form of the interaction potential. I fine tune the strengths of the long- and short-range interactions in our model in such a way that they generate scattering lengths of a natural size. More precisely, I require that the scattering length takes the value $a = \alpha_l/m_l$ ($a = \alpha_s/m_s$) with a dimensionless constant $|\alpha_l| \sim 1$ ($|\alpha_s| \sim 1$) when the short-range (long-range) interaction is switched off. This allows to express the corresponding strengths v_l and v_s in terms of α_l and α_s as follows:

$$v_l = -\frac{8\pi m_l^3 \alpha_l}{m(\alpha_l m_s^2 + m_l^2 \alpha_l - 2m_s^2)}, \quad v_s = -\frac{4\pi m_s \alpha_s}{m(\alpha_s - 1)}. \quad (4.90)$$

One then finds the following expressions for the first three terms in the “chiral” expansion of the scattering length

$$\alpha_a^{(0)} = \alpha_l, \quad \alpha_a^{(1)} = (\alpha_l - 1)^2 \alpha_s, \quad \alpha_a^{(2)} = (\alpha_l - 1)^2 \alpha_l \alpha_s^2, \quad (4.91)$$

and effective range

$$\begin{aligned} \alpha_r^{(0)} &= \frac{3\alpha_l - 4}{\alpha_l}, \\ \alpha_r^{(1)} &= \frac{2(\alpha_l - 1)(3\alpha_l - 4)\alpha_s}{\alpha_l^2}, \\ \alpha_r^{(2)} &= \frac{(\alpha_l - 1)(3\alpha_l - 4)(5\alpha_l - 3)\alpha_s^2 + (2 - \alpha_l)\alpha_l^2}{\alpha_l^3}. \end{aligned} \quad (4.92)$$

Notice that in the model considered the leading terms in the m_l/m_s -expansion of the ERE coefficients are completely fixed by the long-range interaction. The scenario realized corresponds to a strong (at momenta $k \sim m_l$) long-range interaction which needs to be treated non-perturbatively and a weak short-range interaction which can be accounted for in perturbation theory.

Exercise: calculate the T-matrix by solving the LS equation (4.88) for the potential given in Eq. (4.87). Verify the “chiral” expansion for the scattering length and effective range. Work out the first terms in the “chiral” expansion of the shape parameters v_2 and v_3 . The results can be found in Ref. [67].

4.5.2 KSW-like approach

At momenta of the order $k \sim m_l \ll m_s$, the details of the short-range interaction cannot be resolved. An EFT description emerges by keeping the long-range interaction and replacing the short-range one by a series of contact terms $V_{\text{short}}(p', p) = C_0 + C_2(p^2 + p'^2) + \dots$. Iterating such an effective potential in the LS equation leads to ultraviolet divergences which need to be regularized and renormalized. The renormalization prescription plays an important role in organizing the EFT expansion. I first consider the most convenient and elegant formulation by employing the subtractive renormalization which respects dimensional power counting at the level of diagrams. In this sense, the considered formulation is conceptually similar to the KSW framework with perturbative pions discussed above and will be referred to as the KSW-like approach. The available soft and hard scales in the problem are given by $Q = \{k, \mu, m_l\}$ and $\lambda = \{m_s, m\}$, respectively. Here $\mu \sim m_l$ denotes the subtraction point. (There is just a single linearly divergent integral at the order in the low-momentum expansion I will consider.) The contributions to the amplitude up to N²LO in the Q/λ -expansion are visualized in Fig. 11 and can be easily verified using naive dimensional analysis. In particular, the leading term arises at order Q^{-1} is generated by the leading term in the Q/λ -expansion of the long-range interaction

$$\begin{aligned} V_{\text{long}}(p', p) &= v_l F_l(p') F_l(p) \\ &\simeq -\frac{8\pi m_l^3 \alpha_l}{m(\alpha_l - 2)(p^2 + m_l^2)(p'^2 + m_l^2)} \left[1 - \frac{\alpha_l m_l^2}{(\alpha_l - 2)m_s^2} + \frac{p^2}{2m_s^2} + \frac{p'^2}{2m_s^2} + \mathcal{O}\left(\frac{Q^4}{\lambda^4}\right) \right], \end{aligned} \quad (4.93)$$

which scales as Q^{-1} and, therefore, needs to be summed up to an infinite order, see Fig. 11. Notice that the natural size of the short-range effects in our model suggests the scaling of the short-range interactions in agreement with the naive dimensional analysis, i.e. $C_{2n} \sim Q^0$. This leads to the following expression for the on-the-energy shell T-matrix:

$$T^{(-1)} = -\frac{8\pi m_l^3 \alpha_l}{m(k - im_l)^2 [k^2(\alpha_l - 2) + 2ikm_l(\alpha_l - 2) + 2m_l^2]}, \quad (4.94)$$

from which one deduces

$$k \cot \delta = -\frac{4\pi}{m} \frac{1}{T^{(-1)}} + ik = -\frac{m_l}{\alpha_l} + \frac{(3\alpha_l - 4)}{2m_l \alpha_l} k^2 + \frac{(\alpha_l - 2)}{2m_l^3 \alpha_l} k^4. \quad (4.95)$$

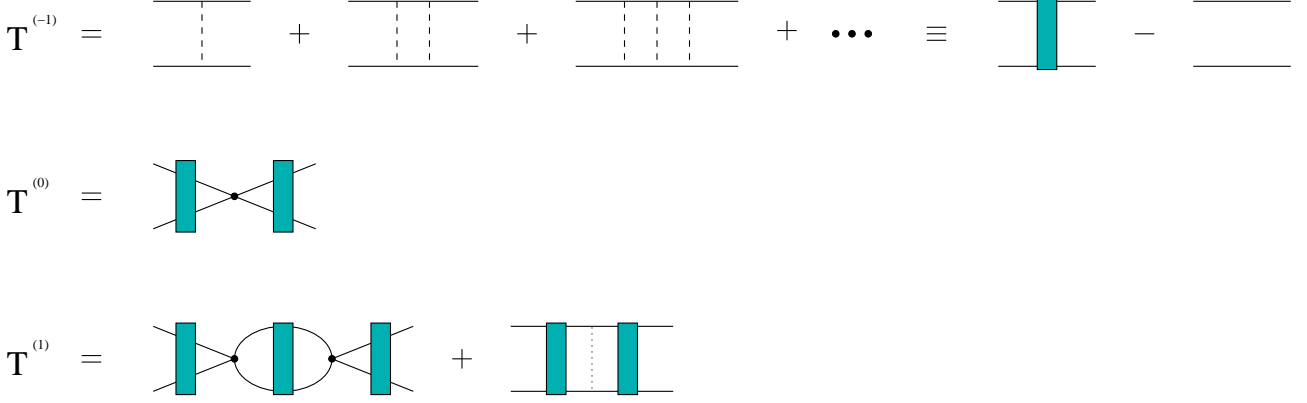


Figure 11: Leading, next-to-leading and next-to-next-to-leading order contributions to the scattering amplitude in the KSW-like approach. The solid lines denote nucleons while the dashed ones represent an insertion of the lowest-order (i.e. $\mathcal{O}(Q^{-1})$) long-range interaction. Solid dots (dotted lines) denote an insertion of the lowest-order contact interaction $\propto C_0$ (subleading order- $\mathcal{O}(Q)$ contribution to the long-range interaction).

Not surprisingly, one observes that the leading terms in the expansion of the ERE coefficients in Eq. (4.89) are correctly reproduced.

The first correction at order Q^0 is given by the leading-order contact interaction dressed with the iterated leading long-range interaction as visualized in Fig. 11. One finds

$$T^{(0)} = \frac{C_0 (k + im_l)^2 [k^2 (\alpha_l - 2) + 2m_l^2 (\alpha_l - 1)]^2}{(k - im_l)^2 [k^2 (\alpha_l - 2) + 2ikm_l (\alpha_l - 2) + 2m_l^2]^2}. \quad (4.96)$$

Notice that all integrals entering $T^{(-1)}$ and $T^{(0)}$ are finite. The effective range function $k \cot \delta$ at NLO can be computed via

$$k \cot \delta = -\frac{4\pi}{m} \frac{1}{T^{(-1)}} \left(1 - \frac{T^{(0)}}{T^{(-1)}} \right) + ik. \quad (4.97)$$

The “chiral” expansion of the coefficients in the ERE results from expanding the right-hand side in this equation in powers of k^2 and, subsequently, in powers of m_l . The LEC C_0 can be determined from matching to $\alpha_a^{(1)}$ in Eq. (4.91) which yields

$$C_0 = \frac{4\pi\alpha_s}{mm_s}. \quad (4.98)$$

This leads to the following predictions for the effective range:

$$r = \frac{1}{m_l} \left[\frac{3\alpha_l - 4}{\alpha_l} + \frac{2(\alpha_l - 1)(3\alpha_l - 4)\alpha_s}{\alpha_l^2 m_s} m_l \right]. \quad (4.99)$$

One observes that $\alpha_r^{(1)}$ is correctly reproduced at NLO. The same holds true for the first shape parameters, see Ref. [67] for explicit expressions. Moreover, using dimensional analysis it is easy to verify that, in fact, $\alpha_{v_i}^{(1)}$ for all i *must* be reproduced correctly at this order. This is a manifestation of the LETs discussed in section 4.2.

At N²LO, the linearly divergent integral $I(k)$ occurs, see Eq. (4.79), which is treated according to Eq. (4.80). Renormalization is carried out by dropping its divergent part $\Delta(\mu)$ and replacing the bare LEC C_0 by the renormalized one $C_0(\mu)$ in the expression for the amplitude. A straightforward calculation using MATHEMATICA yields:

$$T^{(1)} = \frac{(k + im_l)^2}{4\pi^2 m m_s^2 (k - im_l)^2 [k\alpha_l (k + 2im_l) - 2(k + im_l)^2]^2} \left[-32\pi^3 k^2 m_l^3 (\alpha_l - 2) \alpha_l \right. \\ \left. + (C_0(\mu))^2 m^2 m_s^2 [k^2 (\alpha_l - 2) + 2m_l^2 (\alpha_l - 1)]^2 \right. \\ \left. \times \frac{\alpha_l [k^2 (-2\mu - i\pi k) + 2k(\pi k - 2i\mu)m_l + 2\pi m_l^3] + 2(2\mu + i\pi k)(k + im_l)^2}{k\alpha_l (k + 2im_l) - 2(k + im_l)^2} \right]. \quad (4.100)$$

The LEC $C_0(\mu)$ can be written in terms of a perturbative expansion as follows

$$C_0(\mu) = C_0^{(0)} + C_0^{(1)}(\mu) + \dots, \quad (4.101)$$

where the superscript refers to the power of the soft scale Q . The first term does not depend on μ and equals C_0 in Eq. (4.98). The μ -dependence of $C_0^{(1)}(\mu)$ can be determined by solving the renormalization group equation

$$\frac{d}{d\mu} [T^{(-1)} + T^{(0)} + T^{(1)}] = 0. \quad (4.102)$$

One also needs one additional input parameter, such as e. g. $\alpha_a^{(2)}$, in order to fix the integration constant. This leads to

$$C_0^{(1)}(\mu) = \frac{8\mu\alpha_s^2}{mm_s^2}. \quad (4.103)$$

It is then easy to verify that the scattering amplitude $T^{(-1)} + T^{(0)} + T^{(1)}$ is μ -independent up to terms of order Q^2 . Further, the effective range function is given at this order by

$$k \cot \delta = -\frac{4\pi}{m} \frac{1}{T^{(-1)}} \left[1 - \frac{T^{(0)}}{T^{(-1)}} + \left(\frac{T^{(0)}}{T^{(-1)}} \right)^2 - \frac{T^{(1)}}{T^{(-1)}} \right] + ik, \quad (4.104)$$

which can be used to predict the “chiral” expansion for the coefficients in the ERE. Here I list only the result for the effective range which is sufficient for our purposes. The expressions for $v_{2,3}$ can be found in [67].

$$r = \frac{1}{m_l} \left[\frac{3\alpha_l - 4}{\alpha_l} + \frac{2(\alpha_l - 1)(3\alpha_l - 4)\alpha_s}{\alpha_l^2 m_s} m_l + \frac{(\alpha_l - 1)(3\alpha_l - 4)(5\alpha_l - 3)\alpha_s^2 + (2 - \alpha_l)\alpha_l^2 m_l^2}{\alpha_l^3 m_s^2} m_l^2 \right. \\ \left. - \frac{4\mu m_l (\alpha_l - 1)(3\alpha_l - 4)\alpha_s^3 (\pi m_l (3 - 5\alpha_l) + 4\mu\alpha_l)}{\pi^2 \alpha_l^3 m_s^3} + \mathcal{O}(Q^4) \right]. \quad (4.105)$$

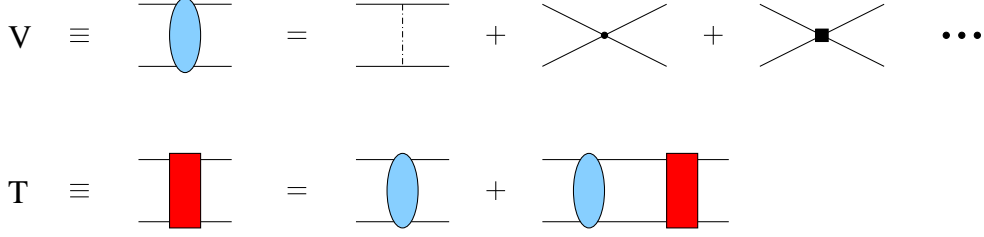


Figure 12: Effective potential and scattering amplitude in the Weinberg-like approach. The dashed-dotted line refers to the full long-range interaction. Solid dot and filled rectangle refer to the leading and subleading contact interactions, respectively. For remaining notation see Fig. 1.

As expected, the first three terms in the “chiral” expansion of r are correctly reproduced at N²LO being protected by the LETs. The same holds true for the shape parameters v_i , see Ref. [67]. The knowledge of $\alpha_{x_j}^{(i)}$ for one particular x_j is sufficient to predict $\alpha_{x_k}^{(i)}$ for all $k \neq j$.

4.5.3 Weinberg-like approach with a finite cutoff

An elegant EFT formulation like the one described above which respects the manifest power counting at every stage of the calculation is not available in the realistic case of nucleon-nucleon interaction. Here, one lacks a regularization prescription for *all* divergent integrals resulting from iterations of the potential in the LS equation which would keep regularization artefacts small without, at the same time, introducing a new hard scale in the problem. Contrary to the considered model, the 1π -exchange potential is non-separable and cannot be analytically resummed in the LS equation. In the context of chiral EFT for few-nucleon systems, the divergent integrals are usually dealt with by introducing an UV cutoff Λ , which needs to be taken of the order $\Lambda \sim m_s$ or higher in order to keep regularization artefacts small. Clearly, cutoff-regularized diagrams will not obey dimensional power counting anymore. This, however, does not mean a breakdown of EFT since power counting is only required for the *renormalized* amplitude. I now consider the Weinberg-like formulation in which the effective potential, given by the long-range interaction and a series of contact terms, is iterated in the LS equation to all orders, see the work by Lepage [74] for a related discussion. This is visualized in Fig. 12. I carry out *renormalization* by literally following the steps outlined in Ref. [74] and summarized in Ref. [75] in the following way: “*The theory is fully specified by the values of the bare constants ... once a suitable regularization procedure is chosen. In principle, the renormalization program is straightforward: one calculates quantities of physical interest in terms of the bare parameters at given, large value of (ultraviolet cutoff) Λ . Once a sufficient number of physical quantities have been determined as functions of the bare parameters one inverts the result and expresses the bare parameters in terms of physical quantities, always working at some given, large value of Λ . Finally, one uses these expressions to eliminate the bare parameters in all other quantities of physical interest. Renormalizability guarantees that this operation at the same time also eliminates the cutoff.*” Notice that by iterating the truncated expansion for the effective potential

in the LS equation one unavoidably generates higher-order contributions without being able to absorb all arising divergences into redefinition of the LECs present in the considered truncated potential. Thus, for the case at hand, cutoff dependence in observables is expected to be eliminated only up to the considered order in the EFT expansion. I further emphasize that expressing the bare parameters (i. e. LECs C_i) in terms of physical quantities is a non-trivial step as the resulting nonlinear equations for $\{C_i\}$ do not necessarily possess real solutions for all values of Λ , especially when it is chosen to be considerably larger than m_s .

To be specific, consider the effective potential at subleading order in the Weinberg-like approach as depicted in Fig. 12

$$V_{\text{eff}}(p', p) = v_l F_l(p') F_l(p) + C_0. \quad (4.106)$$

The off-shell T-matrix $T(p', p; k)$ can be easily calculated by solving the 2×2 matrix equation

$$t(k) = v_{\text{eff}} + v_{\text{eff}} \mathcal{G}(k) t(k) \quad (4.107)$$

where I have defined

$$V_{\text{eff}}(p', p) = \gamma^T(p') v_{\text{eff}} \gamma(p), \quad T(p', p, k) = \gamma^T(p') t(k) \gamma(p), \quad (4.108)$$

with

$$v_{\text{eff}} \equiv \begin{pmatrix} v_l & 0 \\ 0 & C_0 \end{pmatrix}, \quad \gamma(p) \equiv \begin{pmatrix} F_l(p) \\ 1 \end{pmatrix}, \quad \mathcal{G}(k) \equiv \begin{pmatrix} I_l(k) & I_{l1}^{\text{reg}}(k) \\ I_{l1}^{\text{reg}}(k) & I_1^{\text{reg}}(k) \end{pmatrix}. \quad (4.109)$$

The integral $I_l(k)$ is given by

$$I_l(k) = 4\pi m \int_0^\infty \frac{l^2 dl}{(2\pi)^3} \frac{l^2 + m_s^2}{[k^2 - l^2 + i\epsilon][l^2 + m_l^2]^2} = \frac{m(-2ikm_l + m_l^2 + m_s^2)}{8\pi m_l (k + im_l)^2},$$

and is ultraviolet-finite. The divergent integrals $I_1(k)$ and $I_{l1}(k)$ are regularized by means of a finite cutoff Λ :

$$\begin{aligned} I_1^{\text{reg}} &\equiv 4\pi m \int_0^\Lambda \frac{l^2 dl}{(2\pi)^3} \frac{1}{k^2 - l^2 + i\epsilon} = -\frac{m\Lambda}{2\pi^2} - i\frac{mk}{4\pi} + \mathcal{O}(\Lambda^{-1}), \\ I_{l1}^{\text{reg}} &\equiv 4\pi m \int_0^\Lambda \frac{l^2 dl}{(2\pi)^3} \frac{\sqrt{l^2 + m_s^2}}{[k^2 - l^2 + i\epsilon][l^2 + m_l^2]} = \frac{m}{2\pi^2} \left[k \frac{\sqrt{k^2 + m_s^2}}{k^2 + m_l^2} \ln \left(\frac{k + \sqrt{k^2 + m_s^2}}{m_s} \right) \right. \\ &\quad \left. - \frac{m_l m_s s}{2(k^2 + m_l^2)} + \ln \left(\frac{m_s}{2\Lambda} \right) - \frac{i\pi k \sqrt{k^2 + m_s^2}}{2(k^2 + m_l^2)} \right] + \mathcal{O}(\Lambda^{-1}), \end{aligned} \quad (4.110)$$

where $s \equiv \left(2\sqrt{m_s^2 - m_l^2}/m_s \right) \text{arccot} \left(m_l/\sqrt{m_s^2 - m_l^2} \right)$. Neglecting, for the sake of simplicity, the finite cutoff artefacts represented by the $\mathcal{O}(\Lambda^{-1})$ -terms in Eq. (4.110) and performing straightforward calculations, one obtains for the scattering length:

$$a_\Lambda = \frac{\pi m_s \{ C_0 m [2\alpha_l (m_s (\Lambda - sm_l) + 2m_l^2 \ln(m_s/2\Lambda)) + \pi m_l m_s] + 4\pi^2 \alpha_l m_s \}}{m_l \{ 2\pi m_s^2 (C_0 m \Lambda + 2\pi^2) - C_0 m m_l \alpha_l [sm_s - 2m_l \ln(m_s/2\Lambda)]^2 \}}. \quad (4.111)$$

Renormalization is carried out by matching the above expression to the value of the scattering length in the underlying model which is regarded as data,

$$a_{\text{underlying}} = \frac{m_l (2\alpha_l - 1) \alpha_s - \alpha_l m_s}{m_l (m_l \alpha_l \alpha_s - m_s)}, \quad (4.112)$$

and expressing $C_0(\Lambda)$ in terms of $a_{\text{underlying}}$. A straightforward calculation yields the following *renormalized* expression for the effective range:

$$\begin{aligned} r_\Lambda = & \frac{1}{m_l} \left[\frac{3\alpha_l - 4}{\alpha_l} + \frac{2(\alpha_l - 1)(3\alpha_l - 4)\alpha_s}{\alpha_l^2 m_s} m_l + \left(\frac{4(\alpha_l - 2)\alpha_s}{\pi \alpha_l m_s^2} \left(\ln \frac{m_s}{2\Lambda} + 1 \right) \right. \right. \\ & \left. \left. + \frac{(\alpha_l - 1)(3\alpha_l - 4)(5\alpha_l - 3)\alpha_s^2 + (2 - \alpha_l)\alpha_l^2}{\alpha_l^3 m_s^2} \right) m_l^2 + \mathcal{O}(m_l^3) \right]. \end{aligned} \quad (4.113)$$

In agreement with the LETs discussed above, one observes that the subleading terms in the “chiral” expansion of r (and v_i , see [67]) are correctly reproduced once C_0 is appropriately tuned. Notice that the smallness of the subleading correction to r_Λ due to the C_0 -term in the effective potential as compared to the leading contribution given by the first term on the right-hand side of Eq. (4.113) is only guaranteed *after* carrying out renormalization by properly tuning $C_0(\Lambda)$. The sub-subleading and higher-order terms in the “chiral” expansion of r and v_i are not reproduced correctly being not protected by the LETs at the considered order. Moreover, since the included LEC is insufficient to absorb all divergencies arising from iterations of the LS equation, nothing prevents the appearance of positive powers or logarithms of the cutoff Λ in the expressions for $\alpha_r^{(\geq 2)}$. The results in Eq. (4.113) show that this is indeed the case. The dependence on Λ occurs, however, only in contributions beyond the accuracy of calculation and, obviously, does not affect the predictive power of the EFT as long as the cutoff is chosen to be of the order of the characteristic hard scale in the problem, $\Lambda \sim m_s$.

An important misconception that appears frequently in the literature is related to the treatment of the cutoff by employing very large values of Λ or even regarding $\Lambda \rightarrow \infty$. While this is perfectly fine in ChPT, where observables are calculated perturbatively and *all* emerging UV divergencies can be absorbed by the corresponding counterterms at any fixed order in the chiral expansion, this is not a valid procedure for the case at hand. Let us further elaborate on this issue using the above example. At first sight, the appearance of positive powers of Λ and/or logarithmic terms in the predicted “chiral” expansion of the subthreshold parameters, see Eq. (4.113), may give a (wrong) impression that no finite limit exists for r_Λ and $(v_i)_\Lambda$ as $\Lambda \rightarrow \infty$. Actually, taking the limit $\Lambda \rightarrow \infty$ does not commute with the Taylor expansion of the ERE coefficients in powers of m_l . Substituting the value for $C_0(\Lambda)$ resulting from matching Eq. (4.111) to (4.112) into the solution of the LS equation (4.107) and taking the limit $\Lambda \rightarrow \infty$ yields the following finite, cutoff-independent result for the inverse amplitude:

$$\begin{aligned} (T_\infty)^{-1} = & i \frac{km}{4\pi} - \frac{m}{8\pi m_l^3 (k^2 + m_s^2) (\alpha_l m_s + m_l (1 - 2\alpha_l) \alpha_s)} \left(2m_l^4 m_s^2 (m_s - m_l \alpha_l \alpha_s) \right. \\ & + k^2 m_l^2 ((4 - 3\alpha_l) m_s^3 + m_l^2 \alpha_l m_s + m_l \alpha_s ((2\alpha_l - 3) m_s^2 + m_l^2 (1 - 2\alpha_l))) \\ & \left. + k^4 (-\alpha_l m_s (m_l^2 + m_s^2) - m_l \alpha_s (m_l^2 (1 - 2\alpha_l) + m_s^2) + 2m_s^3) \right). \end{aligned} \quad (4.114)$$

The corresponding infinite-cutoff prediction for the effective range has the form:

$$r_\infty = \frac{1}{m_l} \left[\frac{3\alpha_l - 4}{\alpha_l} + \frac{4(\alpha_l - 1)^2 \alpha_s}{\alpha_l^2 m_s} m_l + \frac{\alpha_l^3 (8\alpha_s^2 - 1) + \alpha_l^2 (2 - 20\alpha_s^2) + 16\alpha_l \alpha_s^2 - 4\alpha_s^2}{\alpha_l^3 m_s^2} m_l^2 + \dots \right], \quad (4.115)$$

where the ellipses refer to $\mathcal{O}(m_l^3)$ -terms. One observes that the result after removing the cutoff fails to reproduce the low-energy theorem by yielding a wrong value for $\alpha_r^{(1)}$. This also holds true for the $\alpha_{v_i}^{(1)}$ [67]. Notice that, by construction, the scattering length is still correctly reproduced. The breakdown of LETs in the Weinberg-like approach in the $\Lambda \rightarrow \infty$ limit can be traced back to spurious Λ -dependent contributions still appearing in renormalized expressions for observables, see Eq. (4.113), which are irrelevant at the order the calculations are performed in the regime $\Lambda \sim m_s$ but become numerically dominant if $\Lambda \gg m_s$. Due to non-renormalizability of the effective potential as discussed above, such spurious terms do, in general, involve logarithms and positive powers of Λ which, as Λ gets increased beyond the hard scale m_s , become, at some point, comparable in size with lower-order terms in the “chiral” expansion. For example, the appearance of terms linear in Λ would suggest the breakdown of LETs as the cutoff approaches the scale $\Lambda \sim m_s^2/m_l$. The unavoidable appearance of ever higher power-law divergences when going to higher orders in the EFT expansion implies that the cutoff should not be increased beyond the pertinent hard scale in Weinberg-like or Lepage-like approach to NN scattering leading to $\Lambda \sim m_s$ as the optimal choice. It is furthermore instructive to compare the predictions for the effective range in Eqs. (4.105) and (4.113) corresponding to two different renormalization schemes. One observes that taking $\Lambda \gg m_s$ in Eq. (4.113) has an effect which is qualitatively similar to choosing $\mu \gg m_l$ in Eq. (4.105) and corresponds to an improper choice of renormalization conditions in the EFT framework.

4.5.4 Toy model with local interactions: a numerical example

Having clarified the important conceptual issues related to nonperturbative renormalization in the context of chiral EFT for two nucleons, I now turn to the last toy-model example and give some numerical results.

Consider two nucleons interacting via the local force given by a superposition of two Yukawa potentials corresponding to the (static) exchange of the scalar light and heavy mesons of masses m_l and m_s , respectively:

$$V(r) = \alpha_l \frac{e^{-m_l r}}{r} + \alpha_s \frac{e^{-m_s r}}{r} \quad (4.116)$$

This type of potentials is sometimes referred to as Malfliet-Tjon potential. Motivated by the realistic case of the two-nucleon force, I choose the meson masses to be $m_l = 200$ MeV and $m_s = 750$ MeV. Further, I adjust the dimensionless strengths $\alpha_{l,s}$ in such a way that the potential features an S-wave bound state (“deuteron”) with the binding energy $E_B = 2.2229$ MeV. A suitable combination is given by $\alpha_l = -1.50$ and $\alpha_s = 10.81$. With the parameters specified in this way, the potential is depicted in Fig. 13. The corresponding momentum-space potential can be easily obtained by making the Fourier

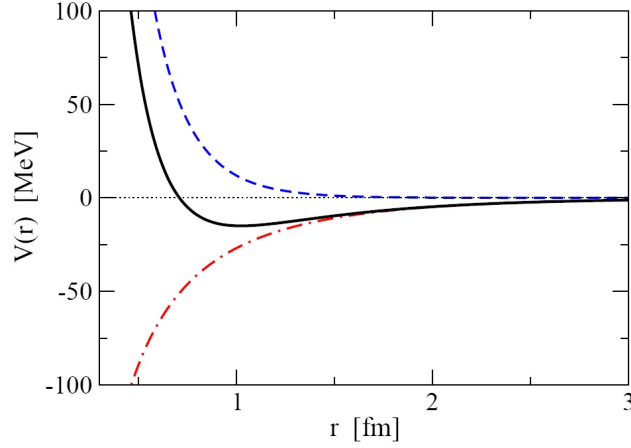


Figure 13: Toy-model potential in Eq. (4.116). The dashed (dashed-dotted) line depicts the short-range (long-range) part proportional to α_s (α_l) while the full potential is shown by the solid line.

transformation:

$$V(\vec{p}', \vec{p}) = \frac{4\pi\alpha_l}{\vec{q}^2 + m_l^2} + \frac{4\pi\alpha_s}{\vec{q}^2 + m_s^2}. \quad (4.117)$$

Here, $\vec{q} = \vec{p}' - \vec{p}$ denotes the momentum transfer. I treat the nucleons in this example as identical, spinless particles. Thus, in the partial wave basis, the only nonvanishing matrix elements $\langle l', j, p' | V | l, j, p \rangle$ correspond to $l = l' = j$. I only consider the S-wave here. Because of no spin dependence, the matrix element $V_0(p', p) \equiv \langle 0, 0, p' | V | 0, 0, p \rangle$ can be obtained by simply integrating over the angle θ between \vec{p}' and \vec{p} :

$$\begin{aligned} V_0(p', p) &= 2\pi \int_{-1}^{+1} d(\cos \theta) V(p', p, \theta) \\ &= \alpha_l \frac{4\pi^2}{p'p} \ln \left(\frac{(p' + p)^2 + m_l^2}{(p' - p)^2 + m_l^2} \right) + \alpha_s \frac{4\pi^2}{p'p} \ln \left(\frac{(p' + p)^2 + m_s^2}{(p' - p)^2 + m_s^2} \right) \\ &\equiv V_0^l(p', p) + V_0^s(p', p). \end{aligned} \quad (4.118)$$

Contrary to the previously considered case of a separable interaction, the LS equation

$$T_0(p, p'; k) = V_0(p, p') + \int \frac{l^2 dl}{(2\pi)^3} V_0(p, l) \frac{m}{k^2 - l^2 + i\epsilon} T_0(l, p'; k), \quad (4.119)$$

cannot be solved analytically for the Malfliet-Tjon-type potentials. It can, however, be solved numerically using the standard methods, see e.g. [12]. With the parameters specified above, one obtains the phase shift which is shown by the solid line in the left panel of Fig. 14. It is fairly similar to the neutron-proton 3S_1 phase shift, cf. the left panel of Fig. 1.

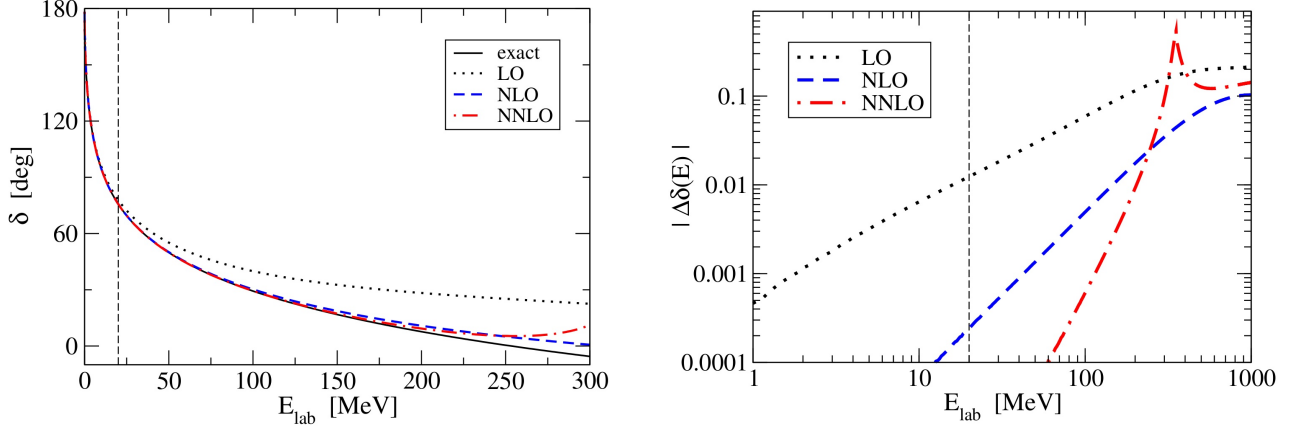


Figure 14: Left panel: phase shifts resulting from the original and effective potentials in Eqs. (4.117) and (4.120), respectively. Right panel: Lepage plot showing the absolute error in phase shifts at various orders in the low-momentum expansion versus lab. energy.

I now develop an effective potential that describes the same physics as the underlying one at momenta of the order of $Q \sim m_l$. Up to N²LO, it takes the form:¹¹

$$V_0^{\text{eff}}(p', p) = V_0^l(p', p) + [C_0 + C_2(p'^2 + p^2) + C_4 p'^2 p^2] f_\Lambda(p', p) \quad (4.120)$$

The regulator function prevents the appearance of ultraviolet divergences in the LS equation and is chosen of the form:

$$f_\Lambda(p', p) = \exp\left(-\frac{p'^2 + p^2}{\Lambda^2}\right). \quad (4.121)$$

I set the cutoff $\Lambda = 500$ MeV, solve the LS equation with the effective potential $V_0^{\text{eff}}(p', p)$ and adjust the LECs to reproduce the coefficients in the ERE as follows:

- LO: $C_2 = C_4 = 0$, C_0 is tuned to reproduce a ;
- NLO: $C_4 = 0$, $C_{0,2}$ are tuned to reproduce $\{a, r\}$;
- N²LO: $C_{0,2,4}$ are tuned to reproduce $\{a, r, v_2\}$.

With the LECs being fixed as described above, the predictions for the S-wave phase shift at various orders in the low-momentum expansion are summarized in the left panel of Fig. 14. The so-called Lepage plot in the right panel of this figure shows absolute errors in the phase shift, $\Delta\delta(E_{\text{lab}}) \equiv \delta_{\text{underlying}} - \delta_{\text{eff}}$, versus energy. It is plotted in radians. One reads off from this plot that the laboratory energy, at which the expansion breaks down, is of the order of $E_{\text{lab}} = 2k^2/m \sim 250$ MeV. This corresponds to the

¹¹One can write down another contact interaction with four derivatives whose matrix elements in the on-shell kinematics, i.e. with $p = p'$, cannot be disentangled from the C_4 -term.

momentum scale of the order of $\tilde{\Lambda} \sim 350$ MeV, in a good agreement with the expected breakdown scale of the modified effective range expansion of the order of $m_s/2$, see section 4.2. Notice that the effective theory is, as desired, able to go beyond the ERE, whose range of convergence is indicated by the vertical lines in Fig. 14. The “deuteron” binding energy is found to be reproduced correctly with 5 significant digits at N²LO:

$$E_B^{LO} + \delta E_B^{NLO} + \delta E_B^{N^2LO} = 2.1594 + 0.638 - 0.0003 = 2.2229 \text{ MeV} . \quad (4.122)$$

For further illustrative quantum mechanical examples and a discussion on renormalization in the context of the Schrödinger equation, the reader is referred to the excellent lecture notes by Lepage [74].

5 Nuclear forces from chiral EFT

In this section I outline and exemplify some methods which can be used to derive nuclear forces from chiral EFT.

5.1 Derivation of nuclear potentials from field theory

The derivation of a potential from field theory is an extensively studied problem in nuclear physics. Historically, the important conceptual achievements in this field have been done in the fifties of the last century in the context of the so-called meson field theory. The problem can be formulated in the following way: given a field theoretical Lagrangian for interacting mesons and nucleons, how can one reduce the (infinite dimensional) equation of motion for mesons and nucleons to an effective Schrödinger equation for nucleonic degrees of freedom, which can be solved by standard methods? It goes beyond the scope of this work to address the whole variety of different techniques which have been developed to construct effective interactions, see Ref. [76] for a comprehensive review. I will now briefly outline a few methods which have been used in the context of chiral EFT. Similar methods are frequently used in computational nuclear physics in order to reduce a problem to a smaller model space which can be treated numerically.

I begin with the approach developed by Tamm [77] and Dancoff [78] which in the following will be referred to as the Tamm-Dancoff (TD) method. Consider the time-independent Schrödinger equation

$$(H_0 + H_I)|\Psi\rangle = E|\Psi\rangle , \quad (5.123)$$

where $|\Psi\rangle$ denotes an eigenstate of the Hamiltonian H with the eigenvalue E . One can divide the full Fock space in to the nucleonic subspace $|\phi\rangle$ and the complementary one $|\psi\rangle$ and rewrite the Schrödinger equation (5.123) as

$$\begin{pmatrix} \eta H \eta & \eta H \lambda \\ \lambda H \eta & \lambda H \lambda \end{pmatrix} \begin{pmatrix} |\phi\rangle \\ |\psi\rangle \end{pmatrix} = E \begin{pmatrix} |\phi\rangle \\ |\psi\rangle \end{pmatrix} , \quad (5.124)$$

where I introduced the projection operators η and λ such that $|\phi\rangle = \eta|\Psi\rangle$, $|\psi\rangle = \lambda|\Psi\rangle$. Expressing the state $|\psi\rangle$ from the second line of the matrix equation (5.124) as

$$|\psi\rangle = \frac{1}{E - \lambda H \lambda} H |\phi\rangle, \quad (5.125)$$

and substituting this in to the first line, one obtains the Schroedinger-like equation for the projected state $|\phi\rangle$:

$$(H_0 + V_{\text{eff}}^{\text{TD}}(E)) |\phi\rangle = E |\phi\rangle, \quad (5.126)$$

with an effective potential $V_{\text{eff}}(E)$ given by

$$V_{\text{eff}}^{\text{TD}}(E) = \eta H_I \eta + \eta H_I \lambda \frac{1}{E - \lambda H \lambda} \lambda H_I \eta. \quad (5.127)$$

This definition of the effective potential corresponds exactly to the one given in section 4.1 in the context of “old-fashioned” time-ordered perturbation theory. To evaluate $V_{\text{eff}}^{\text{TD}}(E)$ one usually relies on perturbation theory. For example, for the Yukawa theory with a single πNN vertex $H_I = g H_1$, $V_{\text{eff}}^{\text{TD}}(E)$ up to the fourth order in the coupling constant g is given by

$$V_{\text{eff}}^{\text{TD}}(E) = -\eta' \left[g^2 H_1 \frac{\lambda^1}{H_0 - E} H_1 + g^4 H_1 \frac{\lambda^1}{H_0 - E} H_1 \frac{\lambda^2}{H_0 - E} H_1 \frac{\lambda^1}{H_0 - E} H_1 + \mathcal{O}(g^6) \right] \eta, \quad (5.128)$$

where the superscripts of λ refer to the number of mesons in the corresponding state. It is important to realize that the effective potential $V_{\text{eff}}(E)$ in this scheme depends explicitly on the energy, which makes it inconvenient for practical applications (especially for calculations beyond the two-nucleon system). In addition, the projected nucleon states $|\phi\rangle$ have a different normalization compared to the states $|\Psi\rangle$ we have started from (which are assumed to span a complete and orthonormal set in the whole Fock space)

$$\langle \phi_i | \phi_j \rangle = \langle \Psi_i | \Psi_j \rangle - \langle \psi_i | \psi_j \rangle = \delta_{ij} - \langle \phi_i | H_I \lambda \left(\frac{1}{E - \lambda H \lambda} \right)^2 \lambda H_I | \phi_j \rangle, \quad (5.129)$$

since the components ψ_i do, in general, not vanish.

The above mentioned deficiencies are naturally avoided in the method of unitary transformation [79, 80]. In this approach, the decoupling of the η - and λ -subspaces of the Fock space is achieved via a unitary transformation U

$$\tilde{H} \equiv U^\dagger H U = \begin{pmatrix} \eta \tilde{H} \eta & 0 \\ 0 & \lambda \tilde{H} \lambda \end{pmatrix}. \quad (5.130)$$

Following Okubo [79], the unitary operator U can be parametrized as

$$U = \begin{pmatrix} \eta(1 + A^\dagger A)^{-1/2} & -A^\dagger(1 + A A^\dagger)^{-1/2} \\ A(1 + A^\dagger A)^{-1/2} & \lambda(1 + A A^\dagger)^{-1/2} \end{pmatrix}, \quad (5.131)$$

with the operator $A = \lambda A \eta$. The operator A has to satisfy the decoupling equation

$$\lambda (H - [A, H] - A H A) \eta = 0 \quad (5.132)$$

in order for the transformed Hamiltonian \tilde{H} to be of block-diagonal form. The effective η -space potential $\tilde{V}_{\text{eff}}^{\text{UT}}$ can be expressed in terms of the operator A as:

$$\tilde{V}_{\text{eff}}^{\text{UT}} = \eta(\tilde{H} - H_0) = \eta \left[(1 + A^\dagger A)^{-1/2} (H + A^\dagger H + H A + A^\dagger H A) (1 + A^\dagger A)^{-1/2} - H_0 \right] \eta. \quad (5.133)$$

The solution of the decoupling equation and the calculation of the effective potential according to Eq. (5.133) can be carried out perturbatively in the weak-coupling case. For the previously considered case of the Yukawa theory, the decoupling equation can be solved recursively by making the ansatz

$$A = \sum_{n=1}^{\infty} g^n A^{(n)}. \quad (5.134)$$

The resulting effective potential $V_{\text{eff}}^{\text{UT}}$ takes the form:

$$\begin{aligned} V_{\text{eff}}^{\text{UT}} = & -g^2 \eta' \left[\frac{1}{2} H_1 \frac{\lambda^1}{H_0 - E_\eta} H_1 + \text{h. c.} \right] \eta - g^4 \eta' \left[\frac{1}{2} H_1 \frac{\lambda^1}{(H_0 - E_\eta)} H_1 \frac{\lambda^2}{(H_0 - E_\eta)} H_1 \frac{\lambda^1}{(H_0 - E_\eta)} H_1 \right. \\ & - \frac{1}{2} H_1 \frac{\lambda^1}{(H_0 - E_{\eta'})} H_1 \tilde{\eta} H_1 \frac{\lambda^1}{(H_0 - E_{\tilde{\eta}})(H_0 - E_{\eta'})} H_1 \\ & + \frac{1}{8} H_1 \frac{\lambda^1}{(H_0 - E_{\eta'})} H_1 \tilde{\eta} H_1 \frac{\lambda^1}{(H_0 - E_{\tilde{\eta}})(H_0 - E_\eta)} H_1 \\ & \left. - \frac{1}{8} H_1 \frac{\lambda^1}{(H_0 - E_{\eta'})(H_0 - E_{\tilde{\eta}})} H_1 \tilde{\eta} H_1 \frac{\lambda^1}{(H_0 - E_{\tilde{\eta}})} H_1 + \text{h. c.} \right] \eta + \mathcal{O}(g^6). \quad (5.135) \end{aligned}$$

Here, η , η' and $\tilde{\eta}$ denote projection operators onto the purely nucleonic states. Different notation is only used to indicate what state the energies in the denominators correspond to. In contrast to $V_{\text{eff}}^{\text{TD}}$, $V_{\text{eff}}^{\text{UT}}$ does not depend on the energy E which enters the Schrödinger equation. Another difference to the Tamm-Dancoff method is given by the presence of terms with the projection operator $\tilde{\eta}$ which give rise to purely nucleonic intermediate states. These terms are responsible for the proper normalization of the few-nucleon states. In spite of the presence of the purely nucleonic intermediate states, such terms are not generated through the iteration of the dynamical equation and are truly irreducible. Since *all* energy denominators entering $V_{\text{eff}}^{\text{UT}}$ correspond to intermediate states with at least one pion, there is no enhancement by large factors of m/Q that occurs for reducible contributions.

Exercise:

1. Calculate A^1 , $A^{(2)}$ and $A^{(3)}$ by solving the decoupling equation for the considered case of Yukawa theory and verify the expression for $V_{\text{eff}}^{\text{UT}}$ in Eq. (5.135).
 2. Consider the disconnected Feynman diagram in Fig. 15 and draw all possible time-ordered diagrams. Using Eqs. (5.128) and (5.135) show that, in contrast to the TD approach, these diagrams do not contribute to the nucleon-nucleon potential in the method of unitary transformation. Use the static approximation for the nucleons in order to simplify the calculations (i.e. set: $E = E_\eta = E_{\eta'} = E_{\tilde{\eta}} = 0$).
-

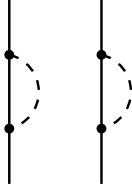


Figure 15: An example of a disconnected diagram that does not contribute to the NN potential in the method of unitary transformation.

The two methods of deriving effective nuclear potentials are quite general and can, in principle, be applied to any field theoretical meson-nucleon Lagrangian. In the weak-coupling case, the potential can be obtained straightforwardly via the expansion in powers of the corresponding coupling constant(s). For practical applications, it is helpful to use time-ordered diagrams to visualize the contributions to the potential, see Fig. 6. In “old-fashioned” perturbation theory or, equivalently, the Tamm-Dancoff approach, only irreducible diagrams contribute to the potential. In the method of unitary transformation one can draw both irreducible and reducible graphs whose meaning, however, differs from that of diagrams emerging in time-ordered perturbation theory. The coefficients in front of various operators and the energy denominators can, in general, not be guessed by looking at a given diagram and have to be determined by solving the decoupling equation (5.132) for the operator A and using Eq. (5.133).

Application of the above methods to the effective chiral Lagrangian requires the expansion in powers of the coupling constants to be replaced by the chiral expansion in powers of Q/Λ_χ . This issue will be dealt with in the next section.

5.2 Method of unitary transformation

To apply the method of unitary transformation to derive nuclear forces in chiral EFT it is useful to rewrite the power counting discussed in section 4.1 into a different form which is more suitable to carry out algebraic manipulations described above.

We begin with Weinberg’s original power counting expression for N -nucleon diagrams involving C separately connected pieces:

$$\nu = 4 - N + 2(L - C) + \sum_i V_i \Delta_i, \quad \Delta_i = d_i + \frac{1}{2}n_i - 2. \quad (5.136)$$

This expression is a generalization of Eq. (4.58) to the case $C > 1$. Its derivation can be found in Ref. [81]. There is one subtlety here that needs to be addressed: according to Eq. (5.136), the chiral dimension ν for a given process depends on the total number of nucleons in the system. For example, one-pion exchange in the two-nucleon system corresponds to $N = 2$, $L = 0$, $C = 1$ and $\sum_i V_i \Delta_i = 0$ and, therefore, contributes at order $\nu = 0$. On the other hand, the same process in the presence of a

third (spectator) nucleon leads, according to Eq. (5.136), to $\nu = -3$ since $N = 3$ and $C = 2$. The origin of this seeming discrepancy is due to the different normalization of the 2N and 3N states:

$$\begin{aligned} 2N : \quad & \langle \vec{p}_1 \vec{p}_2 | \vec{p}_1' \vec{p}_2' \rangle = \delta^3(\vec{p}_1' - \vec{p}_1) \delta^3(\vec{p}_2' - \vec{p}_2), \\ 3N : \quad & \langle \vec{p}_1 \vec{p}_2 \vec{p}_3 | \vec{p}_1' \vec{p}_2' \vec{p}_3' \rangle = \delta^3(\vec{p}_1' - \vec{p}_1) \delta^3(\vec{p}_2' - \vec{p}_2) \delta^3(\vec{p}_3' - \vec{p}_3). \end{aligned} \quad (5.137)$$

It can be circumvented by assigning a chiral dimension to the transition operator rather than to its matrix elements in the N -nucleon space. Adding the factor $3N - 6$ to the right-hand side of Eq. (5.136) in order to account for the normalization of the N -nucleon states and to ensure that the LO contribution to the nuclear force appears at order $\nu = 0$ we obtain

$$\nu = -2 + 2N + 2(L - C) + \sum_i V_i \Delta_i. \quad (5.138)$$

This expression provides a natural qualitative explanation of the observed hierarchy of nuclear forces $V_{2N} \gg V_{3N} \gg V_{4N} \dots$ with

$$\begin{aligned} V_{2N} &= V_{2N}^{(0)} + V_{2N}^{(2)} + V_{2N}^{(3)} + V_{2N}^{(4)} + \dots, \\ V_{3N} &= V_{3N}^{(3)} + V_{3N}^{(4)} + \dots, \\ V_{4N} &= V_{4N}^{(4)} + \dots, \end{aligned} \quad (5.139)$$

as shown in Fig. 16.

The form of power counting in Eq. (5.138) is still of less use for our purpose since the resulting chiral dimension is given in terms of the topological quantities such as N , C and L which is not appropriate for algebraic approaches such as the method of unitary transformation. Using certain topological identities, see [82], Eq. (5.138) can be rewritten in a more suitable form:

$$\nu = -2 + \sum_i V_i \kappa_i, \quad \kappa_i = d_i + \frac{3}{2}n_i + p_i - 4. \quad (5.140)$$

The quantity κ_i which enters this expression is nothing but the canonical field dimension of a vertex of type i (up to the additional constant -4) and gives the inverse mass dimension of the corresponding coupling constant. In fact, this result can be obtained immediately by counting inverse powers of the hard scale Λ_χ rather than powers of the soft scale Q (which is, of course, completely equivalent). Indeed, since the only way for the hard scale to be generated is through the physics behind the LECs, the power ν is just the negative of the overall mass dimension of all LECs. The additional factor -2 in Eq. (5.140) is a convention to ensure that the contributions to the nuclear force start at $\nu = 0$. I encourage the reader to verify the equivalence of Eqs. (5.140) and (5.138) for specific diagrams. One immediately reads off from Eq. (5.140) that in order for perturbation theory to work, the effective Lagrangian must contain no renormalizable and super-renormalizable interactions with $\kappa_i = 0$ and $\kappa_i < 0$, respectively, since otherwise adding new vertices would not increase or even lower the chiral dimension ν . This feature is guaranteed by the spontaneously broken chiral symmetry of QCD which ensures that only non-renormalizable interactions enter the effective Lagrangian.

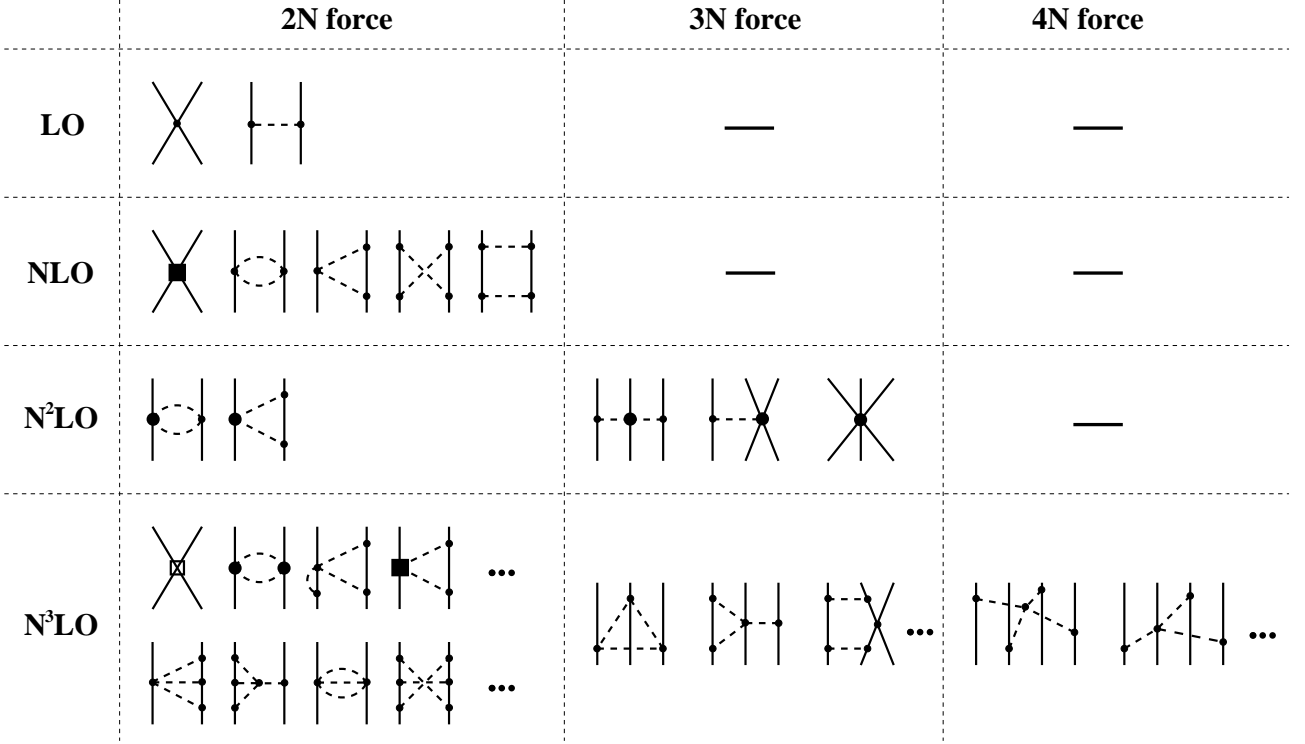


Figure 16: Diagrams that give rise to nuclear forces in ChEFT based on Weinberg's power counting. Solid and dashed lines denote nucleons and pions, respectively. Solid dots, filled circles and filled squares and crossed squares refer to vertices with $\Delta_i = 0, 1, 2$ and 4 , respectively.

While Eq. (5.140) does not say much about the topology and is, therefore, not particularly useful to deal with diagrams, it is very convenient for algebraical calculations. In fact, it formally reduces the chiral expansion to the expansion in powers of the coupling constant, whose role is now played by the ratio Q/Λ . Applying the canonical transformation to the chiral Lagrangian and writing the resulting Hamiltonian in the form

$$H_I = \sum_{\kappa=1}^{\infty} H^{\kappa}, \quad (5.141)$$

the operator A can be calculated by solving Eq. (5.130) recursively,

$$A = \sum_{\alpha=1}^{\infty} A^{(\alpha)}, \quad (5.142)$$

$$A^{(\alpha)} = \frac{1}{E_{\eta} - E_{\lambda}} \lambda \left[H^{(\alpha)} + \sum_{i=1}^{\alpha-1} H^{(i)} A^{(\alpha-i)} - \sum_{i=1}^{\alpha-1} A^{(\alpha-i)} H^{(i)} - \sum_{i=1}^{\alpha-2} \sum_{j=1}^{\alpha-i-1} A^{(i)} H^{(j)} A^{(\alpha-i-j)} \right] \eta.$$

The expressions for the unitary operator and the effective potential then follow immediately by substi-

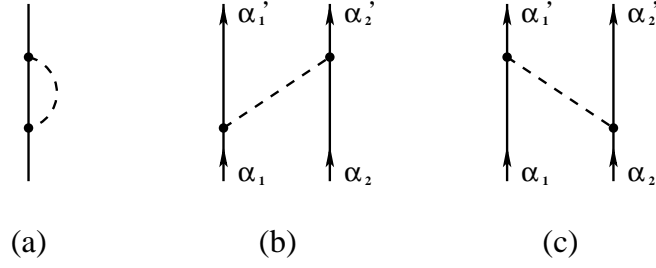


Figure 17: Diagrams that correspond to the operator in Eq. (5.144). Graph (a) yields a single-body contribution to the nuclear Hamilton operator while diagrams (b) and (c) give rise to the 1π -exchange NN potential.

tuting Eqs. (5.141) and (5.142) into Eq. (5.133).

5.3 The 1π - and the leading 2π -exchange potentials

I now illustrate how the above ideas can be applied in practice. I begin with the simple case of the 1π -exchange potential at leading order, i.e. $\nu = 0$. The only relevant contribution to the interaction Hamilton density is given by

$$\mathcal{H}^{(1)} = \frac{g_A}{2F_\pi} N^\dagger \vec{\sigma} \cdot (\vec{\nabla} \boldsymbol{\pi} \cdot \boldsymbol{\tau}) N, \quad (5.143)$$

where the superscript of \mathcal{H} gives the canonical dimension κ_i defined in Eq. (5.140). The relevant operator that contributes to the effective Hamiltonian after performing the unitary transformation is given by the first two terms in Eq. (5.135):

$$V_{\text{eff}}^{\text{UT}} = -\eta H^{(1)} \frac{\lambda^1}{\omega} H^{(1)} \eta, \quad (5.144)$$

where ω denotes the pion free energy and I made use of the static approximation as appropriate at LO.¹² Notice that $V_{\text{eff}}^{\text{UT}}$ in the above equation also gives rise to a one-body operator that contributes to the nucleon mass shift, see graph (a) in Fig. 17. To compute the expression for the 1π -exchange potential I first express the pion and nucleon fields in the interaction picture in terms of the creation and destruction operators:

$$\begin{aligned} \pi_i(x) &= \int \frac{d^3k}{(2\pi)^{3/2}} \frac{1}{\sqrt{2\omega_k}} \left[e^{-ik \cdot x} a_i(\vec{k}) + e^{ik \cdot x} a_i^\dagger(\vec{k}) \right], \\ N(x) &= \sum_{ts} \int \frac{d^3p}{(2\pi)^{3/2}} \sum_{ts} e^{-ip \cdot x} v(s) \epsilon(t) b_t(\vec{p}, s), \end{aligned} \quad (5.145)$$

¹²Corrections to the static 1π -exchange potential are suppressed by Q^2/m^2 .

where $\omega_k = \sqrt{\vec{k}^2 + m_\pi^2}$ and $v(\epsilon)$ denotes a Pauli spinor (isospinor). $a_i(\vec{k})$ and $a_i^\dagger(\vec{k})$ denote a destruction and creation operator of a pion with isospin i . Further, $b_t(\vec{p}, s)$ ($b_t^\dagger(\vec{p}, s)$) is the destruction (creation) operator of a non-relativistic nucleon (i.e. $p_0 = \vec{p}^2/(2m)$) with the spin and isospin quantum numbers s and t and momentum \vec{p} . The creation and destruction operators of the pion (nucleon) field satisfy the usual commutation (anti-commutation) relations. The 1π -exchange potential can be calculated by substituting the expressions in Eq. (5.145) for pion and nucleon fields into Eq. (5.144) and evaluating the matrix element

$$\langle \alpha'_1 \alpha'_2 | -\eta H^{(1)} \frac{\lambda^1}{\omega} H^{(1)} \eta | \alpha_1 \alpha_2 \rangle \equiv \frac{1}{(2\pi)^3} \delta^3(\vec{P}' - \vec{P}) V_{2N}^{1\pi}. \quad (5.146)$$

Here, \vec{P} (\vec{P}') denotes the total momentum of the nucleons before (after) the interaction takes place. Further, α_i and α'_i denote collectively the initial and final quantum numbers of the nucleon i (momentum, spin and isospin). To keep the expressions for the potential compact, they are commonly given in the operator form with respect to the spin and isospin quantum numbers using the corresponding Pauli matrices $\vec{\sigma}_i$ and $\vec{\tau}_i$ of a nucleon i . A straightforward calculation yields the final form of the 1π -exchange potential:

$$V_{2N}^{1\pi} = -\frac{g_A^2}{4F_\pi^2} \frac{\vec{\sigma}_1 \cdot \vec{q} \vec{\sigma}_2 \cdot \vec{q}}{\vec{q}^2 + M_\pi^2} \vec{\tau}_1 \cdot \vec{\tau}_2. \quad (5.147)$$

Clearly, this familiar result for the static 1π -exchange potential can be obtained in a much simpler way by evaluating the corresponding Feynman diagram since it does not generate reducible topologies. One-loop corrections to the static 1π -exchange potential and renormalization within the method of unitary transformation are discussed in detail in Ref. [83]. Notice further that when calculating the matrix element in Eq. (5.146), I discarded the contributions corresponding to graph (a) in Fig. 5.144 with one of the nucleons being a spectator and the contributions from diagrams (b) and (c) with the nucleon labels α'_1 and α'_2 being interchanged. The latter emerge automatically when the potential is inserted into the corresponding dynamical equation due to the antisymmetric nature of the two-nucleon wave function.

As a final example, I discuss the leading 2π -exchange potential arising at order $\nu = 2$ from the box and crossed box diagrams (the last two diagrams in the second row in Fig. 16. Again, the only vertex we need is given in Eq. (5.143). The relevant operators that contribute to the effective nuclear Hamiltonian after performing the unitary transformation are listed in Eq. (5.135)

$$\begin{aligned} V_{\text{eff}}^{\text{UT}} = & -\eta H^{(1)} \frac{\lambda^1}{\omega} H^{(1)} \frac{\lambda^2}{\omega_1 + \omega_2} H^{(1)} \frac{\lambda^1}{\omega} H^{(1)} \eta + \frac{1}{2} \eta H^{(1)} \frac{\lambda^1}{\omega^2} H^{(1)} \eta H^{(1)} \frac{\lambda^1}{\omega} H^{(1)} \eta \\ & + \frac{1}{2} \eta H^{(1)} \frac{\lambda^1}{\omega} H^{(1)} \eta H^{(1)} \frac{\lambda^1}{\omega^2} H^{(1)} \eta. \end{aligned} \quad (5.148)$$

The contribution to the 2π -exchange potential results from evaluating the matrix element $\langle \alpha'_1 \alpha'_2 | V_{\text{eff}}^{\text{UT}} | \alpha_1 \alpha_2 \rangle$ which can be computed along the same lines as above. Calculations of that kind can be optimized by using a diagrammatic approach and formulating a sort of “Feynman” rules. The building blocks are given by vertices and energy denominators that play the role of propagators in Feynman diagrams.

Consider, for example, time-ordered box diagrams (b)-(g) in Fig. 6. All these graphs have an identical sequence of non-commuting vertices generating exactly the same isospin-spin-momentum structure in the resulting potential. Thus, the energy denominators for different diagrams arising from the operators in Eq. (5.148) can be added together yielding the result

$$2 \frac{\omega_1^2 + \omega_1 \omega_2 + \omega_2^2}{\omega_1^2 \omega_2^2 (\omega_1 + \omega_2)}. \quad (5.149)$$

The same result but with an opposite sign is obtained for the sum of the energy denominators for the crossed-box diagrams.

Exercise: show that the operators in Eq. (5.148) do not give rise to the 2π -exchange three-nucleon force. What would be the result for the three-nucleon force if one would employ time-ordered perturbation theory (in the static approximation) instead of the method of unitary transformation?

The vertex in Eq. (5.143) gives rise to the “Feynman” rule

$$i \frac{g_A}{2F_\pi} \tau_i^a \vec{\sigma}_i \cdot \vec{q} \frac{1}{\sqrt{2\omega_q}}, \quad (5.150)$$

for an incoming (outgoing) pion with momentum \vec{q} ($-\vec{q}$) and the isospin quantum number a . Here, i is the nucleon label. Putting everything together, we end up with the contribution from the box diagram of the form

$$\begin{aligned} V_{2N}^{2\pi, \text{box}}(\vec{q}) &= (2\pi)^3 \left(\frac{g_A}{2F_\pi} \right)^4 \tau_1 \cdot \tau_2 \tau_1 \cdot \tau_2 \int \frac{d^3 l_1}{(2\pi)^3} \frac{d^3 l_2}{(2\pi)^3} \vec{\sigma}_1 \cdot \vec{l}_1 \vec{\sigma}_1 \cdot \vec{l}_2 \vec{\sigma}_2 \cdot \vec{l}_1 \vec{\sigma}_2 \cdot \vec{l}_2 \\ &\times \frac{1}{2\omega_{l_1}} \frac{1}{2\omega_{l_2}} 2 \frac{\omega_{l_1}^2 + \omega_{l_1} \omega_{l_2} + \omega_{l_2}^2}{\omega_{l_1}^2 \omega_{l_2}^2 (\omega_{l_1} + \omega_{l_2})} \delta(\vec{l}_1 + \vec{l}_2 - \vec{q}), \end{aligned} \quad (5.151)$$

where the factor $(2\pi)^3$ in front of the integral is due to the normalization of the potential, see Eq. (5.146). The contribution of the crossed-box diagrams can be written as

$$\begin{aligned} V_{2N}^{2\pi, \text{cr.-box}}(\vec{q}) &= -(2\pi)^3 \left(\frac{g_A}{2F_\pi} \right)^4 \sum_a \tau_1^a \tau_1 \cdot \tau_2 \tau_2^a \int \frac{d^3 l_1}{(2\pi)^3} \frac{d^3 l_2}{(2\pi)^3} \vec{\sigma}_1 \cdot \vec{l}_1 \vec{\sigma}_1 \cdot \vec{l}_2 \vec{\sigma}_2 \cdot \vec{l}_2 \vec{\sigma}_2 \cdot \vec{l}_1 \\ &\times \frac{1}{2\omega_{l_1}} \frac{1}{2\omega_{l_2}} 2 \frac{\omega_{l_1}^2 + \omega_{l_1} \omega_{l_2} + \omega_{l_2}^2}{\omega_{l_1}^2 \omega_{l_2}^2 (\omega_{l_1} + \omega_{l_2})} \delta(\vec{l}_1 + \vec{l}_2 - \vec{q}), \end{aligned} \quad (5.152)$$

Adding the two expressions together and performing straightforward simplifications one obtains the total contribution to the leading 2π -exchange proportional to g_A^4 :

$$V_{2N}^{2\pi, \text{total}}(\vec{q}) = -\frac{g_A^4}{32F_\pi^4} \int \frac{d^3 l}{(2\pi)^3} \left[\tau_1 \cdot \tau_2 (\vec{l}^2 - \vec{q}^2)^2 + 6 \vec{\sigma}_1 \cdot \vec{q} \times \vec{l} \vec{\sigma}_2 \cdot \vec{q} \times \vec{l} \right] \frac{\omega_+^2 + \omega_+ \omega_- + \omega_-^2}{\omega_+^3 \omega_-^3 (\omega_+ + \omega_-)}, \quad (5.153)$$

with $\omega_{\pm} \equiv \sqrt{(\vec{q} \pm \vec{l})^2 + 4M_{\pi}^2}$. The integrals appearing in the above expressions are ultraviolet divergent and need to be regularized. This can be achieved using standard methods such as e.g. dimensional regularization. Cutoff regularization can be applied equally well. In the infinite-cutoff limit, $\Lambda \rightarrow \infty$, the regularized integrals can be decomposed into a *finite* non-polynomial part (with respect to the momentum transfer \vec{q}) and polynomial in momenta terms that may diverge as Λ goes to infinity. Such a decomposition follows from the local nature of the ultraviolet divergences and implies the uniqueness of the non-polynomial part (in the limit $\Lambda \rightarrow \infty$). This makes perfect sense from the physics point of view since the nonpolynomial part of the potential controls its long-range behavior which should not depend on the details of regularization at short distances. For the non-polynomial parts of the relevant integrals one obtains:

$$\begin{aligned} I_1 &\equiv \int \frac{d^3l}{(2\pi)^3} \frac{\vec{l}^2}{\omega_+ \omega_- (\omega_+ + \omega_-)} = \frac{1}{6\pi^2} (4M_{\pi}^2 + q^2) L(q) + \dots, \\ I_2 &\equiv \int \frac{d^3l}{(2\pi)^3} \frac{\vec{l}^4 + \vec{q}^4}{\omega_+ \omega_- (\omega_+ + \omega_-)} = -\frac{1}{60\pi^2} \frac{512M_{\pi}^6 + 384M_{\pi}^4 q^2 + 156M_{\pi}^2 q^4 + 23q^6}{4M_{\pi}^2 + q^2} L(q) + \dots, \\ I_3 &\equiv \int \frac{d^3l}{(2\pi)^3} \frac{(\vec{q} \cdot \vec{l})^2}{\omega_+ \omega_- (\omega_+ + \omega_-)} = +\dots, \end{aligned} \quad (5.154)$$

where $q \equiv |\vec{q}|$ and the ellipses refer to terms polynomial in q . Note that I_3 does not give rise to any non-polynomial terms. Further, I have introduced the loop function $L(q)$ defined as:

$$L(q) = \frac{1}{q} \sqrt{4M_{\pi}^2 + q^2} \ln \frac{\sqrt{4M_{\pi}^2 + q^2} + q}{2M_{\pi}}. \quad (5.155)$$

Using the identity

$$\frac{\omega_+^2 + \omega_+ \omega_- + \omega_-^2}{\omega_+^3 \omega_-^3 (\omega_+ + \omega_-)} = -\frac{1}{2} \frac{\partial}{\partial(M_{\pi}^2)} \frac{1}{\omega_+ \omega_- (\omega_+ + \omega_-)}, \quad (5.156)$$

one can express all integrals entering Eq. (5.153) in terms of $I_{1,2,3}$ as follows

$$\begin{aligned} \int \frac{d^3l}{(2\pi)^3} \frac{\omega_+^2 + \omega_+ \omega_- + \omega_-^2}{\omega_+^3 \omega_-^3 (\omega_+ + \omega_-)} (l^2 - q^2)^2 &= -\frac{1}{2} \frac{\partial}{\partial(M_{\pi}^2)} (I_2 - 2q^2 I_1), \\ \int \frac{d^3l}{(2\pi)^3} \frac{\omega_+^2 + \omega_+ \omega_- + \omega_-^2}{\omega_+^3 \omega_-^3 (\omega_+ + \omega_-)} l_i l_j &= \frac{1}{4} \frac{\partial}{\partial(M_{\pi}^2)} \left\{ \left(-I_1 + \frac{1}{q^2} I_3 \right) \delta_{ij} + \left(\frac{1}{q^2} I_1 - \frac{3}{q^4} I_3 \right) q_i q_j \right\}. \end{aligned} \quad (5.157)$$

The final result for the 2π -exchange potential $\propto g_A^4$ then takes the form:

$$\begin{aligned} V_{2N}^{2\pi, \text{total}}(\vec{q}) &= -\frac{g_A^4}{384\pi^2 F_{\pi}^4} \vec{\tau}_1 \cdot \vec{\tau}_2 \left(20M_{\pi}^2 + 23q^2 + \frac{48M_{\pi}^4}{4M_{\pi}^2 + q^2} \right) L(q) \\ &\quad - \frac{3g_A^4}{64\pi^2 F_{\pi}^4} (\vec{\sigma}_1 \cdot \vec{q} \vec{\sigma}_2 \cdot \vec{q} - q^2 \vec{\sigma}_1 \cdot \vec{\sigma}_2) L(q) + \dots \end{aligned} \quad (5.158)$$

The polynomial in momenta, divergent (in the limit $\Lambda \rightarrow \infty$) terms have the form of contact interactions that are anyway present in the potential at a given order and can be simply absorbed into an appropriate redefinition of the LECs C_i .

Exercise: verify the result for the non-polynomial part of $V_{2N}^{2\pi, \text{total}}$ using dimensional regularization. Use the equality

$$\frac{1}{\omega_+ \omega_- (\omega_+ + \omega_-)} = \frac{2}{\pi} \int_0^\infty d\beta \frac{1}{\omega_-^2 + \beta^2} \frac{1}{\omega_+^2 + \beta^2}, \quad (5.159)$$

to get rid of the square roots in the integrand. The resulting integrals can be dealt with in the usual way by introducing the corresponding Feynman parameters.

In coordinate space, contact interactions have the form of the delta function at the origin, $\delta(\vec{r})$, and derivatives thereof. In contrast, the nonpolynomial pieces give rise to the potential at finite distances. To see this let us take a closer look at the obtained expression for the 2π -exchange potential. First, it should be emphasized that the Fourier transformation of the nonpolynomial terms alone is ill defined since they grow as q goes to infinity. The potential $V_{2N}^{2\pi, \text{total}}(\vec{r})$ at a finite distance, $r \neq 0$, can be obtained from $V_{2N}^{2\pi, \text{total}}(\vec{q})$ via

$$V_{2N}^{2\pi, \text{total}}(\vec{r}) = \lim_{\Lambda \rightarrow \infty} \int \frac{d^3 q}{(2\pi)^3} e^{-i\vec{q}\vec{r}} V_{2N}^{2\pi, \text{total}}(\vec{q}) F\left(\frac{q}{\Lambda}\right), \quad (5.160)$$

where $F(q/\Lambda)$ is an appropriately chosen regulator function such as e.g. $F = \exp(-q^2/\Lambda^2)$. Alternatively, one can use a (twice-subtracted) dispersive representation by expressing the potential $V_{2N}^{2\pi, \text{total}}(\vec{q})$ in terms of a continuous superposition of Yukawa functions. For example, the central part of the potential in Eq. (5.158) can be written as [84, 85]

$$V_{2N}^{2\pi, \text{central}}(q) = \frac{2q^4}{\pi} \int_{2M_\pi}^\infty d\mu \frac{1}{\mu^3} \frac{\rho(\mu)}{\mu^2 + q^2}, \quad (5.161)$$

where the spectral function $\rho(q)$ is given by

$$\begin{aligned} \rho(\mu) &= \text{Im} \left[V_{2N}^{2\pi, \text{central}}(0^+ - i\mu) \right] \\ &= -\frac{g_A^4}{768\pi F_\pi^4} \left(20M_\pi^2 - 23\mu^2 + \frac{48M_\pi^4}{4M_\pi^2 - \mu^2} \right) \frac{\sqrt{\mu^2 - 4M_\pi^2}}{\mu} \boldsymbol{\tau}_1 \cdot \boldsymbol{\tau}_2. \end{aligned} \quad (5.162)$$

The Fourier transformation can be easily carried out in this spectral representation by first integrating over \vec{q} and then over the spectrum μ . This leads to the central potential of the form

$$V_{2N}^{2\pi, \text{central}}(r) = -\frac{g_A^4 M_\pi}{128\pi^3 F_\pi^4 r^4} \boldsymbol{\tau}_1 \cdot \boldsymbol{\tau}_2 \left[(23 + 12x^2)K_1(2x) + x(23 + 4x^2)K_0(2x) \right], \quad (5.163)$$

where K_i denote the modified Bessel functions and $x \equiv M_\pi r$. At large distances, the potential behaves as $\exp(-2M_\pi r)/r^{3/2}$. The expressions for the remaining components of the 2π -exchange potential up to

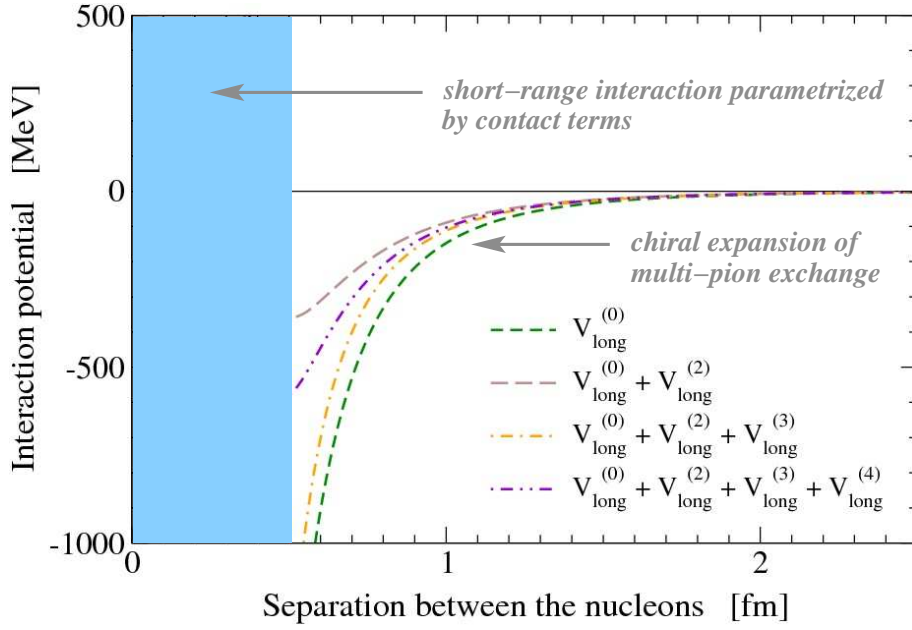


Figure 18: A schematic picture of the two-nucleon potential derived in chiral EFT in a given partial wave.

the chiral order Q^3 , both in momentum and coordinate space, can be found in Ref. [84]. The order- Q^4 contributions are given in Ref. [86]. The expressions for pion exchange potentials derived in chiral EFT at large distances are controlled by low values of μ for which the chiral expansion is expected to converge. At shorter distances, the large- μ components in the spectrum start to contribute which cannot be computed reliably in chiral EFT. This is visualized in Fig. 18. An extended discussion on the resulting theoretical uncertainty can be found in Ref. [85].

It is instructive to compare the toy models considered in section 4.5 with the nucleon-nucleon potential derived in chiral EFT whose structure is symbolically illustrated in Fig. 18. The main conceptual difference is due to the lack of an exact (regular) expression for the long-range force in the realistic case of nucleon-nucleon interaction. Rather, it is represented in terms of the chiral expansion of the pion-exchange potential which is valid at large distances and behaves singular as $r \rightarrow 0$. This raised debates on the relative importance of the long- and short-range components in the potential and the most efficient way to organize the expansion for low-energy observables. There is little consensus on this issue in the literature (yet).

Chiral 2π -exchange potential is, clearly, the most interesting new ingredient of the two-nucleon force from the chiral EFT point of view: it is the next-longest-range contribution after the well established 1π -exchange potential whose form is strongly constrained due to the chiral symmetry of QCD. Notice that three-pion exchange is already considerably less important for low-energy nuclear dynamics. The evidence of the chiral 2π -exchange potential up to $N^2\text{LO}$ has been verified in the Nijmegen PWA [87],

see Ref. [88] for a similar investigation. In their analysis, the Nijmegen group utilized the long-range interaction above some distance b as input in order to constrain the behavior of high partial waves. The missing intermediate and short-range components are simulated by suitably chosen energy-dependent boundary conditions. The number of parameters entering the boundary conditions needed to achieve a perfect description of the data thus may be viewed as a measure of physics that is missing in the assumed long-range force. As demonstrated in Ref. [87], adding the two-pion exchange potential derived at N²LO in chiral EFT to the 1π -exchange potential and the appropriate electromagnetic interactions allowed for a considerable reduction of parameters (from 31 to 23 for $b = 1.4$ fm in the case of proton-proton scattering) with even a slightly better resulting χ^2 . This is a big success of chiral EFT in the two-nucleon sector.

6 Summary

In these lectures, I have outlined the foundations of chiral effective field theory and the application of this theoretical framework to the nuclear force problem. The method allows for a systematic derivation of nuclear forces with a direct connection to QCD via its symmetries. These lecture notes are mainly focused on the conceptual aspects and do not cover applications of the novel chiral potentials to the few-nucleon problem and various related topics such as e.g. isospin breaking effects, few-baryon systems with strangeness, electroweak and pionic probes in the nuclear environment, nuclear parity violation and chiral extrapolations of few-baryon observables. For a discussion on these and other topics as well as for a detailed description of the structure of the two-, three- and four-nucleon forces in chiral EFT the reader is referred to recent review articles [89, 90], see also [64]. There are many frontiers where future work is required. These include a better understanding of the power counting in the few-nucleon sector, the consistent inclusion of electroweak currents, and the development of chiral EFT with explicit $\Delta(1232)$ degrees of freedom.

Acknowledgments

It is a great pleasure to thank Faïçal AZAIEZ and other organizers of the International Joliot-Curie School 2009 for the superb organization and the pleasant atmosphere at the meeting. I also thank all my collaborators for sharing their insights into the topics discussed here. Special thanks are due to Hermann Krebs and Ulf-G. Meißner for a careful reading of the manuscript and their helpful comments. This work was supported by funds provided from the Helmholtz Association to the young investigator group “Few-Nucleon Systems in Chiral Effective Field Theory” (grant VH-NG-222), by the DFG (SFB/TR 16 “Subnuclear Structure of Matter”), and by the EU Integrated Infrastructure Initiative Hadron Physics Project under contract number RII3-CT-2004-506078.

References

- [1] H. Yukawa, Proc. Phys. Math. Soc. (Japan) **17**, 48 (1935).
- [2] N. Ishii, S. Aoki, and T. Hatsuda, Phys. Rev. Lett. **99**, 022001 (2007), nucl-th/0611096.
- [3] W. Glöckle and W. Polyzou, Few-Body Systems **9**, 97 (1990).
- [4] S. Weinberg, Phys. Lett. **B251**, 288 (1990).
- [5] S. Weinberg, Nucl. Phys. **B363**, 3 (1991).
- [6] E. M. Henley and G. A. Miller, Meson theory of charge dependent nuclear forces, in *Mesons and nuclei*, edited by M. Rho and D. H. Wilkinson, volume 1, p. 405, Amsterdam, 1979, North-Holland.
- [7] S. Okubo and R. E. Marshak, Ann. Phys. **4**, 166 (1958).
- [8] E. Epelbaum, W. Glöckle, and U.-G. Meißner, Nucl. Phys. **A747**, 362 (2005), nucl-th/0405048.
- [9] J. Golak *et al.*, (2009), 0911.4173, Eur. Phys. J. A, in press.
- [10] V. G. J. Stoks, R. A. M. Klomp, M. C. M. Rentmeester, and J. J. de Swart, Phys. Rev. **C48**, 792 (1993).
- [11] J. Bystricky, F. Lehar, and P. Winternitz, J. Phys. (France) **39**, 1 (1978).
- [12] W. Glöckle, *The Quantum Mechanical Few-Body Problem* (Springer-Verlag, Berlin, 1983).
- [13] R. Machleidt, Phys. Rev. **C63**, 024001 (2001), nucl-th/0006014.
- [14] R. B. Wiringa, V. G. J. Stoks, and R. Schiavilla, Phys. Rev. **C51**, 38 (1995), nucl-th/9408016.
- [15] V. G. J. Stoks, R. A. M. Klomp, C. P. F. Terheggen, and J. J. de Swart, Phys. Rev. **C49**, 2950 (1994), nucl-th/9406039.
- [16] R. Machleidt and I. Slaus, J. Phys. **G27**, R69 (2001), nucl-th/0101056.
- [17] S. C. Pieper and R. B. Wiringa, Ann. Rev. Nucl. Part. Sci. **51**, 53 (2001), nucl-th/0103005.
- [18] W. Glöckle, H. Witała, D. Hüber, H. Kamada, and J. Golak, Phys. Rept. **274**, 107 (1996).
- [19] S. Weinberg, Physica **A96**, 327 (1979).
- [20] J. Gasser and H. Leutwyler, Ann. Phys. **158**, 142 (1984).
- [21] J. Gasser and H. Leutwyler, Nucl. Phys. **B250**, 465 (1985).
- [22] Particle Data Group, C. Amsler *et al.*, Phys. Lett. **B667**, 1 (2008).
- [23] S. R. Coleman, J. Wess, and B. Zumino, Phys. Rev. **177**, 2239 (1969).
- [24] C. G. Callan, S. R. Coleman, J. Wess, and B. Zumino, Phys. Rev. **177**, 2247 (1969).
- [25] R. Haag, Phys. Rev. **112**, 669 (1958).
- [26] U. L. van Kolck, *Soft physics: Applications of effective chiral lagrangians to nuclear physics and quark models*, PhD thesis, University of Texas, Austin, USA, 1993, UMI-94-01021.
- [27] G. Colangelo, J. Gasser, B. Kubis, and A. Rusetsky, Phys. Lett. **B638**, 187 (2006), hep-ph/0604084.
- [28] I. S. Gerstein, R. Jackiw, S. Weinberg, and B. W. Lee, Phys. Rev. **D3**, 2486 (1971).
- [29] J. Bijnens, Prog. Part. Nucl. Phys. **58**, 521 (2007), hep-ph/0604043.
- [30] G. Colangelo, J. Gasser, and H. Leutwyler, Phys. Lett. **B488**, 261 (2000), hep-ph/0007112.

- [31] J. Bijnens, G. Colangelo, G. Ecker, J. Gasser, and M. E. Sainio, Nucl. Phys. **B508**, 263 (1997), hep-ph/9707291.
- [32] S. Weinberg, Phys. Rev. Lett. **17**, 616 (1966).
- [33] S. Pislak *et al.*, Phys. Rev. **D67**, 072004 (2003), hep-ex/0301040.
- [34] NA48/2, J. R. Batley *et al.*, Eur. Phys. J. **C54**, 411 (2008).
- [35] G. Colangelo, J. Gasser, and A. Rusetsky, Eur. Phys. J. **C59**, 777 (2009), 0811.0775.
- [36] J. R. Pelaez, AIP Conf. Proc. **688**, 45 (2004), hep-ph/0307018.
- [37] J. Gasser, M. E. Sainio, and A. Švarc, Nucl. Phys. **B307**, 779 (1988).
- [38] A. Krause, Helv. Phys. Acta **63**, 3 (1990).
- [39] T. Fuchs, J. Gegelia, G. Japaridze, and S. Scherer, Phys. Rev. **D68**, 056005 (2003), hep-ph/0302117.
- [40] E. Jenkins and A. V. Manohar, Phys. Lett. **B255**, 558 (1991).
- [41] V. Bernard, N. Kaiser, J. Kambor, and U.-G. Meißner, Nucl. Phys. **B388**, 315 (1992).
- [42] L. L. Foldy and S. A. Wouthuysen, Phys. Rev. **78**, 29 (1950).
- [43] T. Mannel, W. Roberts, and Z. Ryzak, Nucl. Phys. **B368**, 204 (1992).
- [44] N. Fettes, U.-G. Meißner, and S. Steininger, Nucl. Phys. **A640**, 199 (1998), hep-ph/9803266.
- [45] H. Leutwyler, Principles of chiral perturbation theory, in *Hadron Physics 94: Topics on the Structure and Interaction of Hadronic Systems, Rio Grande Do Sul, Brazil 10-14 April 1994*, edited by V. Herscovitz, C. Vasconcellos, and E. Ferreira, pp. 1–46, Singapore, 1995, World Scientific.
- [46] U.-G. Meißner, (1997), hep-ph/9711365.
- [47] G. Ecker, (1998), hep-ph/9805500.
- [48] A. Pich, (1998), hep-ph/9806303.
- [49] J. Gasser, Lect. Notes Phys. **629**, 1 (2004), hep-ph/0312367.
- [50] B. Kubis, (2007), hep-ph/0703274.
- [51] S. Scherer, Adv. Nucl. Phys. **27**, 277 (2002), hep-ph/0210398.
- [52] V. Bernard, N. Kaiser, and U.-G. Meißner, Int. J. Mod. Phys. **E4**, 193 (1995), hep-ph/9501384.
- [53] V. Bernard, Prog. Part. Nucl. Phys. **60**, 82 (2008), arXiv:0706.0312 [hep-ph].
- [54] Proceedings of the 6th International Workshop on Chiral Dynamics, PoS(CD09)001-122, see: <http://pos.sissa.it/cgi-bin/reader/conf.cgi?confid=86>.
- [55] S. S. Schweber, *An introduction to relativistic quantum field theory* (Harper and Row, New York, Evanston & London, 1966).
- [56] J. M. Blatt and J. D. Jackson, Phys. Rev. **76**, 18 (1949).
- [57] H. A. Bethe, Phys. Rev. **76**, 38 (1949).
- [58] H. van Haeringen and L. P. Kok, Phys. Rev. **A26**, 1218 (1982).
- [59] A. M. Badalian, L. P. Kok, M. I. Polikarpov, and Y. A. Simonov, Phys. Rept. **82**, 31 (1982).
- [60] J. V. Steele and R. J. Furnstahl, Nucl. Phys. **A637**, 46 (1998), nucl-th/9802069.
- [61] D. B. Kaplan, M. J. Savage, and M. B. Wise, Phys. Lett. **B424**, 390 (1998), nucl-th/9801034.

- [62] D. B. Kaplan, M. J. Savage, and M. B. Wise, Nucl. Phys. **B534**, 329 (1998), nucl-th/9802075.
- [63] S. R. Beane, P. F. Bedaque, W. C. Haxton, D. R. Phillips, and M. J. Savage, nucl-th/0008064.
- [64] P. F. Bedaque and U. van Kolck, Ann. Rev. Nucl. Part. Sci. **52**, 339 (2002), nucl-th/0203055.
- [65] E. Braaten and H. W. Hammer, Phys. Rept. **428**, 259 (2006), cond-mat/0410417.
- [66] L. Platter, (2009), 0910.0031.
- [67] E. Epelbaum and J. Gegelia, Eur. Phys. J. **A41**, 341 (2009), 0906.3822.
- [68] T. D. Cohen and J. M. Hansen, Phys. Rev. **C59**, 13 (1999), nucl-th/9808038.
- [69] T. D. Cohen and J. M. Hansen, Phys. Rev. **C59**, 3047 (1999), nucl-th/9901065.
- [70] M. Pavon Valderrama and E. R. Arriola, Phys. Rev. **C72**, 044007 (2005).
- [71] S. Fleming, T. Mehen, and I. W. Stewart, Nucl. Phys. **A677**, 313 (2000), nucl-th/9911001.
- [72] S. R. Beane, D. B. Kaplan, and A. Vuorinen, Phys. Rev. **C80**, 011001 (2009), 0812.3938.
- [73] D. R. Entem and R. Machleidt, Phys. Rev. **C68**, 041001 (2003), nucl-th/0304018.
- [74] G. P. Lepage, nucl-th/9706029.
- [75] J. Gasser and H. Leutwyler, Phys. Rept. **87**, 77 (1982).
- [76] R. J. N. Phillips, Reports on Progress in Physics **XXII**, 562 (1959).
- [77] I. Tamm, J. Phys. (USSR) **9**, 449 (1945).
- [78] S. M. Dancoff, Phys. Rev. **78**, 382 (1950).
- [79] S. Okubo, Prog. Theor. Phys. (Japan) **12**, 603 (1954).
- [80] N. Fukuda, K. Sawada, and M. Taketani, Prog. Theor. Phys. (Japan) **12**, 156 (1954).
- [81] S. Weinberg, Phys. Lett. **B295**, 114 (1992), hep-ph/9209257.
- [82] E. Epelbaum, Eur. Phys. J. A **34**, 197 (2007), arXiv:0710.4250 [nucl-th].
- [83] E. Epelbaum, U.-G. Meißner, and W. Glöckle, Nucl. Phys. **A714**, 535 (2003), nucl-th/0207089.
- [84] N. Kaiser, R. Brockmann, and W. Weise, Nucl. Phys. **A625**, 758 (1997), nucl-th/9706045.
- [85] E. Epelbaum, W. Glöckle, and U.-G. Meißner, Eur. Phys. J. **A19**, 125 (2004), nucl-th/0304037.
- [86] N. Kaiser, Phys. Rev. **C64**, 057001 (2001), nucl-th/0107064.
- [87] M. C. M. Rentmeester, R. G. E. Timmermans, J. L. Friar, and J. J. de Swart, Phys. Rev. Lett. **82**, 4992 (1999), nucl-th/9901054.
- [88] M. C. Birse and J. A. McGovern, Phys. Rev. **C70**, 054002 (2004), nucl-th/0307050.
- [89] E. Epelbaum, Prog. Part. Nucl. Phys. **57**, 654 (2006), nucl-th/0509032.
- [90] E. Epelbaum, H.-W. Hammer, and U.-G. Meißner, Rev. Mod. Phys. **81**, 1773 (2009), 0811.1338.